Cindy Duarte de Oliveira

Licenciada em Bioquímica

A gold nanoparticle based colorimetric test allied to *Salmonella* LAMP amplification: toward the revolution of Food Quality Control

Dissertação para obtenção do Grau de Mestre em Biotecnologia

Orientador: Prof. Pedro Viana Baptista

Júri:

Presidente: Prof. Doutora Ana Cecília Afonso Roque
Arguente: Prof. Doutora Maria Alexandra Núncio de Carvalho Ramos Fernandes
Vogal: Prof. Doutor Pedro Miguel Ribeiro Viana Baptista

FACULDADE DE CIÊNCIAS E TECNOLOGIA
UNIVERSIDADE NOVA DE LISBOA

setembro de 2016

UNIVERSIDADE NOVA DE LISBOA
FACULDADE DE CIÊNCIAS E TECNOLOGIAS
DEPARTAMENTO DE CIÊNCIAS DA VIDA

Cindy Duarte de Oliveira

Licenciada em Bioquímica

A gold nanoparticle based colorimetric test allied to *Salmonella* LAMP amplification: toward the revolution of Food Quality Control

Dissertação para obtenção do Grau de Mestre em Biotecnologia

Orientador: Prof. Pedro Viana Baptista

Setembro de 2016

A gold nanoparticle based colorimetric test allied to *Salmonella* LAMP amplification: toward the revolution of Food Quality Control

ACKNOWLEDGMENTS

Ao professor Pedro Viana Baptista pela oportunidade de desenvolver o meu projeto no seu grupo de investigação, pela disponibilidade com que esclareceu todas as minhas questões, por todas as sugestões que me deu e por me fazer ver o que era realmente ciência, ensinando-me a ver para além do que está diante dos nossos olhos.

Aos meus colegas do 315 (que considero meus amigos após este ano de tanta partilha, parvoíces e união): **Fábio** por toda a ajuda que me deste, entre umas risadas e uns insultos, obrigada por estares sempre lá quando precisei. Dás vida àquele laboratório!; **Milton** por, apesar das boquinhas medíocres que mandas, estares sempre disposto a ajudar e a dar uma palavra amiga!; **Kelinha**, pela tua alegria contagiante e boa disposição que, sem dúvida, ajudaram a ultrapassar os momentos mais difíceis;**Sofia**, pelos desabafos, por todas as brincadeiras e pela ajuda que me deste!; **Pedrosa**, que estiveste lá sempre para ajudar em tudo ou simplesmente disponível para gozar comigo; **Fabiana**, por todas as vezes que me ouviste e me fizeste sentir que estava a ir bem mesmo quando eu achava o contrário e pelas vezes que adoçaste os nossos dias por nos desencaminhares para os brownies; **Beatriz**, pelas nossas risadas e pela simplicidade que tanto admiro em ti; **Catarina**, pelas vezes que, na brincadeira, disputamos o microplacas ou a chama para fazer um LAMP, são esses momentos que ajudam a atenuar o stress do dia-a-dia; **Toino**, que apesar de estares há pouco tempo no laboratório animaste os meus dias com as tuas brincadeiras ou simplesmente ouviste os meus desabafos. Enfim, este ano provou que tudo se consegue e, mesmo que não se consiga, a amizade ajuda sem dúvida atenuar os dias menos bons. Por isso, um obrigada especial à **Rita** que, apesar de só ter conhecido este ano, sinto que somos amigas há bem mais tempo! Obrigada pelos momentos que passámos, por cada membro que me deste quando mais precisei, aquele ombrinho ou aquela mão, pelas parvoíces e pelas gargalhadas! Sem dúvida que sem ti este ano não teria sido o mesmo!

Aos meus amigos André, Lucas, Carolina, Marisa e Filipa pelas conversas e bons momentos passados e, em especial, ao Dani, que por sermos tão parecidos, me percebes tão bem e estás sempre disponível para me ouvir ou simplesmente para ter conversas parvas e me animares o dia!

Às minhas amigas Carina, Cindy, Inês e Helena, as pessoas que mais me marcaram nestes cinco anos de faculdade! Obrigada por me deixarem ser quem sou, pelas gargalhadas e momentos inesquecíveis que passamos! Levo-vos comigo para a vida!

À Vanessa e à Andreia pela amizade e por estarem sempre lá para me ouvirem ou para passarmos momentos bem animados!

Ao Fábio por teres tido tanta paciência para o meu mau feitio este ano quando as coisas corriam menos bem (só pode ser amor!), por ajudares a ver sempre a vida com mais leveza e simplicidade, por me conseguires pôr sempre um sorriso na cara e por acreditares sempre nas minhas capacidades mesmo quando eu não acredito.

Ao meu Ruben por, com essa simplicidade de criança me pôres sempre um sorriso na cara e me ajudares a relativizar as coisas, mostrando-me que a felicidade está nas coisas simples da vida!

À minha irmã por estares lá sempre para me falares com a voz da experiência, me dares aqueles conselhos ou por estares lá simplesmente para me fazer rir.

Aos meus pais, por todo o amor e apoio incondicionais, por terem feito de mim quem sou hoje, por me ouvirem sempre e por quererem sempre o melhor para mim mesmo que eu nem sempre perceba isso! Esta tese é dedicada a vocês porque simboliza o fim de mais uma etapa e o culminar dos nossos sonhos e esforço! Obrigada por tudo!

RESUMO

Os microrganismos são a causa primária da deterioração de alimentos e das doenças transmitidas por estes. Anualmente, 1 300 mil milhões de casos de infeção originada por *Salmonella* surgem a nível mundial, acarretando grandes encargos para os países desenvolvidos e em desenvolvimento. Apesar dos grandes desenvolvimentos em tecnologia ocorridos na última década, os métodos atualmente utilizados na deteção de *Salmonella* não são suficientemente rápidos e fidedignos. De modo a solucionar estas questões, um teste baseado nas propriedades colorimétricas das nanopartículas de ouro foi combinado com a técnica de LAMP para a deteção de *Salmonella.*

As nanopartículas de ouro foram sintetizadas e funcionalizadas com oligonucleótidos de DNA modificados com um grupo tiol (nanossondas de ouro) com a capacidade de reconhecer a sequência alvo – locus *ttrRSBCA* de *Salmonella.* Este foi amplificado por LAMP, técnica otimizada ao longo deste estudo.

Quatro *batches* de nanossondas de ouro foram sintetizadas a partir de dois *batches* distintos de nanopartículas de ouro sob diferentes condições de pH. As nanossondas resultantes apresentaram diferenças entre si, nomeadamente na sua estabilidade e capacidade de deteção. Estas diferenças foram investigadas e as suas causas relacionadas com as condições de funcionalização, nomeadamente ultrassons, força iónica e tamanho das nanopartículas de ouro. O último fator foi confirmado por TEM.

As nanossondas de ouro foram utilizadas num método colorimétrico para a deteção de DNA, seguindo uma abordagem non-cross-linking – após um aumento da força iónica, as nanossondas de ouro agregam e a solução muda de vermelho para azul devido à deslocação para comprimentos de onda maiores da banda de ressonância de plasmónica superficial (SPR), típica das nanopartículas de ouro; a presença de um alvo complementar à sequência da nanossonda impede a agregação das nanossondas de ouro e a solução mantém a sua cor vermelha original.

A capacidade de deteção das nanossondas de ouro foi avaliada em produtos de LAMP e PCR, tendo-se verificado uma melhor discriminação em produtos de PCR.

O sistema desenvolvido neste projeto apresenta diversas vantagens, no entanto necessita de otimização para utilizações posteriores na deteção de agentes patogénicos em produtos alimentares.

Palavras-chave: Amplificação isotérmica de DNA mediada por LOOP (LAMP), nanopartículas de ouro, SPR, *Salmonella.*

ABSTRACT

Microorganisms are the primary cause of food spoilage and foodborne illness. Every year *Salmonella* causes 1.3 billion cases of disease worldwide, representing a considerable burden in both developing and developed countries. Despite of great advances in technologies in the last decade, current *Salmonella* detection methods are not fast and reliable enough. In order to address these issues a test based in the colorimetric properties of gold nanoparticles was combined with LAMP technique for the detection of *Salmonella*.

Gold nanoparticles were synthesized and functionalised with thiol-modified DNA oligonucleotides (Gold nanoprobes) able to recognize the target sequence - *ttrRSBCA* locus from *Salmonella*. It was amplified by LAMP technique, which was optimized in this study.

Four batches of gold nanoprobe were synthesized from two different batches of gold nanoparticles and under different pH. The arising gold nanoprobes showed some differences between them, namely in their stability and their detection capacity. These differences were investigated and it was verified that their cause was related to the conditions of functionalisation, namely ultrasound, ionic strength and nanoparticles size. The last was confirmed with TEM.

Au-nanoprobes were then used in a colorimetric method for DNA detection based on a non-cross-linking approach - upon increasing ionic strength, Au-nanoprobes aggregate and the solution changes colour from the original red to blue, due to the red-shift of the typical Surface Plasmon Resonance (SPR) band of gold nanoparticles; the presence of a complementary target to the probe sequence, prevents aggregation of the Au-nanoprobes and the solution remains red.

Gold nanoprobes detection capacity was tested with LAMP and PCR products and it was verified that a better discrimination is achieved with PCR products.

The system developed here presents some advantages but still needs optimisation for further application in pathogen detection in food.

Keywords: Loop-mediated isothermal amplification (LAMP), gold nanoparticles, SPR, *Salmonella*.

TABLE OF CONTENTS

FIGURE INDEX

TABLE INDEX

SYMBOLS AND ABBREVIATIONS

Abs – Absorbance

A525/600 - Ratio between 525 nm and 600nm

Au- Gold

AuNPS – Gold Nanoparticles

bp – base pair

DLS - Dynamic Light Scattering

DMSO - Methyl Sulfoxide

DNA - Deoxyribonucleic Acid

dNTPs - Deoxyribonucleotide Triphosphate

dsDNA - Double strand Deoxyribonucleic Acid

DTT - DL-Dithiothreitol

LAMP – Loop Mediated Isothermal Amplification

NTS – Non-Typhoid Salmonellosis

PCR - Polymerase Chain Reaction

SPR - Surface Plasmon Resonance

ssDNA - Single strand Deoxyribonucleic Acid

UV-vis – Ultraviolet-visible spectroscopy

“É preciso perder para depois se ganhar
E mesmo sem ver, acreditar”

Mariza

1 INTRODUCTION

1.1 Nanotechnology

Nanotechnology can be defined as the ability to understand, control and manipulate matter at the level of individual atoms and molecules (Bhattacharyya et al.,2009). It was in 1959 that the concepts that seeded this capability were first discussed. The physicist Richard Feynman described in his talk “There’s Plenty of Room at the Bottom” the possibility of synthesis at the molecular level via direct manipulation of atoms (Feynman, 1959).

Nanoscience and nanotechnology have faced an exponential progress in the last decade (Chandra et al., 2013).The production and characterization of new materials consisting of particles with dimensions in the order of a few nanometres allowed the development of a wide range of fields, such as electronics, mechanics and, especially, biomedicine (Chandra et al., 2013; Eustis & el-Sayed, 2006; Ghosh & Chattopadhyay, 2013) Carbon nanotubes, quantum dots, nanorods and noble metal nanoparticles are examples of these materials(Chandra et al., 2013; Eustis & el-Sayed, 2006).

1.1.1 Gold Nanoparticles and their properties

Gold nanoparticles (AuNPs) are among the most extensively studied nanomaterials (Ghosh & Chattopadhyay, 2013). AuNPs’ popularity is attributed to their ease of synthesis, chemical stability and unique physical and optical properties dependent of their interesting size (Khlebtsov & Dykman, 2010; Baptista et al., 2011). The incomparable characteristics of gold nanoparticles are making them responsible for a revolution occurring in biomedicine (Eustis & el-Sayed, 2006). AuNPs nanoscale properties make them very suitable for molecular imaging, photothermal treatment of diseases (Ghosh & Chattopadhyay, 2013) and molecular diagnostics (Baptista et al. 2006). Their high-surface-area-to-volume ratio make them great vectors for drug delivery (Dreaden et al., 2012; Veigas et al., 2012).

Among the remarkable properties of gold nanoparticles (AuNPs), their intense colours associated with their interesting optical properties are of great importance (Liz-Marzán, 2006). A solution of monodisperse gold nanoparticles appears red and exhibits a 520 nm centred band in the UV-visible spectrum, characteristic of LSPR – Localised Surface Plasmon Resonance (Doria et al., 2007).This phenomenon is related with nanoparticles size. According to Gustav Mie, for a spherical particle much smaller than the wavelength of light, an electromagnetic field at a certain frequency causes the induction of a resonant, coherent oscillation of the metal free electrons across the nanoparticle (LSPR) (Louis & Plucherry, 2012). This effect is responsible for the strong enhancement of absorption and scattering of electromagnetic radiation that allow for higher sensitivity in optical detection methods(Jain et al., 2006).

LSPR is strongly affected by changes in shape and inter-particle distance (Baptista et al. 2008; Rai & Kon 2015). The last can be influenced by NaCl addition, which may cause surface

charge shielding, leading to a concomitant inter-particle distance decrease. Thus, a solution containing aggregated gold nanoparticles shows a blue colour, which is a consequence of a redshift in the surface plasmon resonance to higher wavelength (Doria et al., 2007). A plethora of colorimetric detection schemes is based on this condition, taking advantage of the optical properties of disperse against aggregated gold particles for biodetection assays (Baptista et al., 2011; Rai & Kon, 2015).

Modulation of these properties of AuNPs can be easily achieved by adequate synthetic strategies.

1.1.2 Synthesis and functionalisation

Gold nanoparticles are associated colloids, which can be synthesised with dimensions ranging from 0.8 to 250 nm (Doria et al., 2007). Several physical and chemical techniques have been described for gold nanoparticles synthesis. These methods generate nanoparticles with high homogeneity and adequate morphology, size dispersion and surface functionalities (Yeh et al., 2012).

The most commonly used method for preparation of spherical AuNPs is Turkevich Method (Turkevich et al.,1951). It starts with the dissolution of chlorohauric acid ($HAuCl_4$) in water. Then a reducing agent (sodium citrate) is added, causing the reduction of Au^{3+}ions to Au^0, and consequently, the nucleation of neutral charged NPs (Ji et al., 2007). These nanoparticles grow in diameter until they get saturated of sodium citrate. Therefore, higher concentrations of sodium citrate promote the formation of smaller nanoparticles. Besides controlling size, this reagent prevents nanoparticles from aggregation due to electrostatic repulsion between citrate-capped AuNPs. Thus, sodium citrate acts also as a capping agent since it confers stability to nanoparticles (Wilcoxon & Abrams, 2006). As a result, this method produces monodisperse gold nanoparticles, forming an homogeneous colloid that does not suffer from precipitation nor aggregation (Ji et al., 2007). The use of citrate is very advantageous, since it can be easily replaced by other capping agents. It allows the functionalisation of gold nanoparticles surface with ligands, making them very suitable for use in biodetection assays. Thiol-linking of DNA and chemical functionalisation of gold nanoparticles for specific protein/antibody binding are the most common approaches (Baptista et al. 2008).

Functionalisation of AuNPs with biomolecules occurs generally through thiolmetal quasi-covalent bonds. It takes advantage of the strong affinity between the metal and sulfur that either exist in the biomolecule (e.g., proteins) or can be easily added (e.g., oligonucleotides) (Zhao et al., 2013). The use of thiol-linked oligonucleotide modified gold nanoparticles (Au nanoprobes) for the colorimetric detection of DNA targets was described for the first time by Mirkin et al in 1996 (Doria et al. 2007). A cross-linking approach was developed with the use of single-stranded oligonucleotides targets which could be detected using two species of Au-nanoprobes (Rai & Kon, 2015). Each nanoprobe was functionalized with a DNA-oligonucleotide complementary to one half of the given target (Doria et al. 2007). If sequence complementarity occurred between the

target and the two probes, NP aggregation would be observed and, consequently, a visual change from red to blue would take place (Mirkin et al., 1996).

1.1.3 Non-cross-linking approach

Baptista et al described a new strategy for the detection of nucleic acids– the non-cross-linking approach. This method only needs one Au-nanoprobe for molecular detection, which aggregates by the increase of ionic strength of the media (salt addition). In the presence of a specific complementary target, Au-nanoprobe stabilise and the solution remains red (Baptista et al., 2006). This occurs, possibly, due to the existence of electrostatic interactions between the negatively charged phosphate groups of the nucleic acid and the high polarisable gold nanoparticles (Doria et al., 2007). On the other hand, as a result of aggregation, the solution becomes blue in the absence of a specific complementary target (Baptista et al., 2006).

The development of this approach was only possible due to gold NPs extraordinary properties. Since LSPR confers them bright intense colours in solution, these nanoparticles present particular relevance for use in colorimetric tests to characterize and identify pathogens, such as *Salmonella* (Kalidasan et al., 2013).

1.2 *Salmonella spp.*

1.2.1 Taxonomy

Salmonella are facultative, anaerobic gram-negative bacilli belonging to the Enterobacteriaceae family (Kokkinos et al., 2014). The genus *Salmonella* contains two species: S. *bongori*, which is commonly associated with reptiles and *S. enterica*, which includes serotypes usually associated with the majority of food-related infections(Baylis et al., 2011). Six subspecies are differentiated within *S. enterica* based on their biochemical and genomic characteristics (Meneses et al., 2010). Belonging to these species there have been identified over 2500 serotypes. Based on Kauffmann-White method they are distinguished by their flagellar, carbohydrate and lipopolysaccharide (LPS) antigenic structures (Coburn, Grassl, & Finlay, 2007; Meneses, 2010). The serotypes of most concern with regard to food safety belong to *S.enterica* subsp. enterica, causing 99% of *Salmonella* infections(Coburn et al., 2007). *S. Typhimurium* and *S. Enteritidis* represent two of the more prominent *Salmonella* serotypes associated with human infections (Park et al., 2014).

1.2.2 Epidemiology

Foodborne illnesses continue to be a serious concern as a public health issue for the food industry. Viruses are major causative agents for foodborne illnesses (59%), followed by bacteria (39%). Each year, roughly 1 in 6 people in the US gets sick from eating contaminated food. *Salmonella* species were considered as the leading cause for the more severe cases resulting in

35% of the hospitalisations and 28% of the deaths(Park et al., 2014). *Salmonella* infection represents a considerable burden in both developing and developed countries, causing 1.3 billion cases of disease annually worldwide (Coburn et al., 2007) with costs of billions of dollars in medical services and incalculable losses to the reputations of implicated agricultural products and producers regardless of the true source of contamination(Kokkinos et al., 2014).

The majority of the infections are associated with ingestion of contaminated foods such as eggs, chicken, beef, pork, milk products, fruits, and vegetables (Kokkinos et al., 2014; Martelli & Davies, 2012). The epidemiology of *Salmonella spp*. associated infections varies widely depending on the type of *Salmonella spp*. involved (Sánchez-Vargas et al., 2011). While enteric fever, caused by *S. Typhi* and *S. Paratyphi*, generally leads to a severe and life-threatening disease, Non-Typhoid Salmonellosis (NTS) infections tend to be self-limiting, causing intestinal/ diarrheal disease (Baylis et al., 2012).

High portion of these infections take place in Africa, Asia, Latin America, with 80% of cases in Bangladesh, China, India, Indonesia, Nepal or Vietnam (Ao et al., 2015; Chau et al., 2007) (**Figure 1.1**).

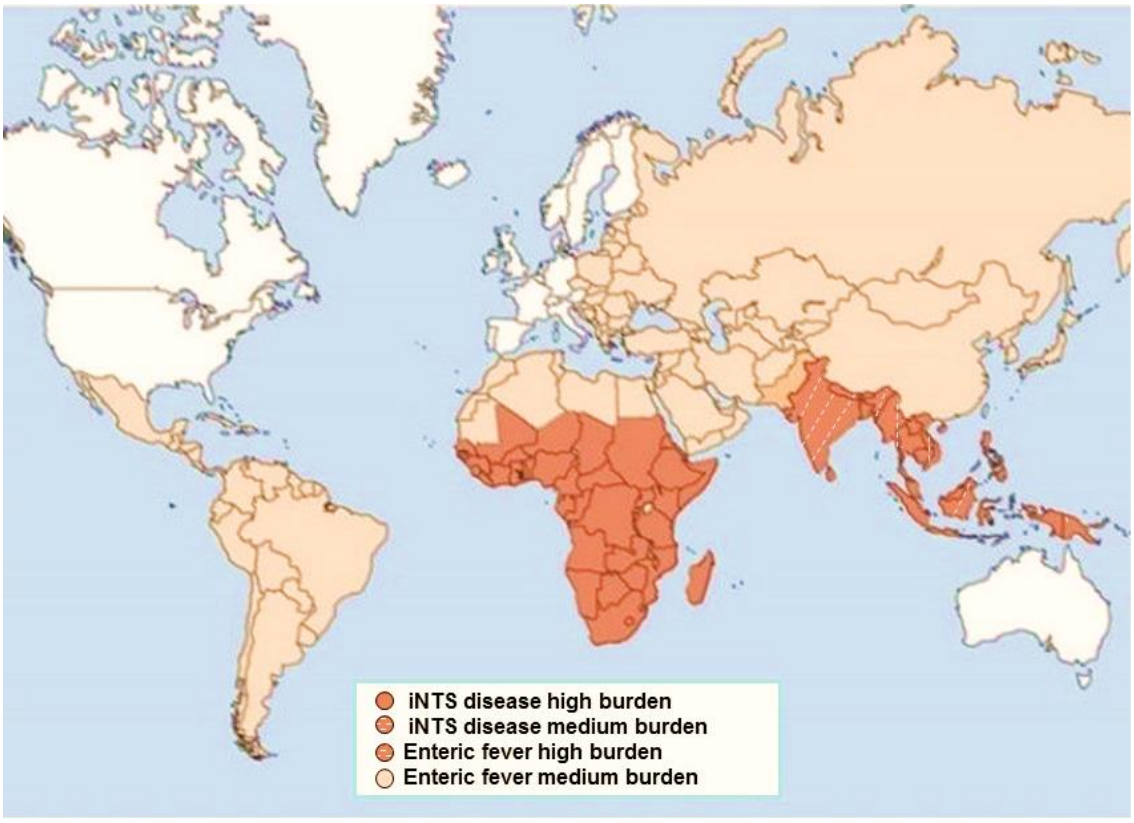

Figure 1.1. **Geographical distribution of enteric fever and Non-Typhoid Salmonellosis (iNTS) disease**. High disease burden is defined as greater than 100 cases per 100,000 population per year, and medium disease burden as 10–100 cases per 100,000 population per year (Gilchrist et al., 2015).

1.2.2.1 Typhoid Fever

Once ingested the bacteria pass through the stomach and enter the intestine where multiplication occurs. Transportation of the bacteria from the small intestine to the mesenteric lymph nodes is via microfold cells (also termed M cells) of the Peyer's patches (aggregations of lymphoid tissue usually found in the lowest portion of the ileum) (D'Aoust et al., 1991). The bacteria perforate and enter through the intestinal wall and are phagocytosed by macrophages, where they can exist and avoid destruction by neutrophils, complement and the immune response. While inside the macrophages, the bacteria spread via the lymphatic system and blood stream. This gives them access to the different organs throughout the body (Baylis et al., 2011).

1.2.2.2 Non-Typhoid Salmonellosis (NTS)

Salmonella generally cause illness by localised infection of the gastrointestinal tract (Morgan et al., 2004), leading to the development of nausea, vomiting, fever and diarrhoea (Andino & Hanning, 2015). Colonisation and attachment to epithelial cells with subsequent invasion of the intestinal tissue characterise *Salmonella* infection (C. Baylis, M. Uyttendaele, Han Joosten & Davies, 2011). During this invasive process, the bacterium secrets a heat labile enterotoxin that precipitates a net efflux of water and electrolytes into the intestinal lumen resulting in diarrhoea (Coburn et al., 2007). During infection by *Salmonella* a strong innate immune/inflammatory response is induced in the host (Hur et al., 2012).

1.2.3 Pathogenicity

Significant inflammatory disease is a common feature of typhoid and enterocolitis (Meneses et al., 2010). The various virulence programs employed by *Salmonella* species interact with host defence mechanisms at various tissues in different stages of infection resulting in significant host immunopathology, morbidity and mortality(Coburn et al., 2007). The severity of illness in individuals with salmonellosis is determined not only by host properties but also by the virulence factors of the infecting strain(Baylis et al., 2011).

The chromosomes of enteric bacteria are mosaics, composed of collinear regions interspersed with 'loops' or 'islands' unique to certain species (McClelland et al., 2001). Virulence genes often cluster on large plasmids or in the localised regions of the chromosome, termed *Salmonella* pathogenicity islands (SPI) (Hur et al., 2012). These islands are of critical importance for in vivo virulence, in particular SPI-1 and -2 (Andino & Hanning, 2015).Both SPIs encode a molecular apparatus called a type III secretion system (T3SS) capable of injecting bacterial proteins known as 'effectors' through bacterial and host membranes into host cells (translocation) or the extracellular milieu (secretion) to directly influence host biochemistry and cell physiology(Coburn et al., 2007).*Salmonella* pathogenicity island 1 (SPI-1) encodes genes necessary for invasion of intestinal epithelial cells and induction of intestinal secretory and inflammatory responses (Watson et al., 1995). *Salmonella* pathogenicity island 2 (SPI-2) encodes

genes essential for intracellular replication, and is necessary for establishment of systemic infection beyond the intestinal epithelium (Coburn et al., 2007).

1.3 Challenges and current needs

The incidence of *Salmonella* infections has not declined over the past 16 years, underscoring the critical need for prevention and control (Q. Yang et al., 2015). The large number of outbreaks produced by this bacterium worldwide indicates its importance and impact (Majowicz et al., 2010; Tirado & Schmidt, 2001).

Interventions, which demonstrate effective reductions in the occurrence and levels of pathogenic bacteria at different processing steps, have been included in production lines to keep critical points under control (Meneses et al., 2010). Despite the existence of high regulated government monitoring programs, such as the Hazard Analysis and Critical Control Point (HACCP) plans for food industry, preventing *Salmonella* remains challenging (Mead et al., 1999). The difficulty in controlling *Salmonella* lies in its ability to survive extreme environmental conditions (Meneses et al., 2010). Its existence in many different types of foods and the possibility of contamination occurrence anywhere from production and manufacturing to distribution and consumption also difficult its control.

Detecting microbial pathogens and toxins in foods faces many inherent challenges associated with food analysis. The complexity of food matrices and compositions presents a major obstacle to developing effective sampling, sample preparation, and testing strategies, mainly in solid food. Food matrices frequently harbour inhibitors for key reagents used in detection assays, such as PCR enzymes. Furthermore, raw foods naturally contain high levels of normal flora, which may interfere with the performance of a wide array of pathogen detection technologies. On the other hand, the attributes of target analytes in foods also significantly impact the detection efficiency. For example, pathogens in foods are generally present at a much lower level and are frequently injured during food processing, which demands improved detection sensitivity and pre-enrichment to resuscitate the injured cells. Additionally, the heterogeneous distribution of pathogens and toxins in foods presents a challenge for effective and statistically sound sampling procedures, particularly when detecting pathogens that cause severe illness in humans with very low infectious doses (Ge & Meng 2009).

In order to overcome these difficulties, enrichment, concentration and extraction techniques are strategies commonly applied to food samples before they are actually subjected to the detection assay. However, these methods may be labour intensive, increase the total analysis time and inhibit certain detection assays, reducing their sensitivity and efficiency (Ge & Meng 2009).

Increased public awareness related to health and economic impacts of food-borne contamination and illness has resulted in greater efforts to develop more sensitive, rapid, and inexpensive method of pathogenic microbe detection and identification (Deguo et al., 2008).

1.4 Classical and Molecular Methods for *Salmonella* Detection

1.4.1 Culture Methods – The "gold standards" in food detection

Reference methods for bacterial detection or identification rely mainly on culture based approaches (Francois et al., 2011). Generally regarded as the "gold standard" for food detection, conventional culture technique for *Salmonella* standardised by the International Organization for Standardisation (ISO6579:2002) and the United States Food and Drug Administration includes pre-enrichment, selective enrichments, and plating on selective agar media followed by biochemical and serological tests(Ge & Meng, 2009; Lee et al., 2015).

Despite the great development of these methods, they are time consuming, requiring 4 to 5 days to obtain presumptive or negative results; and can take up to 7 days depending on the realization of biochemical and serological confirmations (Park et al., 2014). Antibiotic treatment, inadequate sampling, presence of other competing organisms during enrichment step and small number of viable microorganisms in samples can affect cultures sensitivity(Lee et al., 2015; Zadernowska & Chajecka, 2012). Moreover, these tests demand large volumes usage of liquid and solid media and reagents (Odumeru & León-Velarde, 2012).

Although traditional culture based methods detect "viable" bacterial cells, they do not detect potentially infectious non-culturable cells, and these techniques are not specific enough to detect and characterize *Salmonella* at the strain level, particularly when a large number of samples are involved (Maciorowski et al., 2006).

For public health and the food industry, rapid, sensitive and specific methods to detect *Salmonella* are required.

1.4.2 Rapid Methods

Recent advances on technology have made the detection of this pathogen more rapid and convenient, while achieving improved sensitivity and specificity in comparison to conventional methods(Ge & Meng, 2009). Rapid methods include convenience-based, antibody-based, Fluorescent *in situ* hybridisation (FISH) and nucleic acid-base assays (Lee et al., 2015; Park et al., 2014) (**Table 1.1**).

Convenience-based assays are used in food industry for sanitation control. They include hydratable gel cards and portable device for testing ATP activities. It provides immediate feedback on the sanitation conditions of food contact surfaces and the environment, while not being a direct indicator of microbial contamination of food products(Ge & Meng, 2009).

Immunological based methods, which employ specific mono- or polyclonal antibodies binding with somatic or flagella antigens, contain diverse assays, including ELISA (Lee et al., 2015; Odumeru & León-Velarde, 2012). Enzyme-linked immunosorbent assay (ELISA) is a biochemical technique used to detect the presence of an antibody or an antigen in a sample (Lee et al., 2015). In the ELISA assay, an antigen specific to *Salmonella spp*. is bound to the appropriate antibody linked to a solid matrix. After forming the antigen-antibody complex, the

concentration of the antigen and the presence of *Salmonella spp.* can be measured through the change in colour caused by the enzymatic cleavage of a chromogenic substrate(Park et al., 2014).

FISH (Fluorescent *in situ* hybridisation) technique consists in hybridisation of the rRNA sequence of immobilised cells by a fluorescently-labelled 16S rRNA oligonucleotide probe (Zwirglmaier et al., 2005), which is a short fragment of deoxyribonucleic acid that hybridizes or is paired with complementary sequences of DNA or RNA extracted from the analysed microorganisms. Probes are most often marked on one or on both ends with a fluorescent dye, binding only with the DNA of the identified organism (Zadernowska & Chajecka, 2012). This method includes preparation and permeabilisation of cells, hybridisation, washing off the excess unbound probe and detecting the signal with the application of fluorescence microscopy (Jasson et al., 2010).

Next Generation Sequencing (NGS) came as a response to the ultimate goal in foodborne detection – the ability to distinguish subtle strain genetic differences of a pathogen. It has led to the rapid assembly of microbial sequences encoding complete genome within a day. NGS technologies allow an extensive parallel sequencing approach of a large number of template fragments(Park et al., 2014).

In the last decade nucleic acid-based assays have suffered an exponential development since they offer great sensitivity and specificity over other methods, being able to identify rapidly *Salmonella* in the absence of pure cultures (Glynn et al. 2006). These techniques consist of two main types, hybridisation using probes and amplification by PCR and related techniques (Ge & Meng, 2009). The nucleic acid-based assays are *Salmonella* detection tests that use a specific nucleic acid target sequence within the organism (Lee et al., 2015) and have been successfully used for the detection of food-borne pathogens, including *Salmonella* (Kokkinos et al., 2014). DNA microarrays involve the use of selected single stranded oligonucleotide probes attached to a solid surface of glass slides or fluorescently encoded beads. Subsequently, the probe hybridises with target DNA isolated from samples that are labelled with a fluorophore (Park et al., 2014). Probes directed to specific gene regions of the *Salmonella* genome have proven to be more specific than culture and immunological assays (Manzano et al., 1998).

Even though these molecular methods have the potential to reduce detection time to less than 3 days (Zhang et al., 2011), they present several drawbacks (**Table 1.1**). Therefore, in order to prevent and control the spread of *Salmonella*, the development and validation of faster screening and robust diagnostic assays for this pathogen are crucial (Yang et al., 2010).

Table 1.1. Advantages and Disadvantages of rapid detection methods (adapted from Park et al. 2014).

Method	Advantages	Disadvantages
ELISA	• More rapid than culture-based methods (2 d vs 5-7d) • Can be automated to reduce assay time and manual labor input • Able to handle large number of samples • More specific than cultural methods	• Low sensitivity • Limited multiplexing ability • False negative results • Difficulty in detecting damaged or stresses cells • Pre-enrichment for production of cell surface antigens • Cross-reactivity with antigens of closely related bacteria
FISH	• Determines only the number of physiologically active cells • Sensitive (able to detect viable but not culturable cells) • Specific (information available concerning RNA sequences from organisms very closed genetically) • Fast and cheap	• False positive results • Specificity of probe affected by the food matrix
NGS	• Sensitive, specific and accurate • Sequencing without electrophoresis • Rapid (7-10h)	• Data storage and data release • Need skill person for data analysis • High cost • No detection of viable cells without pre-enrichment • Samples need to be prepared and amplified
Microarray	• Rapid than culture-based methods (2 d vs 5-7d) • Multiplex analysis (Up to 100 different beads commercially available) • High sensitive and specific (probe design to genome) • Labor effective (can be applied to 96-well format)	• Difficulty in distinguishing live and dead cells • High cost • Need skill person and support
Conventional PCR	• Rapid than culture-based methods (4-24h vs 5-7d) • High specific and sensitive • Automated • Multiplex potential	• Difficulty in distinguishing live and dead cells • Prone to PCR inhibitors, non-target DNA and physicochemical parameter modifications • Requirement of thermal cycler and gel documentation system • Post-PCR handling leading to carry over contaminations • Less sensitive, thereby missing borderline cases with low gene copy numbers
Real-Time PCR	• Simultaneous amplification and detection during exponential amplification • Increased sensitivity due to fluorescent chemistry • Lower carry over contamination due to closed tube operation	• Difficulty in multiplex assay • Expensive detection equipments and consumables • Need skilled person • Prone to PCR inhibitors, non-target DNA and physicochemical parameter modifications
LAMP	• Isothermal field-based gene amplification without requiring thermal cycler • Amplification can be accomplished with water bath/ heating block • Real-time as well as quantitative • Requirement of fewer operation steps compared to PCR assays	• Complicated primer design • Laboratory based • Limitations for multiplexing

1.4.2.1 Loop-mediated isothermal technique (LAMP) technique

Developed by Notomi et al. in 2000, LAMP has become a promising alternative to PCR for pathogen detection (Notomi et al., 2000), due to its high specificity and sensibility, simple operation and low cost (Shao et al., 2011). Its mechanism is described in **Figure 1.2.**

This method is based on the use of a specially designed set of four target-specific primers (F3, B3, FIP and BIP), which are able to recognise six distinct sites flanking the amplified DNA sequence (F1c, F2c, F3c sites on the 3' side and B1, B2, B3 sites on the 5' side) (**Figure 1.2 a**). One pair of primers, F3 and B3, represents the ordinary, single-domain primers (they each recognise one of the six sites and so amplify the entire target region), and these are supplemented by an additional pair of composite, double-domain primers, FIP and BIP, which recognise two of the six sites each and play the major role in the LAMP reactions (FIP and BIP primers are used in excess, compared to F3 and B3 primers). The LAMP reaction is considered to progress through two steps by DNA polymerase with strand displacement activity: starting structure producing step (**Figure 1.2 b**) and cycling amplification step (**Figure 1.2 c**) (Tomita et al., 2008).

The final amplification products are mixtures of many different sizes of stem-loop DNAs with several inverted repeats on the target sequence and cauliflower-like structures with multiple loops (Notomi et al., 2000; J. L. Yang et al., 2010). At the end of the reaction, the presence or absence of the target DNA is judged visually by the appearance of a white magnesium pyrophosphate precipitate, by a colorimetric change on addition of SYBR Green I to the mixture or agarose gel (Kokkinos et al., 2014).

LAMP assays have been developed for the detection of *Salmonella* in different food matrices, including liquid egg (Hara-Kudo et al., 2005), meat products (Y. Wang et al., 2009), milk (Shao et al., 2011), chicken, yogurt, omelet, hamburger, beef, and apple juice (Chen et al.,2011).

Recently, this technique has also been used to overcome a major limitation of DNA-based molecular detection assays – the inability to differentiate live versus dead cells (Ge & Meng, 2009). Incorporation of propidium monoazide during the sample preparation steps, allowed the chemicals to intercalate into free DNA (dead cells) but not in intact live cells, preventing amplification of dead cell DNAs (S. Chen et al., 2011).

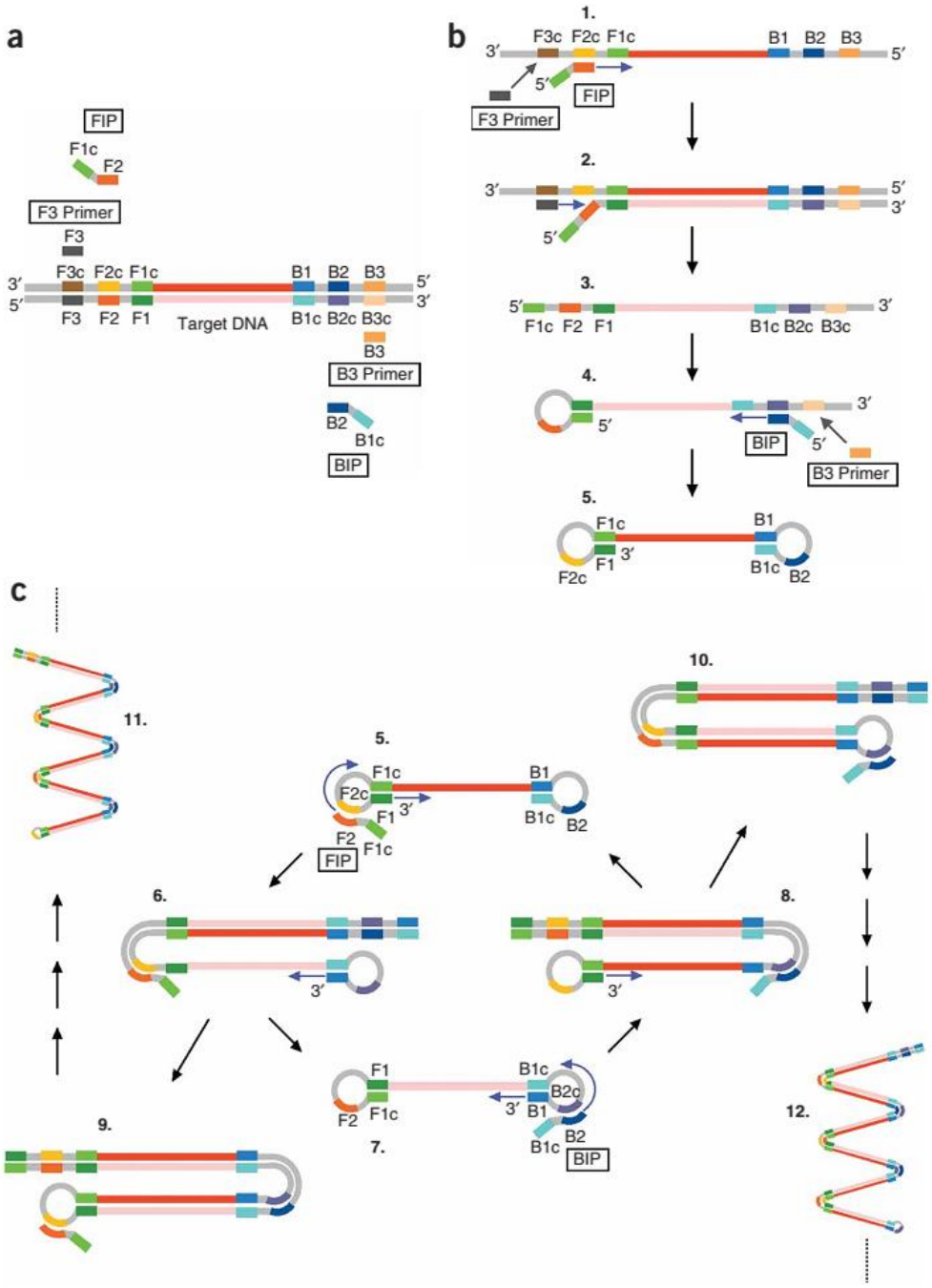

Figure 1.2 Principle of loop-mediated isothermal amplification (LAMP) method. (a) Primer design of the LAMP reaction. Six distinct regions are designated on the target DNA, labelled F3, F2, F1, B1c, B2c and B3 from the 5' end. As c represents a complementary sequence, the F1c sequence is complementary to the F1 sequence. Two inner primers (FIP and BIP) and outer primers (F3 and B3) are used in the LAMP method. FIP (BIP) is a hybrid primer consisting of F1c (B1c) sequence and the F2 (B2) sequence**. (b) Starting structure producing step.** DNA synthesis initiated from FIP proceeds as follows. The F2 region anneals to the F2c region on the target DNA and initiates the elongation. DNA amplification proceeds with BIP in a similar manner. The F3 primer anneals to the F3c region on the target DNA, and strand displacement DNA synthesis takes place. The DNA strand elongated from FIP is replaced and released. The released single strand forms a loop structure at its 3' end (structure 3). DNA synthesis proceeds with the single-strand DNA as the template, and BIP and B3 primer, in the same manner as described earlier, to generate structure 5, which possesses the loop structure at both ends (dumbbell-like structure). **(c) Cycling amplification step.** Using self-structure as the template, self-primed DNA synthesis is initiated from the 3' end F1 region, and the elongation starts from FIP annealing to the single strand of the F2c region in the loop structure. Passing through several steps, structure 7 is generated, which is complementary to structure 5, and structure 5 is produced from structure 8 in a reaction similar to that which led from structures 5–7. Structures 9 and 10 are produced from structures 6 and 8, respectively, and more elongated structures (11, 12) are also produced (Tomita et al. 2008).

1.4.2.1.1 LAMP *Salmonella* amplification allied to a gold nanoprobe based colorimetric test

An ideal detection system should include high specificity and sensitivity; fast response time; capability for mass production; elimination or simplification of sample preparation steps; minimal perturbation of sample and providing continuous data analysis (Ge & Meng, 2009).

When used for the detection of pathogens and toxins in foods, the rapid methods described above are used primarily as a screening tool (Ge & Meng, 2009). Negative results are definitive, while positive are regarded as presumptive, requiring further confirmation by traditional culture-based methods(Park et al., 2014). Moreover, the majority of antibody-based and nucleic acid-based assays, require enrichment to achieve the necessary sensitivity require of food testing, which results in a great increase of time analysis (Ge & Meng, 2009).

Therefore, in this thesis LAMP amplification method was joined to gold nanoprobes. Even though these two methods have already been used individually for *Salmonella* detection (Prasad, Shankaracharya, & Vidyarthi, 2011; Zhuang et al., 2014), their combination make easier the achievement of the required test specificity and sensitivity allied to some degree of rapid detection.

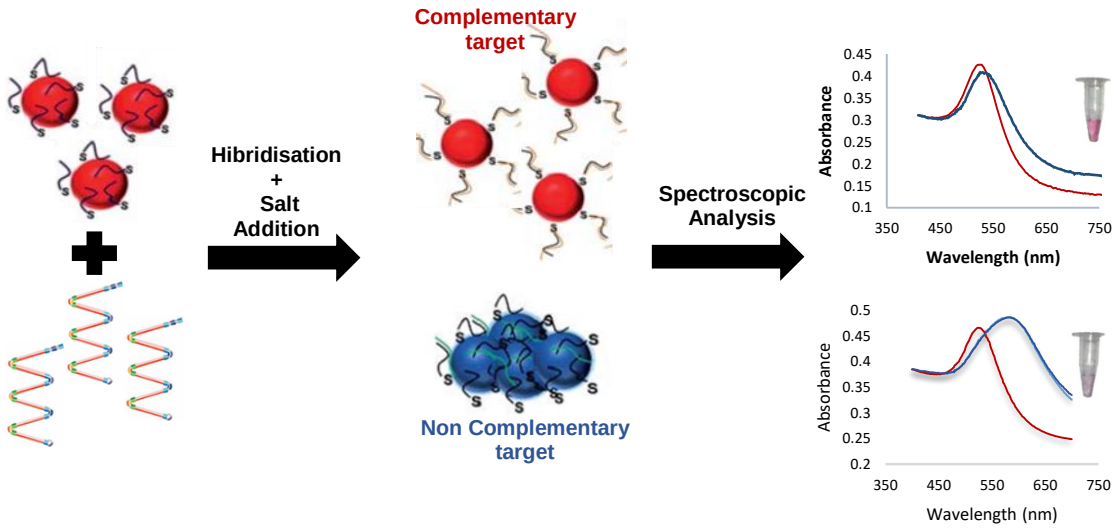

Figure 1.3. Au-nanoprobes non-cross-linking method applied to *Salmonella* LAMP amplified detection.

1.5 Thesis Scope

Salmonella has been recognised as a major and important foodborne pathogen for humans and animals over more than a century, causing human foodborne illness as well as high medical and economical cost.

Despite the advances made in technology in the past decades, the detection of microbial pathogens and their toxins in foods remains a challenging task. Rapid methods have been developed but limitations still exist.

Considering this issue, this thesis aims to develop a colorimetric test for the detection of *Salmonella* allied to LAMP technique. In order to attain this milestone, the project proposed intends to:

- Design probes *in silico* with the ideal characteristics to detect *ttrRSBCA* locus from *Salmonella*;
- Design and optimise LAMP reaction;
- Synthesize, functionalise and characterise gold nanoparticles for non-cross linking method;
- Study the underlying mechanisms involved in the non-cross-linking detection, towards the optimisation of the method;
- Couple LAMP with Au-nanoprobes;
- Compare LAMP products detection with PCR gold-standard.

2 MATERIALS AND METHODS

2.1 Materials

2.1.1 Equipment

- Balance Sartorius BP 610 (DWS, USA)
- Gel Doc XR + Molecular Imager system (Bio-Rad, USA)
- Microplate reader Infinite M200 with Absorbance module (Tecan, Switzerland)
- pH meter Basic 20 with combined glass electrode 5209 (Crison, Spain)
- Sigma 1-14 Microfuge (SciQuip, UK)
- Thermal Cycler MyCycler (Bio-Rad, USA)
- Thermal Cycler Tgradient (Biometra, Germany)
- Ultrasonic bath Elmasonic S10H (Elma, Germany)
- UV-Vis Spectrophotometer Nanodrop ND-1000 (Nanodrop Technologies, USA)
- UV-Vis Spectrophotometer UV Mini-1240 (Shimadzu, Germany)
- Wide Mini-Sub Cell GT electrophoresis cell with PowerPac Basic power supply (Bio-Rad, USA)
- 384 well small volume, LoBase Polystyrene microplates, black (Greiner Bio-One, Germany)
- NAP-5 columns (GE Healthcare, Sweden)
- Quartz Absorption Cell – 105.202-QS (Hellma, Germany)

2.1.2 Chemical Reagents

Table 2.1. Chemical Reagents

Reagents	CAS number	Distributor
Agarose	9012-36-6	VWR
Betaine	107-43-7	Sigma-Aldrich
Bromophenol Blue	115-39-9	Merck
Dithiothreitol (DTT)	3483-12-3	Sigma-Aldrich
Ethylenediaminetetraacetic acid (EDTA)	25102-12-9	Merck
Glycerol	56-81-5	Sigma-Aldrich
Gold (III) chloride trihydrate	16961-25-4	Sigma-Aldrich
Hydrochloric acid	7647-01-0	Sigma-Aldrich
Magnesium chloride hexahydrate	7791-18-6	Merck
Nitric acid	7697-37-2	Sigma-Aldrich
Sodium Chloride	7647-14-5	Merck
Sodium phosphate dibasic	10028-24-7	Sigma-Aldrich
Sodium phosphate monobasic monohydrate	10049-21-5	Sigma-Aldrich
Trisodium Citrate	03-04-6132	Merck

2.1.3 Solutions and buffers

Ultrapure sterile water (> 16.2 MΩ.cm) from Merck Millipore Milli-Q system was used to prepare all needed solutions and dilutions.

AGE I

2% SDS

10 mM phosphate buffer (pH 8)

Sterilised by filtration (0.22 µm) and stored at 4 ºC. Warm up to 37 ºC before used.

AGE II

0.01% (w/v) SDS

1.5 M NaCl

10 mM phosphate buffer (pH 8)

Sterilised by filtration (0.22 µm) and stored at 4ºC. Warm up to 37ºC before used.

Aqua Regia

One volume of HNO_3 to three volumes of HCl

Phosphate buffer

According to the desired pH and concentration (from Sambrook and Russel 2001).

Table 2.2. Phosphate buffer (10mM) at different pH values.

pH	Na_2HPO_4 (mL)	NaH_2PO_4 (mL)
7	57.7	42.3
8	93.2	6.8

Sterilised by autoclaving and stored at 4ºC.

TAE Buffer (50x)

2 M Tris-Acetate

0.05 M EDTA

Tris-acetate was made with Tris-Base and Glacial Acetic Acid. The solution was sterilised by autoclaving and stored at room temperature until further use.

2.1.4 Biological Material

2.1.4.1 Biological Reagents

Table 2.3. Biological Reagents

Reagents	Distributor
Betaine (5M)	Sigma-Aldrich
Bst DNA polymerase large fragment (8000U/µL)	New England Biolabs
dNTP mix (10 mM)	Thermoscientific
GelRed ® (10000X)	Fermentas
GeneRuler™ DNA Ladder Mix, ready-to-use	Fermentas
Magnesium chloride (25mM)	Sigma-Aldrich
Oligonucleotides	STAB VIDA, Lda
Thermo Buffer Termopol reaction buffer (10X)	New England Biolabs

2.1.4.2 Molecular Biology Kits

GenElute™ Bacterial Genomic DNA Kit (Sigma-Aldrich, Germany)

2.1.4.3 *Salmonella* strains

Salmonella enterica serovar Typhimurium 14208 was provided by Prof. Luís Jaime Mota, Assitant professor and Member of the Molecular Biology Research group at DCV Department, FCT, UNL.

2.1.4.4 DNA oligonucleotides

All oligonucleotides were acquired from STAB VIDA (Portugal). Non-modified oligonucleotides (LAMP primers and synthetic ssDNA target) were resuspended in sterile milli-Q H_2O to achieve a final concentration of 100 µM and stored at -20ºC. Modified oligonucleotide (*ttrRSBCA* probe) was resuspended in 100 µL of 1 M Dithiothreitol (DTT) and 900 µL of sterile milli-Q H_2O and stored at -20ºC. Sequences and specifications are displayed below.

Table 2.4. DNA oligonucleotides

Designation	Sequence (5' to 3')	Tm (ºC)	%GC	Comments
FIP (F1c) *ttrRSBCA*	AGTCCGTTCAGCGTTTCACGAA	59.2	50.0	Primer
FIP (F2) *ttrRSBCA*	GCTGGCTGGCTATTCTCG	56.0	61.0	Primer
BIP (B2) *ttrRSBCA*	ACCCGTCGTCAGTGGCTAAAAG	59.4	54.5	Primer
BIP (B1c) *ttrRSBCA*	CATCACGGTAGCTCAGACCA	56.5	55.0	Primer
F3 *ttrRSBCA*	CTTACTCGTTACCAGGCGG	55.2	57.9	Primer
B3 *ttrRSBCA*	ACAGGCCATCAATTGCGC	56.8	55.6	Primer
ttrRSBCA target	GCTCAGACCAAAAGTGACCATCCCACCGACGGCGAGACCG	-	62.5	Synthetic
ttrRSBCA probe	Thiol - GGTCTCGCCGTCGGTGG	-	76.5	Probe

2.2 Methods

2.2.1 Molecular Biology

2.2.1.1 Genomic DNA extraction from *Salmonella*

Genomic DNA was extracted at Prof. Luís Jaime Mota Laboratory, Assitant professor and Member of the Molecular Biology Research group at DCV Department, FCT, UNL, who gently provided *Salmonella enterica* serovar Typhimurium 14208 strain and a Genomic DNA extraction kit. Firstly, a liquid culture of the provided strain was let to grow overnight at 25 ºC, then genomic DNA was extracted using GenElute ™ Bacterial Genomic DNA Kit from Sigma-Aldrich as described below.

1. Bacterial cells were harvested in a microcentrifuge in tubes of 1.5 mL by centrifugation at 14,000 × g for 2 minutes. The supernatant was discarded.
2. Cell pellets were re-suspended thoroughly in 180 µl Lysis Solution T and 20 µL of RNase A solution were added. Then all components were mixed and incubated for 2 minutes at room temperature.
3. Proteinase K solution (20µL) was added and mixed by vortexing. After 30 minutes' incubation at 55 ºC, 200 µL of Lysis Solution C were added, followed by thorough vortexing and incubation for 10 minutes at 55 ºC.
4. In order to prepare the GenElute Miniprep binding Column, 500 µL of the Column Preparation Solution were added to the column and centrifuged at 12,000xg for 1 minute. The eluate was discarded.
5. In order to prepare the lysate for binding, 200 µL of ethanol (95-100%) were added to the lysate and mixed thoroughly by vortex for 10 seconds. A homogeneous mixture was obtained.
6. Using a wide bore pipette, the entire contents of the tube were transferred into the binding column and centrifuged at 6,500 x g for 1 minute. The collection tube containing the eluate was discarded and the column was placed in a new 2 mL collection tube.
7. After addition of Wash solution 1 to the column, a centrifugation ate 6,500 x g was carried out for 1 minute. The collection tube containing the eluate was discarded again and the column was placed in a new 2 mL collection tube.
8. The column was filled with 500 µL of Wash Solution and followed by centrifugation for 3 minutes at maximum speed to dry the column. The collection tube containing the eluate was discarded and the column was placed in a new 2 mL collection tube. **Note:** In order to execute step 9 (DNA elution), the column must be free of ethanol. After the centrifugation there was still residual ethanol in the column, thus an additional centrifugation of 20 minutes was carried out.
9. Centrifugation was carried out for 1 minute at 6,500 x g after pipetting 200 µL of the Elution Solution onto the centre of the column and incubation for 5 minutes at room temperature.

10. In order to improve the DNA yield, a second elution was performed by repeating step 9 with an additional 200 µL of Elution Solution and eluting into a new 2mL collection tube.
11. The obtained DNA was quantified by UV-Vis spectroscopy with help of NanoDrop and stored at -20ºC.

2.2.1.2 Target amplification by Loop-mediated isothermal amplification (LAMP)

2.2.1.2.1 Reaction mixture

LAMP amplification was carried out in a total 25 µL reaction mixture containing two inner primers (0.8 µM FIP and 0.8 µM BIP) and two outer primers (0.2 µM F3 and 0. 2 µM B3), 400 µM of dNTP mixture, 5 M Betaine, 25 mM $MgCl_2$,1 µL (8U) of *Bst* DNA polymerase and 30 ng of double-stranded target DNA.

2.2.1.2.2 Reaction Program

1. Reaction mix was briefly vortexed, mixed and distributed to 0.2 mL microtube;
2. 30 ng of previously extracted DNA (See subsection **2.2.1.1**.) was added to 0.2 mL microtube;
3. The mixture was heated at 95ºC for 5 minutes and then chilled on ice for 1 minute;
4. *Bst* DNA polymerase was added to the mixture and incubated at 65ºC for 45 minutes.
5. The mixture was heated at 80ºC for 10 minutes in order to terminate the reaction.

2.2.1.3 Target amplification by Polymerase Chain Reaction (PCR)

2.2.1.3.1 Reaction mixture

PCR amplification was carried out in a total 50 µL reaction mixture containing two primers (0. 4 µM F3 and 0. 4 µM B3), 200 µM of dNTP mixture, 1 µL (5U) of *Bst* DNA polymerase and 30 ng of double-stranded target DNA.

2.2.1.3.2 Reaction Program

1. Reaction mix was briefly vortexed, mixed and distributed to 0.2 mL microtube;
2. 30 ng of previously extracted DNA (See subsection **2.2.1.1.**) was added to 0.2 mL microtube;
3. Reaction was briefly mixed and vortexed and incubated in the thermocycler for amplification reaction. Several steps were followed: Pre-Denaturation (1 min 95°C); Denaturation (30s 95°C); Annealing (30 s 60°C); Extension (30s 72°C) and 4°C. Denaturation, annealing and extension were repeated for 33 cycles.

2.2.1.4 Digestion with *AluI* restriction enzyme

1. 1 Unit of Alu*I* was mixed with the respective Buffer and 100 ng of Loop-mediated isothermal amplification product and fulfilled with H_2O to a final volume of 50 µL.
2. Mixture was incubated for 1 hour at 37 °C. Digestion was confirmed by electrophoretic analysis in 2% agarose gel.

2.2.2 Nanotechnology

2.2.2.1 Synthesis of Gold Nanoparticles (adapted from Lee & Meisel, 1982)

1. All glassware was previously immersed in Acqua Regia for 2 hours.
2. Glassware was vigorously washed with Mili-Q water (18.2 $M\Omega.cm^{-1}$ at 25ºC).
3. Using a 500 mL round bottom flask with a condenser, 250 mL of a 1 mM $HAuCl_4$ solution were boiled with vigorous stirring.
4. While in reflux 25 mL of 38.8 mM sodium citrate were quickly added and, upon verifying the subsequent colour change, both heat and stirring were maintained for 15 minutes.
5. After 15 minutes, the heat was turned off and stirring kept for an additional 20 minutes. The solution was then stored in the dark at room temperature overnight.
6. Characterisation of the AuNPs was performed by UV-Vis spectroscopy, Transmission Electron Microscopy (TEM) and Dynamic Light Scattering (DLS).

2.2.2.2 Synthesis of Gold nanoprobes

2.2.2.2.1 AuNPs functionalisation (Salt-Aging Method)

1. One volume of thiol-modified oligonucleotide was extracted with two volumes of ethyl acetate.
2. The organic phase was discarded after centrifuging for 5 minutes at 21,460 g.
3. Two more extractions were performed repeating steps 1 and 2.
4. The remaining aqueous phase was further purified through a desalting NAP-5 column, accordingly to manufacturer's instructions, using 3 volumes of phosphate buffer 10 mM (pH 8) as eluent.
5. After three extractions complete, the aqueous phase was loaded into the column for the thiol-modified oligonucleotide to adsorb to the resin.
6. When adsorption was complete and the first fraction washed out, the adsorbed thiol-modified oligonucleotide was eluted with 1 mL of phosphate buffer 10 mM (pH 8.0), collected and immediately placed into ice.
7. The purified thiol-modified oligonucleotide was quantified by UV/Vis spectroscopy using NanoDrop, to assess OD_{260} and ensure no traces of DTT were still on solution.
8. In a polypropylene 25 mL vial with a conical skirted base, the purified thiol-modified oligonucleotide was mixed with a ~15 nM AuNPs solution in a theoretical ratio of 1:200 (AuNP:oligos).

9. AGE I solution was then added to achieve a final concentration of 10 mM phosphate buffer, 0.01% (w/v) SDS. The solution vial was then submersed in an ultrasound bath for10 seconds and let to rest at room temperature for 20 minutes.
10. After 20 minutes, the salt-aging procedure began. AGEII solution was added, to reach a final NaCl concentration of 0.05 M. The solution was sonicated for 10 s and incubated for 20 minutes at room temperature.
11. After 20 minutes, AGE II solution was added again in order to reach a final NaCl concentration of 0.1 M. The solution was sonicated for 10 s and let to rest at room temperature for 20 minutes before the next increment.
12. After 20 minutes, final NaCl concentration was raised to 0.2 M with the addition of AGE II solution. The solution was sonicated for 10 s and incubated for 20 minutes at room temperature.
13. After 20 minutes, final NaCl concentration was raised to 0.3 M. The solution was sonicated for 10 s and let to rest at room temperature for 16h period.
14. The functionalised AuNPs were distributed in 1.5 mL tubes and centrifuged at 21,460 g for 20 min.
15. The supernatant was discarded and the resulting oily pellet was washed twice with 10 mM phosphate buffer pH 8 and once with 10 mM phosphate buffer pH 8 0.1M NaCl in the conditions of step 13.
16. The resulting pallets were than mixed and the nanoprobe solution was analysed via UV-Vis spectrophotometry to determine its concentration by the Lambert–Beer law assuming a calculated molar absorptivity for the SPR peak (525 nm) of 2.33×10^{8} M^{-1} cm^{-1} (Baptista et al., 2005).
17. By diluting the resulting functionalised AuNPs solution (stock solution) with 10mM phosphate buffer pH 8 0.1M NaCl a final concentration of 15 nM was obtained and the colloidal solution was stored in the dark at 4ºC.

2.2.2.2.2 Nanoprobes Stability Assays

1. A solution containing 15 nM Au-nanoprobe (Au-nanoprobe final concentration of 2.5 nM) and 10 mM phosphate buffer pH 8 + 0,1M NaCl alone was prepared by heating for 5 minutes at 95ºC and cool down for 10 minutes at room temperature. **NOTE:** Other solutions of phosphate buffer (pH8, pH7 + 0.1M NaCl, pH7) were also tested during optimisation.
2. The solution was mixed with increasing concentrations of $MgCl_2$ solution to a total volume of 30 µL.
3. The solutions were transferred to microplate wells and UV-visible spectroscopic measurements were registered 5 minutes after salt addition in a microplate reader. **NOTE:** Some measurements were also registered after 10 and 15 minutes.

2.2.2.2.3 Non-cross-linking Detection Assays

1. Assay solutions containing the Au-nanoprobes and target DNA were prepared by mixing the appropriate DNA sample with the Au-nanoprobe solution (final concentration 2.5 nM), and by using 10 mM phosphate buffer pH 8 +0,1M NaCl to fulfil the 30 µL final volume. A blank solution was prepared by replacing the DNA for an equivalent volume of 10 mM phosphate buffer pH 8.
2. The solutions were heated for 10 min at 95ºC and then allowed to cool down for 20 minutes at 24 ºC.
3. The solutions were mixed with a specific concentration of MgCl2 solution to fulfil a total volume of 30 µL (Au-nanoprobe final concentration of 2.5 nM).
4. The solutions were transferred to microplate wells and UV-visible spectroscopic measurements were registered 15 minutes after salt addition in a microplate reader.

2.2.2.3 UV-Vis Analysis

The behaviour of the synthesised colloidal gold solution was analysed from 400 to 800 nm, on a 1240 UV-Mini spectrophotometer from Shimadzu (Japan). After dilution of an aliquot of the AuNPs solution, the concentration was determined by the Lambert–Beer law assuming a molar absorptivity for the SPR peak (525 nm) of $2.33\times108\ M^{-1}\ cm^{-1}$ (Baptista et al., 2005).

2.2.2.4 TEM Analysis

Samples of AuNPs were analised by TEM at the Microlab, Instituto Superior Técnico facilities in Lisbon, Portugal. First, 10µL of the prepared colloidal suspensions were deposited in carbon copper grids, then were washed twice with10 µL of Mili-Q water and, finally, air dried. TEM was performed with a HITACHI H-8100 microscope operated at 200 kV. Particles size and shape were determined by analysing the TEM pictures using the imaging software ImageJ.

2.2.2.5 DLS Analysis

The hydrodynamic diameter of AuNPs was determined by DLS, at REQUIMTE, Departamento de Química, Faculdade de Ciências e Tecnologias, UNL. Analysis was carried out on a SZ-100 Nanoparticle Analyzer from Horiba Scientific (Japan), at a temperature of 25 °C a scattering angle of 90 °C. An aliquot of colloidal gold solution was diluted to reach a final concentration of ≈ 2 nM. Samples of 60 µL were measured after stabilization for 5 minutes.

3 RESULTS AND DISCUSSION

3.1 Design and characterization of *ttrRSBCA* target, probe and primers

3.1.1 Target selection

Salmonella infection represents a considerable global burden, with significant health and economic impacts (Kokkinos et al., 2014). Sensitive and rapid detection methods for *Salmonella* in food are required. Many detection methods have been developed in recent years(Lee et al., 2015). Molecular methods designed for targeting *Salmonella* DNA have focused on genes such as *Salmonella* invasion gene *(invA), fimC, phoP* and other genome markers (Kokkinos et al., 2014). The use of some of these genes as target can be disadvantageous since some of them might be localised in regions which sometimes suffer from deletion. Genes *inv, spa* and *hil* from *Salmonella* pathogenicity island 1 are examples of these cases(Malorny et al., 2004). Considering this and the commercial interests of BIOPREMIER, *ttrRSBCA* locus, which was first used for *Salmonella* detection by Malorny and co-workers (Malorny et al., 2004), was the selected region for this study. Since this locus is responsible for tetrathionate respiration, it has great significance in *Salmonella* spp life cycle (Malorny et al., 2004). Thus, *ttr* genes should be genetically stable in all *Salmonella* strains, making this colorimetric test more reliable. This hypothesis was confirmed by alignment of 103 strains of *Salmonella* from GenBank by BioEdit software with the published DNA sequence of *S.enterica* serotype Typhimurium *ttr* locus (GenBank accession no. AF282268) and the part of this region shared by all the aligned sequences was used as target in this study (**Figure A2 Appendix**). This region has 232 bp, which is a length included in the range of target sizes (130-200 pb) where the best results were obtained in previous studies. The size of target DNA is an important factor that LAMP efficiency depends on, because the rate limiting step for amplification is strand displacement DNA synthesis(Saleh, 2009).

The primers and probe designed for the assay anneal in a highly conserved region of the *Salmonella*-specific *ttr* locus (**Figure 3.1**). It consists of five genes organised as an operon. The genes *ttrA*, *ttrB*, and *ttrC* encode the tetrathionate reductase structural proteins, and the *ttrS* and *ttrR* genes encode the sensor and response regulator components of a two-component regulatory system (Hensel et al., 1999).

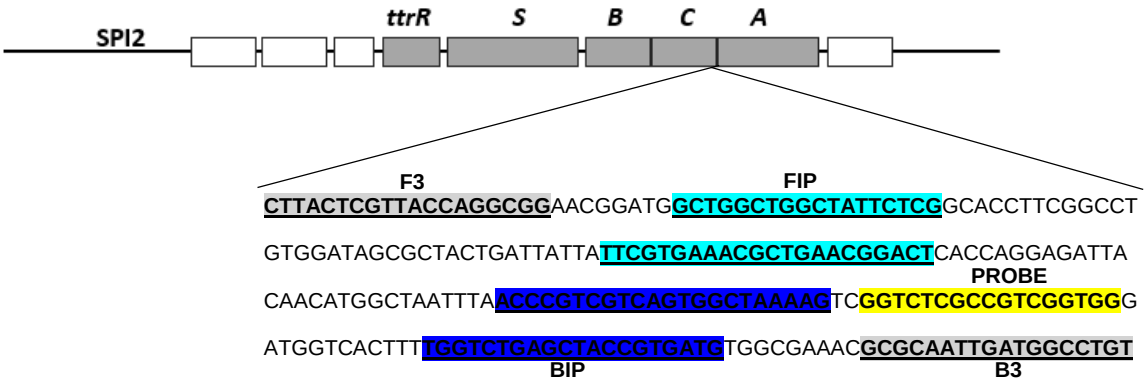

Figure 3.1 Schematic map of the *ttr* locus adjacent to the *Salmonella* Pathogenicity Island 2 (SPI2). Primers and probe location within the sequence region developed for LAMP assay for detection of Salmonella. F3 and B3 primers are represented in grey. FIP primer appears in light blue and BIP primer in dark blue. Probe is represented in yellow.

3.1.2 Primers and Probe Design

Based on the alignment and the target selected previously, LAMP primers were designed using primer explorer v4 software. Several primers set were appraised, with the most effective set selected to this study. The size and sequence of the primers were chosen so that their melting temperature (T_m) was between 60-65 °C, the optimal temperature for *Bst* polymerase. The F1c and B1c T_m values should be a little higher than those of F2 and B2 to form the looped out structure (**Table 5 section 2.1.4 Materials and Methods**). The T_m values of the outer primers F3 and B3 have to be lower than those of F2 and B2 to assure that the inner primers start synthesis earlier than the outer primers (Notomi et al., 2000).

After selection of the target, a probe was designed for *ttrRSBCA* locus. In this design, several criteria were considered. Probe length is an important factor. Since longer probes will result in longer hybridisation times and low synthesis yields and shorter probes will lack specificity, this probe was designed with a length of 17 bases. Base composition has also an effect in the probe behaviour. In order to decrease the probability of occurrence of nonspecific hybridisation, a composition of 40-60% G-C must be guaranteed. In this case, the probe has ~70% GC, which may influence the hybridisation efficiency, factor that will be discussed after. It should also be guaranteed that no complementary regions are present within the probe, which could result in the formation of “hairpin” structures that would inhibit hybridisation to target. Therefore, gold nanoprobe structure was theoretically studied at different temperatures. 4°C and 25°C were selected as they correspond to the storage temperature and laboratory temperature, respectively. Since at these temperatures it was observed hairpin structure formation by the nanoprobe, higher temperatures were tried (**Figure 3.2**). It was observed no formation of hairpin at 57° C. Therefore, this condition was chosen to make the synthesis of the last two batches of the gold nanoprobe. On the other hand, 25°C was the temperature used to synthesize the first two batches. This difference of synthesis conditions would influence probe hybridisation in parallel to the used pH values. These issues will be discussed in the next sections in more detail.

Even though gold nanoprobes are stored at 4°C and at this temperature it may be formed a loop structure, when the hybridisation and stability tests are performed the first step is boil at 95°C (**sections 2.2.2.2.2 and 2.2.2.2.3**) which ensures the opening of the DNA chain and the exposure of DNA bases to the target.

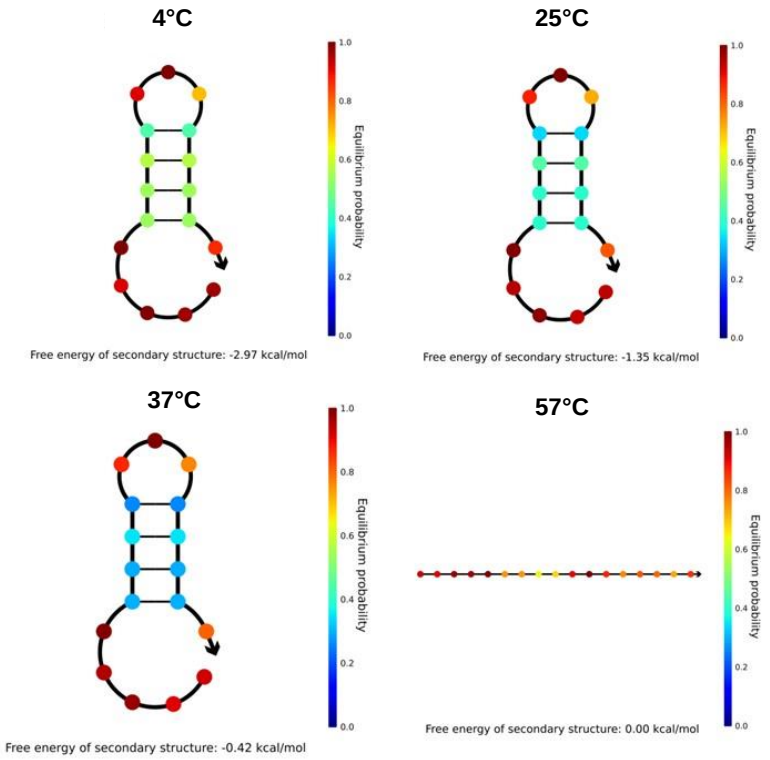

Figure 3.2 Study of *ttrRSBCA* gold nanoprobe behaviour at different temperatures. The coloured band at the right side of each picture represents the probability of equilibrium from lower (blue) to higher probability (red). Considering this scale 57°C was the selected temperature.

It is more important to ensure gold nanoprobe stability in its synthesis than in its storage conditions. If the nanoprobe is produced in conditions that favour its instability, it will be more likely to lose the oligonucleotides at the surface and aggregate, leading to trouble in hybridisation. This phenomenon is affected by the differences in nucleotide affinity, which can result in variations in the reactivity of thiolated DNA oligonucleotides to AuNPs. A- and C-containing oligonucleotides have a higher affinity for AuNPs than the G- and T-containing. Since the synthesized gold nanoprobe has only 4 C bases in its structure and no A bases, it may lead to non-specific adsorption(Brown et al., 2008). It might result in lower coverage ratio and inhibit proper reaction of the thiol with the AuNP surface, leading to the decrease of the extent of hybridisation (Brown et al., 2008).

3.2 LAMP - Loop Isothermal Mediated Amplification

After the previously described *in silico* tests in order to design probe and primers with the ideal characteristics to detect the intended target, LAMP amplification assays were performed.

LAMP amplified products were then analysed using 1% agarose gel electrophoresis. In **Figure 3.3A** it is observed, as expected, a banding pattern characteristic of the presence of mixtures of many different sizes of stem-loop DNA products. In this gel one can also observe the existence of a smear, which may be related to the reaction temperature or LAMP reaction components. Maybe the reaction temperature used was too low for the primers annealing, causing a non-specific binding to the template or the thermocycler ramping is too slow, leading to spurious annealing and to its non-specificity. On the other hand, the dNTPs, water or the used primers may contain impurities, leading to non-specific amplification. The template concentration might also be too high, inhibiting *Bst* polymerase due to inefficient denaturation time. Increase denaturation time or reduce the template concentration would be considerable hypotheses since LAMP technique is very sensitive and specific, having the capability of synthesizing a large amount of DNA (10-20µg/25µl) from an infinitesimal quantity of template(Chen et al., 2011).

Figure 3.3B shows the same results as **Figure 3.3A**, except that the negative controls show a banding pattern with an intensity similar to the positive sample, indicating that the non-specific amplification was as intense as the target DNA amplification.

Assuming that the false positives were due to a reagent/ carry-over contamination of a positive sample, all the reagents were freshly prepared. Strict precautions were made to avoid any possible contamination. Separate working areas and pipettes with filtered pipette tips were used for each step of the reaction procedure. The bench tops and pipettes were thoroughly disinfected with 70% ethanol, before and after setting up the reaction. However, none of these safety measures reduced the non-specific amplification in the negative control.

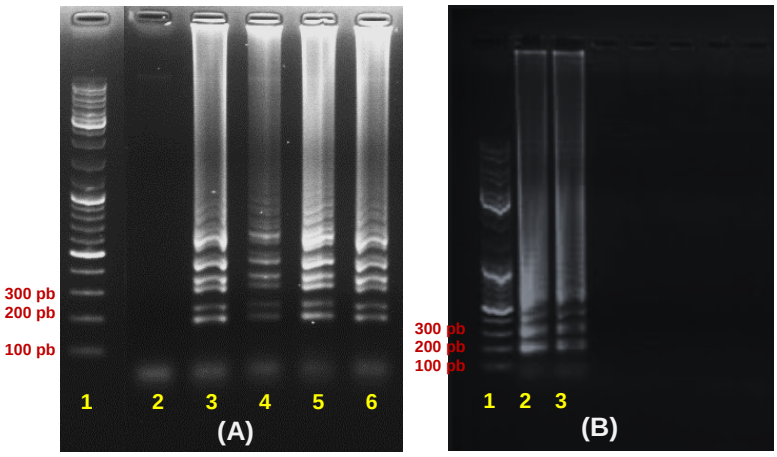

Figure 3.3 Agarose gel 1% electrophoresis in 100 mL TAE 1x + 15µL of gel red (85 V 70 min) of amplification products of *ttrRSBCA* locus from *Salmonella.* (A) 1 – Gene Ruler DNA Ladder; 2 - Negative control of LAMP amplification reaction where is evident the absence of non-specific amplification; 3,4,5,6- LAMP product at 65ºC for 45 minutes; **(B)** 1 – Gene ruler DNA ladder; 2 - Negative control of LAMP amplification reaction where non-specific amplification is present; 3- LAMP product at 65ºC for 45 minutes.

Non-specific amplification and false positive occurrence has been reported previously in LAMP technique (Senarath et al., 2014; Wang et al., 2015).

Several hypotheses may explain the non-specific amplification/ contamination visualised in the Negative control of LAMP reaction. It can be caused by *Salmonella* or by other species which belong to the *Enterobacteriaceae* family such as *Shigella* and *E. coli (***Figure 3.4**).

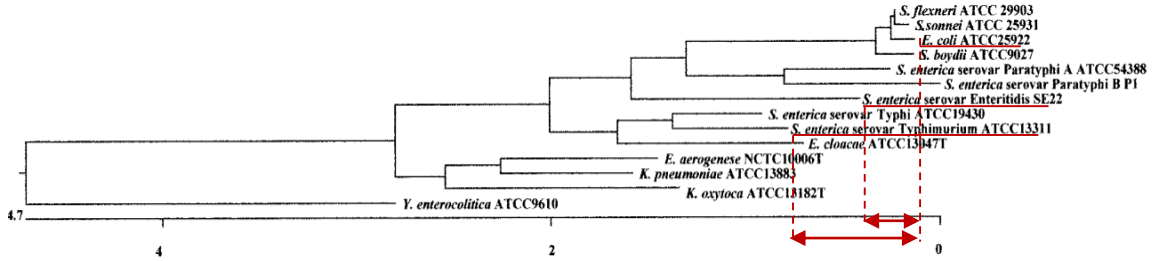

Figure 3.4 Phylogenetic tree based on the nucleotide sequences of 16S rRNA genes. The scale indicates the percentage of base difference (percent divergence). The phylogenetic analysis includes the following strains: *E. coli* (ATCC 25922), *S. enterica serovar Enteritidis* (SE22), *S. enterica serovar Paratyphi* A (ATCC 54388), *S. enterica serovar Paratyphi B,* S. *enterica serovar Typhi* (ATCC 19430), *S. enterica serovar Typhimurium* (ATCC 13311), *S. boydii* (ATCC 9027), *S. flexneri* (ATCC 29903), *S. sonnei* (ATCC 25931), *Y. enterocolitica* (ATCC 9610), *E. aerogenes* (NCTC10006T), *E. cloacae* (ATCC 13047T), *K. oxytoca* (ATCC 13182T), and *K. pneumoniae* (ATCC 13883) (Fukushima et al. 2002). *Salmonella* serovars, namely *S. Enteritidis* and *S. Typhimurium*, and *E. coli* have a divergence value below 1% which is highlighted by red arrows.

In the phylogenetic tree represented above *Salmonella* species strains were grouped into two clusters. The first cluster contained *S. enterica* serovar Paratyphi A, *S. enterica* serovar Paratyphi B, and *S. enterica* serovar Enteritidis, while the second cluster contained *S. enterica* serovar Typhi and *S. enterica* serovar Typhimurium. It can be observed that the percent divergence between the represented species is very low, namely between two of the most prominent *Salmonella* serotypes associated with human infection (*S. Enteritidis* and *S. Typhimurium*) and *E. coli* is below 1%.

E. coli can cause severe illness in humans with very low infectious doses and its symptoms in humans are similar to that caused by *Salmonella* infection (Ge & Meng, 2009). Considering that these species are closely related and possess the highly conserved 16S rRNA region, the genetic distance for this gene was analysed by Fukushima and co-workers(Fukushima et al., 2002) (**Table 3.1**).

Table 3.1 16S rRNA gene sequence similarity and divergence of each pair for *E. coli, Salmonella, Shigella, Enterobacter, Klebsiella,* and *Yersinia.* The red table highlights the similarity between *E. coli* and *Salmonella* strains (Fukushima et al. 2002).

Strain no.	Strain name	% Similarity with strain no.													
		1	2	3	4	5	6	7	8	9	10	11	12	13	14
1	*E. coli* ATCC 25922		99.6	97.4	97.2	96.5	95.4	99.6	99.9	99.8	95.0	95.9	95.4	95.1	93.0
2	*S. enterica* serovar Enteritidis ES22	2.6		97.6	97.4	97.4	97.1	96.7	96.9	96.9	95.1	96.9	95.1	95.5	91.6
3	*S. enterica* serovar Paratyphi A ATCC 54388	2.3	2.3		98.6	97.6	96.7	97.5	97.4	97.3	94.6	96.2	94.8	94.8	91.5
4	*S. enterica* serovar Paratyphi B P1	2.5	2.6	1.3		97.1	96.3	97.2	97.2	97.1	94.5	96.1	94.5	94.6	91.3
5	*S. enterica* serovar Typhi ATCC 19430	3.4	2.3	2.1	2.6		97.8	96.8	96.7	96.6	95.6	97.4	95.7	95.9	92.0
6	*S. enterica* serovar Typhimurium ATCC 13311	3.4	2.1	2.4	2.9	1.1		95.4	95.4	95.3	95.0	96.6	95.3	95.4	91.1
7	*S. boydii* ATCC 9207	0.4	2.8	2.1	2.4	3.1	3.4		99.7	99.7	94.6	95.5	95.1	94.7	92.8
8	*S. flexneri* ATCC 29903	0.1	2.6	2.2	2.4	3.3	3.4	0.3		99.9	94.9	95.7	95.3	95.0	93.0
9	*S. sonnei* ATCC 25931	0.2	2.6	2.3	2.5	3.4	3.4	0.3	0.1		94.8	95.6	95.1	94.8	93.0
10	*E. aerogenes* NCTC10006T	4.0	4.2	4.8	5.0	3.4	3.6	4.3	4.0	4.1		97.5	97.8	98.1	93.2
11	*E. cloacae* ATCC 13047T	3.3	2.6	3.1	3.4	1.6	1.9	3.6	3.3	3.4	2.2		97.2	98.3	92.1
12	*K. oxytoca* ATCC 13182T	3.8	4.4	4.8	5.1	3.4	3.4	3.9	3.8	3.9	1.8	2.6		97.4	92.3
13	*K. pneumoniae* ATCC 13883	4.0	3.9	4.5	4.8	3.1	3.1	4.2	4.0	4.0	1.5	1.5	2.6		93.0
14	*Y. enterocolitica* ATCC 9610	5.6	6.7	6.9	7.1	6.8	6.6	5.9	5.6	5.7	4.4	6.2	5.7	4.9	

In this table, one can observe that *E. coli* presents approximately 96% of similarity to the several *Salmonella* serotypes, which may explain the non-specific amplification obtained in the negative control. Since they have this high degree of similarity the LAMP primers could anneal and amplify *E. coli*.

It should be considered that LAMP reactions took place in a lab where cloning is often performed in *E. coli*., which is a technique also performed in this organism in other laboratories of our department. This may lead to aerosol generation which can easily affect LAMP due to its sensitivity, resulting in false positive samples.

In order to check this hypothesis, an alignment between LAMP primers and this region was performed (**Figure A3 Appendix**). Even though the annealing observed between these sequences presents low values, it must be considered that LAMP is a very sensitive technique because it occurs in the presence of 4 primers, which anneal to 6 regions of the target. Thus, even there is a low number of bases annealing to this region, amplification still may occur.

To confirm what was being amplified in negative control in the absence of target DNA, LAMP amplified products were subjected to restriction enzyme followed by agarose gel electrophoresis analysis. In this process, it was used enzyme *AluI* which contains its recognition site within the region being amplified (**Figure 3.5**).

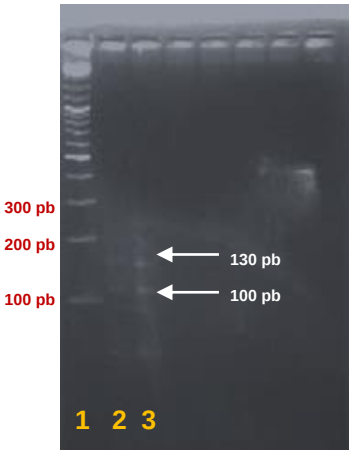

Figure 3.5 Agarose gel 2% electrophoresis in 50 mL TAE 1x + 10µL of gel red (60 V 100 min) of LAMP amplification products of *ttrRSBCA* locus from *Salmonella* digested by *AluI* enzyme. 1) Gene Ruler DNA Ladder; 2) Digestion of negative control from LAMP Amplification reaction; 3) Digestion of positive control from LAMP amplification reaction. As a result, 2 bands of 100pb and 130pb can be observed.

The results of restriction digestion of the LAMP amplified products with *AluI* enzyme yielded the expected fragments of 100 pb and ~ 130 pb indicating the specific amplification of the target *ttrRSBCA* locus sequence by LAMP (**Figure A4 Appendix**). These results were shared by negative and positive controls of the reaction. It suggests that the non-specific amplification presented in the negative controls is from *Salmonella,* caused possibly by open-tube procedures after amplification such as gel electrophoresis. Therefore, amplified DNA products from previous LAMP reactions may generate aerosols or contaminate laboratory material (for example tubes) and become templates for re-amplification that lead to false positive results (Hu et al., 2015; Tomita et al., 2008).

Currently, there is no effective means for eliminating LAMP carryover contamination. Recently, Hsieh and co-workers reported the integration of LAMP amplification with uracil-DNA-glycosylase (UDG) digestion to eliminate false-positive results arising from carryover contaminants (Hsieh et al., 2014).

On the other hand, a cause of this amplification in negative control can be the self-amplification of primers as described by Wang and co-workers (Wang et al., 2015). Considering this possibility, different variables were tested.

DMSO is an agent that binds to DNA at cytosine residue, changing its conformation and making the DNA molecule more labile for heat denaturation. As a result, DNA chain will be more exposed and the formation of secondary structures is less likely to happen (Lv et al., 2015). It will also interfere in self- complementary of primers, which is expected to facilitate their annealing to the template (Lv et al., 2015; Chakrabarti & Schutt, 2001). Therefore, DMSO was added to the reaction in different concentrations. The applied gradient is represented below (**Figure 3.6**).

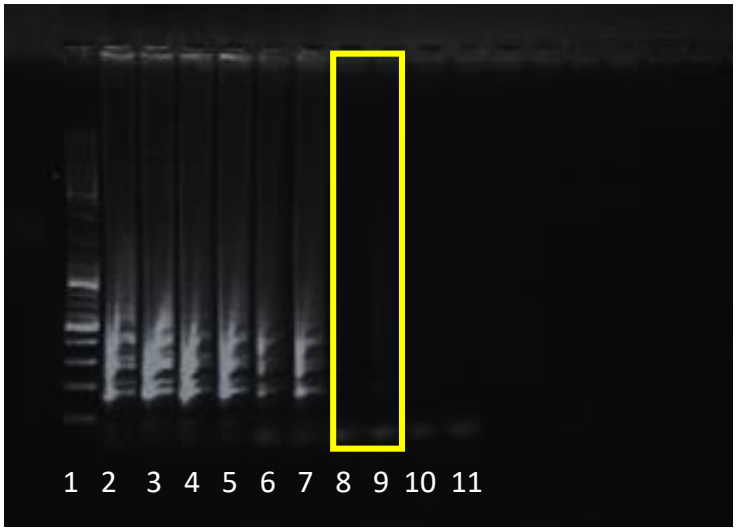

Figure 3.6 Agarose gel 1% electrophoresis in 100 mL TAE 1x +15µL of gel red (85 V 70 min) of optimisation of LAMP amplification of *ttrRSBCA* locus from *Salmonella*. 1) Gene Ruler DNA Ladder; **2) 0 % DMSO:** negative control (no DNA template added); **3) 0 % DMSO:** positive control; **4) 1% DMSO**: negative control (no DNA template added); **5) 1% DMSO**: positive control; **6) 2,5% DMSO**: negative control (no DNA template added); **7) 2,5% DMSO**: positive control; **8) 5 % DMSO**: negative control (no DNA template added); **9) 5 % DMSO**: positive control; **10) 7,5 % DMSO:** negative control (no DNA template added); **11**)**7,5% DMSO**: positive control.

In fact, as observed in **Figure 3.6**, the use of 5% DMSO increased the specificity of the reaction. Even though in this percentage the yield of the reaction is decreased in comparison to values below 5% DMSO, it is observed an amplification in control positive without unspecific amplification in negative control. Thus, the purpose of this gradient was achieved.

In order to optimize this condition, an evaluation of different amplification temperatures (65ºC to 69ºC), the reaction time (30, 45, 60, 90 min) and the ratio of outer and inner primers (1:1 to 1:12) were carried out (**Figure 3.7**).

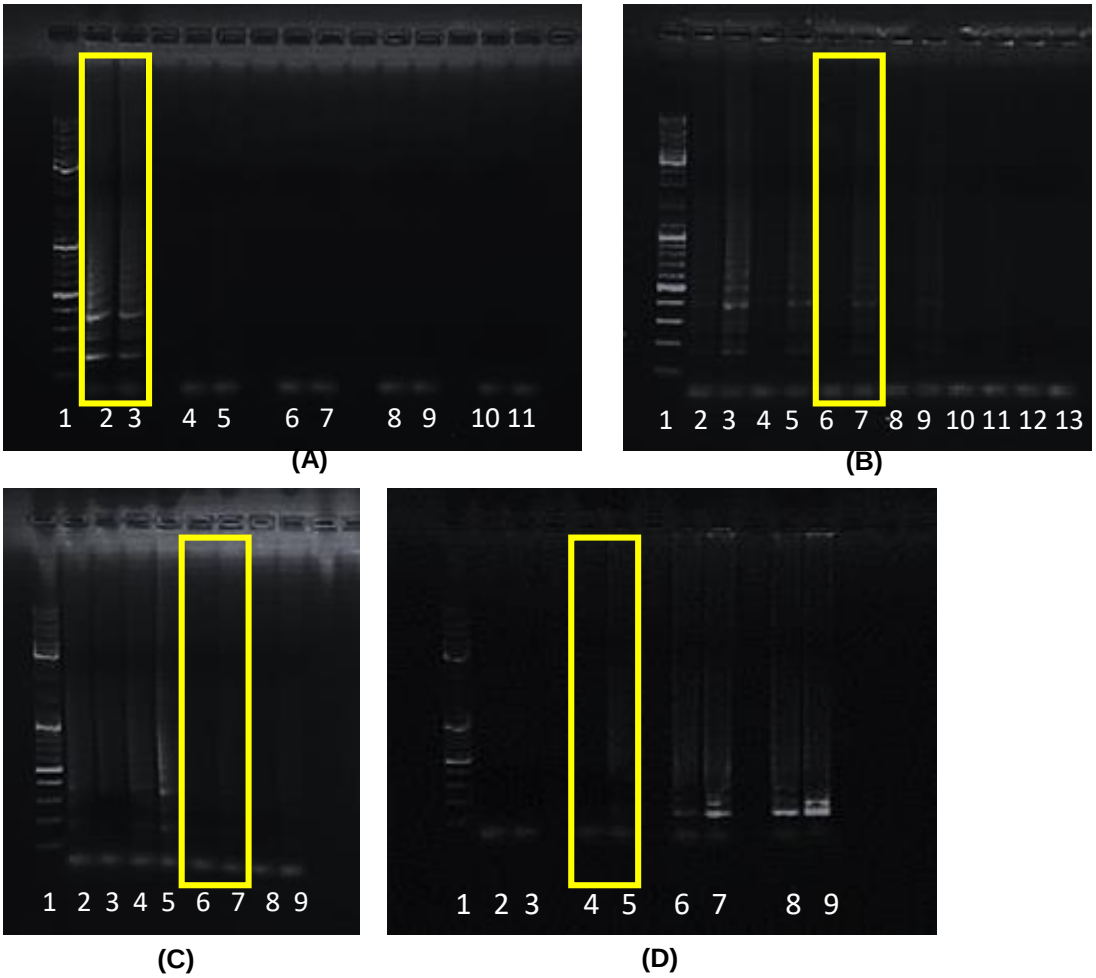

Figure 3.7 Agarose gel electrophoresis in 100 mL TAE 1x +15µL of gel red (85 V 70 min) of optimisation of LAMP amplification of *ttrRSBCA* locus from *Salmonella*. A) The effect of temperature:1) Gene Ruler DNA Ladder; **2) 65 °C:** negative control; **3) 65°C:** positive control; **4) 66°C:** negative control; **5) 66°C**: positive control**; 6) 67°C**: negative control; **7) 67°C**: positive control; **8) 68°C**: negative control; **9) 68°C**: positive control; **10) 69ºC:** negative control**; 11) 69°C:** positive control; **B**) **The effect of temperature: 1)** Gene Ruler DNA Ladder; **2) 65 °C**: negative control; **3) 65 °C:** positive control; **4) 65.2 °C:** negative control;**5) 65.2 °C:** positive control; **6) 65.4 °C**: negative control; **7) 65.4 °C**: positive control; **8) 65.8 ºC:** negative control; **9) 65.8 ºC:** positive control **C**) **The effect of the ratio of outer and inner primers: 1)** Gene Ruler DNA Ladder; **2) 1:3**: negative control; **3) 1:3** positive control; **4) 1:4:** negative control; **5) 1:4**: positive control; **6) 1:8**: negative control; **7)1:8**: positive control; **1:12**: negative control; **1:12**: positive control; **D) The effect of reaction time**: **1)** Gene Ruler DNA Ladder; **2) 30 minutes**: negative control; **3) 30 minutes**: positive control; **4) 45 minutes**: negative control; **5) 45 minutes**: positive control; **6) 60 minutes**: negative control; **7) 60 minutes**: positive control; **8) 90 minutes:** negative control; **9) 90 minutes:** positive control.

Annealing temperature is an important requirement in LAMP. It is based on the melting temperature of the primer-template pair and is affected by the other reagents of the reaction and concentration of primers and the template. Therefore, it is difficult to find the right annealing temperature for a given primer/ template combination. Too low annealing temperatures can lead to primer-dimer formation and non-specific products (Rychlik et al., 1991). To avoid this result, an increasing gradient of temperatures was performed (**Figure 3.7 A**).

It was observed that at higher temperatures the yield reduced, possibly due to poor primer annealing (Rychlik et al., 1991). On the other hand, it favours only the accumulation of

amplicons whose primer-template complementarity is the highest. 65ºC was the selected temperature as it was the only condition where the amplification was visible, but it was present in both controls. In order to eliminate the unspecific amplification on negative control, a new temperature gradient between 65 and 66 ºC was tried (**Figure 3.7 B**). 65.4ºC was found as the ideal temperature.

Then, primer ratios ranging from 1:3 to 1:12 were tested. Although a more distinct pattern was shown when the ratio was above 1:8, 1:8 is the condition that eliminates the non-specific amplification in negative control. Since outer primers are present in lower concentration than in the previous reactions (**Figure 3.7 C**), they are less likely to form self-dimer.

Finally, as the aim of this thesis was the development of a rapid test for *Salmonella* detection, different times of reaction were performed. The results proved that amplification in positive control in the absence of negative control amplification are only observed in 45 minutes of reaction (**Figure 3.7 D**). At higher reaction times this condition is not witnessed, although there was obtained a higher yield. Higher time of reaction possibly facilitates the occurrence of unspecific amplifications since primer self-assembly will be more likely to happen. Or, if there is an infinitesimal amount of template DNA in the negative control of the reaction it is more likely to be amplified.

Taken together, the optimal conditions for the LAMP assay were determined to 65.4ºC for 45 minutes with 5% DMSO and 1:8 primers ratio (**Figure 3.7D**). The initial conditions of the other reagents were maintained.

The positive LAMP reaction generated a laddering pattern with a set of bands of different sizes consisting of several inverted-repeat structure. Even though it was obtained a low yield or even when no amplification is observed in the gel it is not synonym of no occurrence of the reaction. It is necessary to take into account the detection limit of gel red added to the agarose gel. Moreover, despite the importance of LAMP amplification technique, the crucial part of this project relies on the development of a gold nanoprobe, which is responsible for the sensitivity and specificity of the test. Therefore, the next step was the synthesis and characterization of gold nanoprobes.

3.2.1 Synthesis and characterisation of gold nanoprobes

The aim of this project was the development of a colorimetric test based on gold nanoprobes for detection of specific DNA sequences from *Salmonella*. Similar non-cross linking approaches for the detection of pathogens described the use of citrate gold nanoparticles of 14 nm diameter (Veigas et al., 2013). Throughout this project the gold nanoprobe schematized in **Section 3.1** (**Figure 3.1**) was synthesized four times. These syntheses were made from two different batches of gold nanoparticles which may present different features. In order to assess the size of the synthesized citrate capped AuNPs three different techniques were used.

First, the UV-Vis spectrum was analysed, presenting a single SPR peak of 520 nm (**Figure 3.8 A**), which indicated the presence of relatively monodisperse spherical particles.

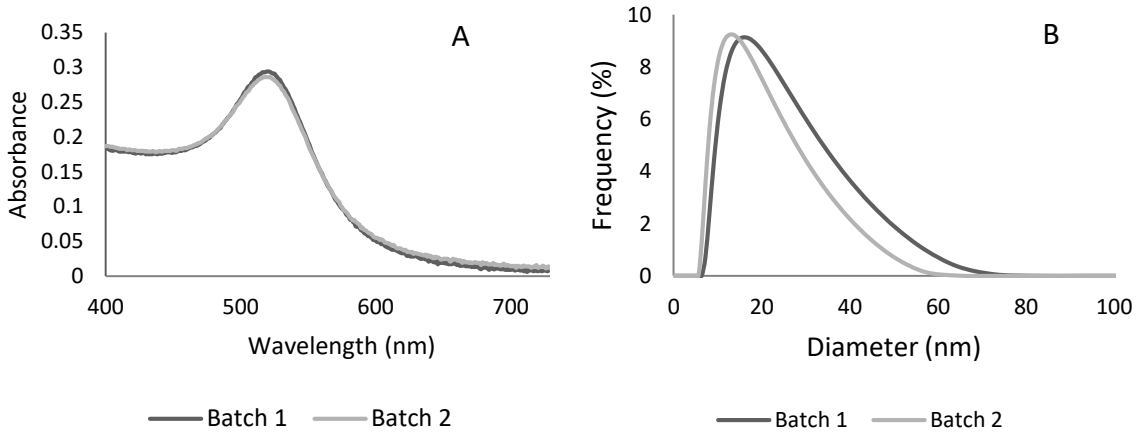

Figure 3.8 Characterisation and comparison between the two synthesized batches of citrate gold nanoparticles. A) UV-Vis spectrum of spherical AuNPs, with a characteristic maximum absorption peak at 520 nm; **B)** DLS of the two batches of the synthesized gold nanoparticles.

The theoretical size of gold nanoparticles was also calculated based on a model proposed by Haiss and co-workers. As represented in the following equation (**Equation 1**), the ratio of the absorbance of AuNPs at the surface plasma resonance peak (Aspr) to the absorbance at 450 nm (A450), estimated a mean diameter of 14.3 nm for Batch 1 and 12.4 nm for Batch 2 of the synthesized gold nanoparticles (Haiss et al., 2007).

$$d = \exp\left(3\frac{Aspr}{A450} - 2{,}2\right)$$

Equation 1. Calculation of AuNPs mean size using UV-vis spectrum (Haiss et al., 2007).

Dynamic Light Scattering (DLS) was also used to confirm the nanoparticles size. Based on the differential scattering of colloids according to their Brownian movement in solution, it is directly related to AuNPs hydrodynamic radius (Lim et al., 2013). DLS indicated an AuNPs mean diameter of 14.5 nm which is a value higher than the obtained by the previous method. Since hydrodynamic radius of AuNPs is influenced by the molecules at its surface, this difference of values can be explained by the citrate capping of gold nanoparticles (Kato et al., 2009). Moreover,

the technique used by Haiss *et al* was performed for monodisperse and perfectly spherical particles, whereas the experimental data collection is over a distribution of particle sizes and shapes.

Finally, TEM was also performed (**Figure 3.9**). It allowed the quantitative measurement of physical size and morphology of AuNPs. The predicted size and shape were confirmed, with an obtained diameter of 13 nm (±2.8 nm) for Batch 1 of the spherical gold nanoparticles and 14.3 nm (± 2.7 nm). Thus, the used methods for the characterization of the citrate-capped AuNPs seem to be in agreement. The slightly differences between the two synthesized batches of gold nanoparticles might have influenced the synthesis of gold nanoprobes and will be discussed in the next sections.

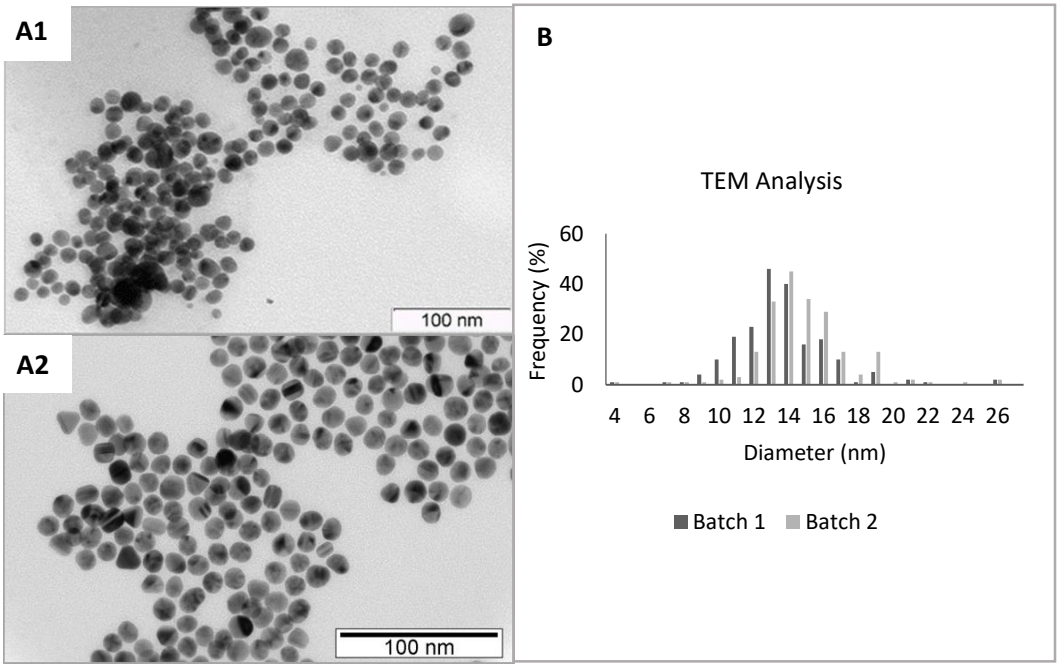

Figure 3.9 Characterisation of the synthesized citrate gold nanoparticles by TEM. A) TEM picture of spherical nanoparticles with approximate 14 nm diameter size: **A1** –Gold nanoparticles Batch 1, used in the synthesis of Batches 1 and 2 of gold nanoprobes; **A2** – Gold nanoparticles Batch 2, used in the synthesis of Batches 3 and 4 of gold nanoprobes; **B)** Histogram of analysed particles by measured diameter, with a mean diameter of 13 nm for Batch 1 and 14 nm for Batch 2. Five random pictures were taken from each batch and nanoparticle size was measured representing a total of 200 measurements for each batch.

After physical characterization, guaranteeing the desired size and shape of gold nanoparticles, the following step was their functionalisation with thiol-modified oligonucleotides by salt aging method (**section 2.2.2.2.1.**). Four batches of Au-nanoprobe where synthesized throughout this project, with a variation in their synthesis process, namely the phosphate buffer used for their storage. Batches 1 and 2 where stored with phosphate buffer at pH8+0.1M NaCl, whereas pH7+0.1M NaCl was used to store gold nanoprobe batches 3 and 4. These conditions will be discussed and compared in the following sections.

In order to confirm functionalisation, the four batches of Au-nanoprobe obtained were submitted to the similar approaches previously used to evaluate gold nanoparticles.

First, the expected increase in the hydrodynamic radius as a result of the bounding of the thiol-modified oligonucleotide to the AuNP surface (Lim et al., 2013), was verified in UV-vis spectra since the SPR peak shifted to the right (from 520 nm to 525 nm). This shift was a result of an increase in the local refractive index at the gold nanoparticle surface (**Figure 3.10**).

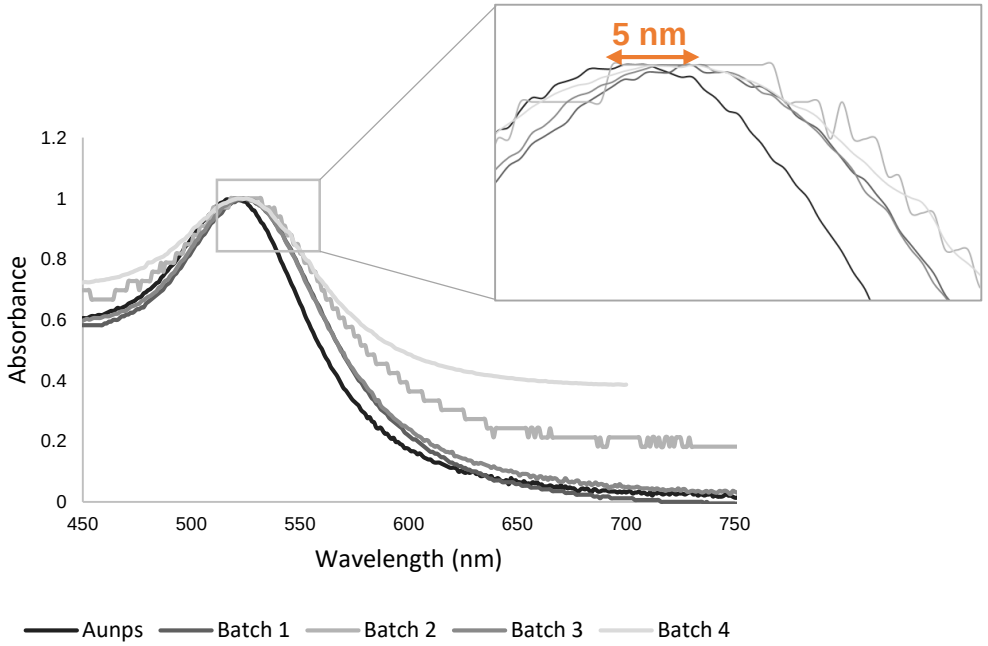

Figure 3.10 Characterisation of the synthesized gold nanoprobes by UV-vis spectra. A shift in the maximum absorption peak of gold nanoparticles is observed from 520 nm to 525 nm as evidence of functionalisation.

In this figure it is also observed that the gold nanoprobe Batch 2 presents an irregular profile when compared with the other synthesized nanoprobes. It may arise due to low concentration of the sample when it was measured in the spectrophotometer. Low concentration leads to low absorbance. In these cases, noise in the measurements results in a loss of precision with a concomitant loss of accuracy in the measurement.

The DLS results corroborated the spectrophotometric data since it was confirmed an increase in the diameter from 14.5 nm to an average of approximately 30 nm (**Figures A5 and A6 Appendix**). Thus, an increase of 20 nm in the hydrodynamic radius was observed. This higher diameter directs to the citrate substitution by the thiol-modified oligonucleotides(Pellegrino et al.,2007). Taking into account that the distance between dsDNA base pairs is 0.34 nm (Watson and Crick, 1953) and that the probe has 17 nucleotides it would be expected a value of 26 nm for the hydrodynamic diameter (14.5 nm from gold nanoparticles and 5.8 nm for each side). This mismatch observed between theoretical and experimental values may be justified by the no consideration of the thiol group size (Parak et al., 2003).

Another parameter that can be used to prove AuNPs functionalisation is stability.

3.2.2 Au-Nanoprobes stability assays

Noble metal nanoparticles brought new possibilities for biodetection. Gold nanoparticles gained special interest due to their colorimetric properties, namely intense colours and LSPR, which are very useful for biomolecular assays(Conde et al., 2014). As referred before, surface plasmon resonance is dependent on size, shape and interparticle distance (Baptista et al., 2008). The last constitutes the foundations for most AuNP-based colorimetric assays, namely those in non-cross-linking format, which is being applied in this project (Baptista et al., 2011).

As previously referred, non-cross-linking approach is based in the induction of Au-nanoprobes aggregation by an increasing salt concentration. This change in stability is reflected in colorimetric variations of the gold nanoprobes solutions in the presence of a complementary or non-complementary target (Baptista et al., 2008). Therefore, the stability characterisation of Au-nanoprobes is a key step for this method.

Four batches of gold nanoprobes were synthesized and their stability was evaluated. The minimal electrolyte concentration needed to induce Au-nanoprobes aggregation was determined through Au-nanoprobes stability assays against salt-induced aggregation. This characteristic was determined with the registration of UV-vis spectra (400nm-700nm) for different $MgCl_2$ concentrations (**Figure 3.11**).

Citrate capped AuNPs tend to aggregate by the increase of the ionic strength in solution. Their stability is maintained with the functionalisation process, which through the oligonucleotides protects AuNPs from aggregation (Sato et al., 2003).

Inter-particle distance between NPs strongly affects their SPR absorbance band due to plasmon coupling (Jain et al., 2007). The addition of electrolyte causes the decrease of this distance, increasing nanoparticles size. Consequently, occurs a shift in the SPR absorbance band of dispersed AuNPs (520 nm) towards longer wavelengths (600 nm), with a concomitant colour change from red to blue (Baptista et al., 2008).

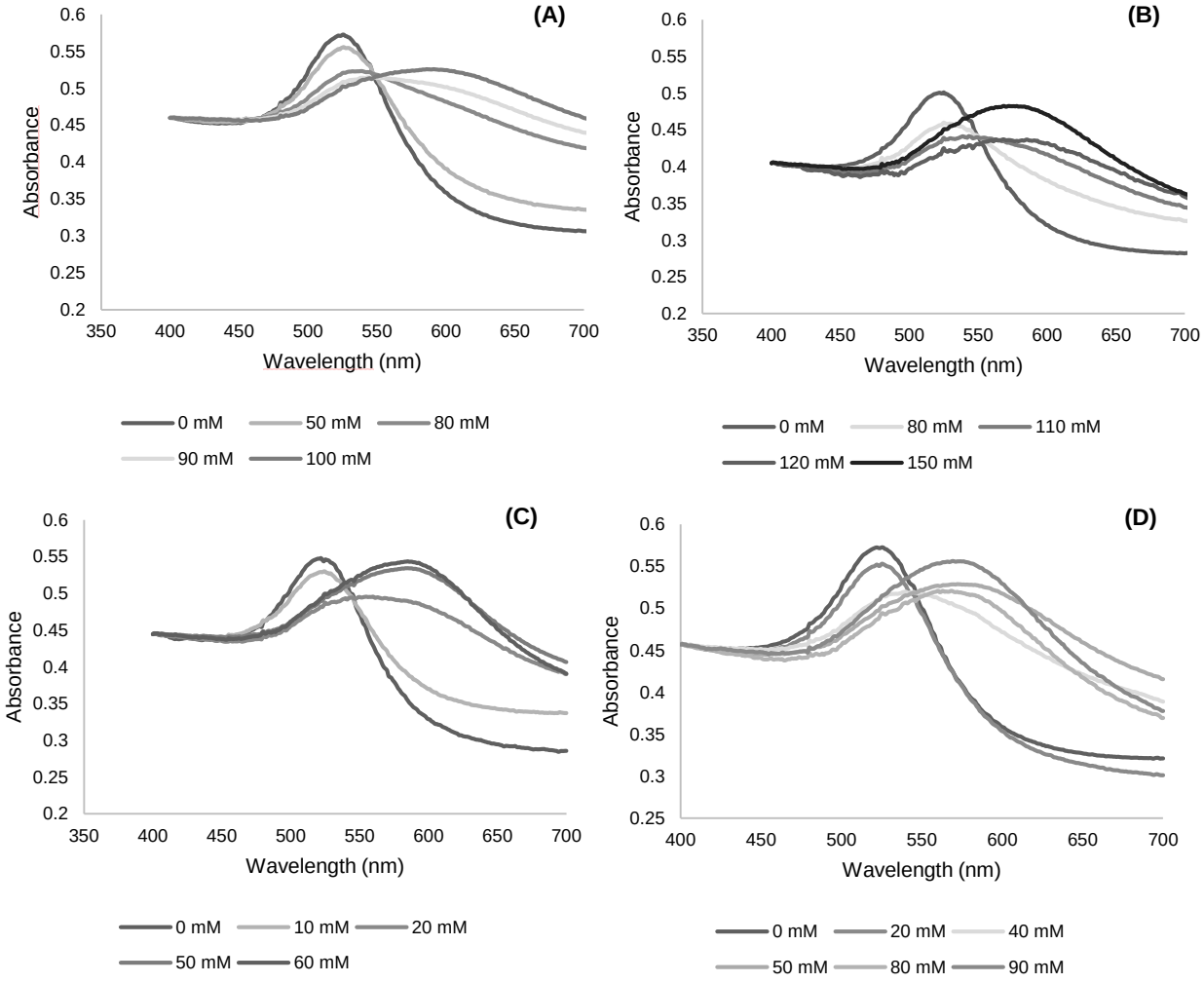

Figure 3.11 Au-nanoprobes stability by increasing $MgCl_2$ concentration. UV-Vis spectra registered 15 minutes after salt addition to Au-nanoprobes batches 1(**A**), 2(**B**), 3(**C**) and 4 (**D**) in pH7+0.1M NaCl phosphate buffer 10 mM at different $MgCl_2$ concentrations

In the figure above, one can observe that, for the same phosphate buffer, this shift occurs at different electrolyte concentrations for the 4 batches of gold nanoprobes. This issue will be discussed in more detail below (**Figure 3.14**).

Several factors may interfere in the spectrophotometer reading. For example, during data acquisition along this thesis precipitation of Au-nanoprobes occurred often. This can lower the absorbance of the aggregated Au-nanoprobes registered, which can lead to a misinterpretation of the observed aggregation. We also need to take into account that there is an error associated to the used equipment, causing a variation in the optical path. In order to overcome this question, data normalisation was performed.

3.2.2.1 Data Analysis

Based on the obtained UV-Vis spectrum after electrolyte addition in increasing concentrations (**Figure 3.11**), a ratio (r) between the absorbance of the single wavelengths that are characteristic of dispersed (Abs 525nm) and aggregated nanoparticles (Abs 600 nm) was performed. It allowed to determine that for r(Abs)<1, Au-nanoprobes are mainly aggregated, meaning that the absorbance value of aggregated species is higher than the absorbance value of non-aggregated species, resulting in a blue coloured solution. On the other hand, a r (Abs)>1 is related to a non-aggregated state, where the absorbance value of the non-aggregated species is higher than the absorbance value of the aggregate species, associated to a red solution.

It is also relevant to mention that the SPR peak of the aggregation fraction may suffer some variations around the 600 nm for lower or high wavelengths (Pedrosa et al., 2014). In this thesis these variations were studied in order to achieve the conditions that showed a better spectrophotometric discrimination between complementary and non–complementary target, according to the obtained colorimetric results. Even though the most important of colorimetric tests is the colour visualised after the test, it is important to acquire and analyse spectrophotometric data to guarantee the reproducibility of the results. In this study, although the maximum absorbance registered in the spectra for the aggregated species in solution was not 600 nm, this was the selected absorbance. This value corresponded to the position in the spectrum where the absorbance of aggregated species is maximum at the same time that the absorbance of non-aggregated species is minimum, allowing a better discrimination. Illustrative examples are represented in **Figure A7 Appendix.**

For AuNPs systems, it is of utmost importance to attain a balance between oligonucleotide surface coverage, particle stability, and hybridisation efficiency (Veigas et al.,2015). Several factors can influence these parameters. The effect of pH in Au-nanoprobes stability in salt induced aggregation was evaluated herein.

3.2.2.2 pH effect

The behaviour of the synthesized nanoprobes was followed in four 10 mM phosphate buffers at different values of pH, namely pH7 and pH8, in the presence or absence of 0.1 M NaCl. A narrow range of pH values was used, since DNA hybridization is a crucial factor for non-cross-linking method and only occurs between 6.5 and 8 pH value (Zhang et al., 2012). Moreover, Au-nanoprobes are stable between pH 4 and pH 12, aggregating outside this range(Sun et al., 2009). The results are represented below.

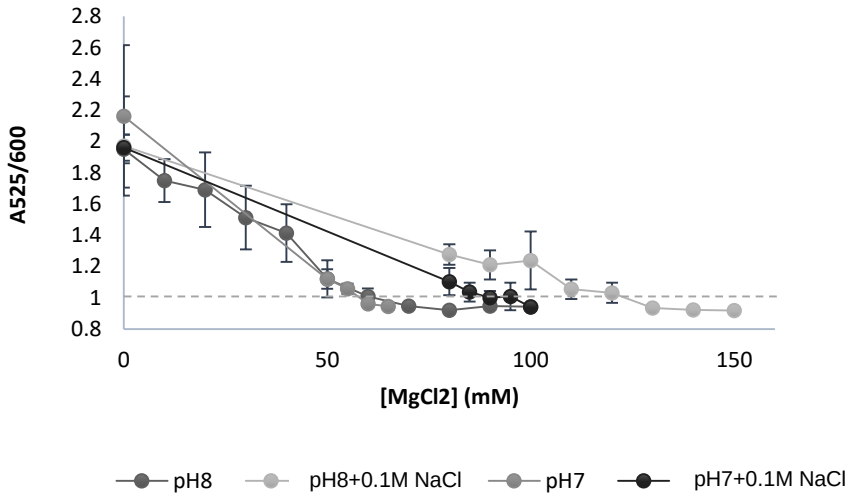

Figure 3.12 *ttrRSCBCA* Au-nanoprobe (Batch 1) salt induced aggregation profile for different phosphate buffers. Determination of *ttrRSBCA* Au-nanoprobe stability profile by $MgCl_2$ concentration increase. All data was collected 15 minutes after salt addition

Results show that pH influences nanoprobe stability. For batch 1, the minimum electrolyte concentration needed to cause nanoprobe aggregation varies between the used buffers. The most remarkable difference is observed for the same value of pH, for example between pH7 and pH7+0,1M NaCl, where the minimum electrolyte concentration needed to cause aggregation were 60 mM and 100 mM, respectively. The presence of salt ions in the phosphate buffer stabilizes the phosphate-phosphate repulsion present between the probe strands at the surface of the gold nanoparticles (Doktycz, 1997). Thus, in the presence of pH7+0.1M NaCl phosphate buffer, a higher concentration of electrolyte is needed to destabilize nanoprobes and, consequently, cause its aggregation. The same explanation can be applied to the difference between pH8 and pH8+0.1M NaCl phosphate buffers.

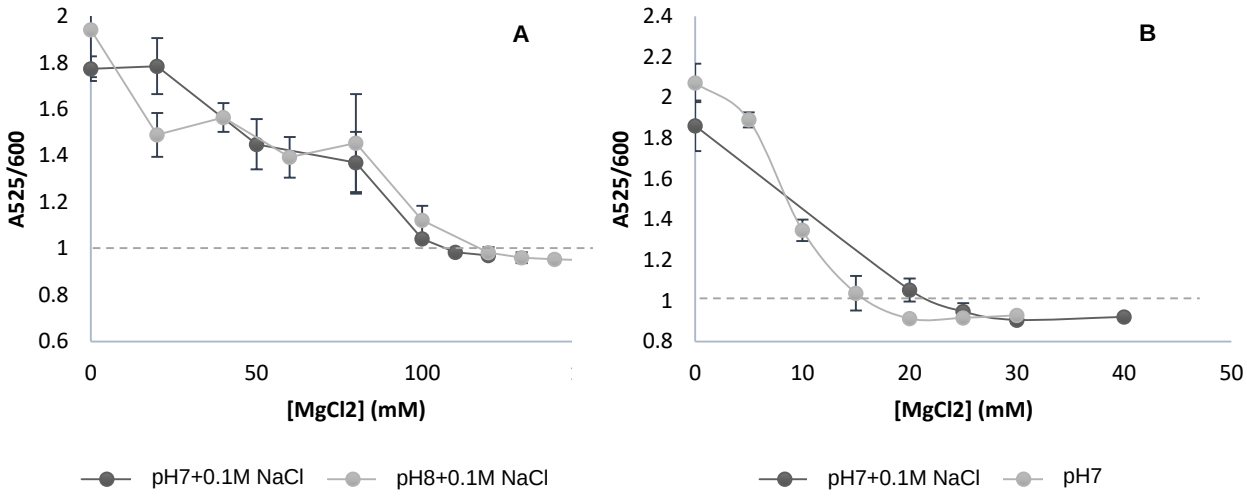

Figure 3.13 ***ttrRSBCA*** **Au-nanoprobes salt induced aggregation profile for different phosphate buffers.** All data was collected 15 minutes after salt addition. **A)** Determination of *ttrRSBCA* Au-nanoprobe (Batch 2) stability profile by $MgCl_2$ concentration increase; **B)** Determination of *ttrRSBCA* Au-nanoprobe (Batch 3) stability profile by $MgCl_2$ concentration increase

For batch 2 (**Figure 3.13 A**), when the nanoprobe stability is compared between phosphate buffer at pH7+0.1M NaCl and pH8+0.1M NaCl, it is observed that the minimum values of electrolyte needed to nanoprobe cause aggregation (r<1) are similar (110 mM and 120 mM, respectively). The fact that for a lower pH less amount of salt is needed to cause this phenomenon, might be related to the DNA protonation. At lower pH values, probe molecules are partially protonated and an electrostatic attraction between them causes the strands to bend to each other (Ravan et al., 2014), making them more likely to aggregate, needing less concentration of salt to this effect.

These values are also close for batch 3 (**Figure 3.13 B**), where the minimum electrolyte concentration needed is 20 mM for pH7 and 25 mM for pH7+0.1M NaCl. The differences registered can be explained by the presence of salt in one of the phosphate buffers, that interact with the negative-charged phosphate groups of the oligonucleotide probes. Thus, the electrostatic repulsion between surface probes is minimised, stabilising them and making necessary the addition of a higher amount of electrolyte to cause their aggregation (Ravan et al., 2014). This difference of salt needed to cause aggregation was also previously described for batch 1(**Figure 3.12**), however the registered difference there was significantly higher. This difference observed between probes behaviour might be related to their functionalisation efficiency upon synthesis. Possibly, batch 3 contains less amount of oligonucleotides at its surface, being more influenced by changes in the surrounding environment.

The comparison between the studied nanoprobes is represented below.

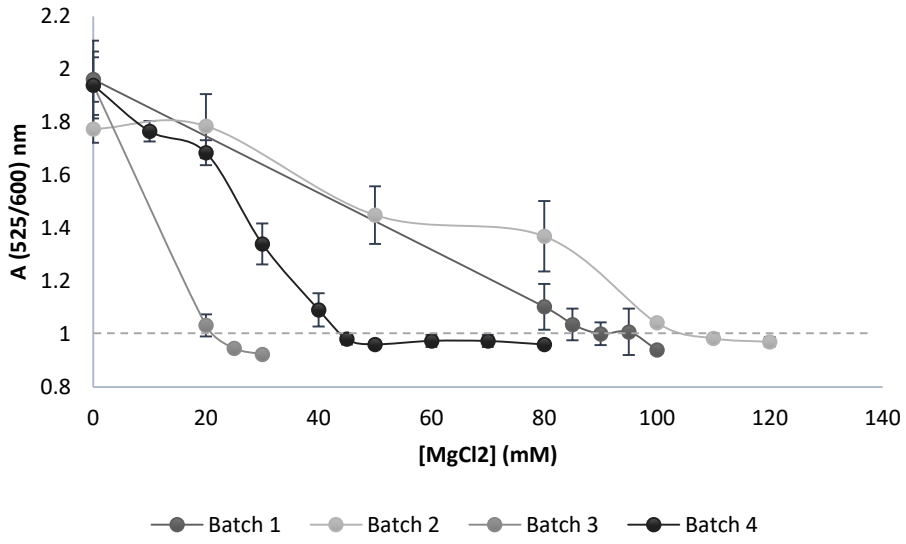

Figure 3.14 Comparison between *ttrRSBCA* Au-nanoprobes salt induced aggregation profile for pH7+0.1M NaCl phosphate buffer. All data was collected 15 minutes after salt addition.

After analysis of the figure above (**Figure 3.14**), one can observe that batch 2 nanoprobe stability profile presents irregularity. After addition of increasing electrolyte concentrations, it was expected to verify a reduction in r (A525/A600) as consequence of the increase of aggregated species in solution (increase of A600). Nevertheless, it was not verified when the electrolyte concentration increased from 50 mM to 80 mM. This fact might me associated with a pipetting error which may have influenced electrolyte concentration in the final test. Since the volume of electrolyte added was lower than desired, gold nanoprobe aggregation tendency was lower and, consequently, A525/A600 ratio presented a higher value than expected.

This figure shows also that for the same buffer, the four batches of nanoprobes differ in their stabilities. Gold nanoprobes batches 3 and 4 need less electrolyte concentration to aggregate when compared to batches 1 and 2. This difference may arise from their syntheses. Batches 1 and 2 were synthesized in pH8 buffer whereas the last two batches were resuspended in pH7 buffer, which make them more likely to aggregate as explained in figure **3.13 A** case.

For example, a remarkable difference is registered for phosphate buffer pH7+0.1M NaCl between batch 3, where is shown that the minimum electrolyte concentration needed to cause nanoprobes aggregation is 30 Mm against batches 1 and 2 where is needed around 100 mM. This observation may be justified by several factors.

Despite following the same experimental protocol, the different batches of probes might be associated to different Au-nanoprobe functionalisation. Higher densities of thiol-modified oligonucleotides bound to the AuNPs surface have been associated with Au-nanoprobes with higher stability (Storhoff et al., 2002). Therefore, batches 1 and 2 of probe may have higher densities of thiol-modified oligonucleotides, presenting greater stability than the last synthesized probes. These differences of stability might be associated to non-specific adsorptions occurred

during functionalisation process, possibly as a result of insufficient or absence of ultrasound time (Hurst et al.,2006).

These non-specific adsorptions might also be related to the ionic strength of the immobilisation solution. Kinetics of probe immobilisation on the gold surface depends strongly on this property(Peterson et al., 2001). In the presence of a high ionic strength, the repulsions between probes are efficiently screened by the salt ions, allowing many more probes to adsorb to the surface. On the other hand, at low ionic strength, electrostatic repulsions between probes tend to supress the adsorption of DNA strands on the surface(Peterson et al., 2001). Therefore, some phenomenon might have occurred during salt aging course (**section 2.2.2.2.1**) in the synthesis of batch 3 of gold nanoprobe, in comparison to batches 1 and 2, that prevented the ionic strength increase, resulting in a poor functionalisation of this batch.

In order to support this hypothesis, an oligo quantification must have been done during synthesis process. The densities of thiolated oligonucleotides should have been determined by fluorescence measurements after their displacement with DTT (Sato et al., 2003).

Another way to infer about nanoprobes functionalisation could also be the evaluation of their electrophoretic mobility (Pellegrino et al., 2007). The DNA attachment to Au nanoparticles can be clearly observed by gel electrophoresis (Zanchet et al.,2001). Their mobility on the gel depends on size and charge. Bigger sizes cause a slower migration of nanoparticles on the gel. Therefore, upon attachment of DNA, the mobility of the resulting conjugates is decreased as a consequence of the increase in their effective diameter (Pellegrino et al., 2007). These assumptions could be applied in the explanation of the differences in functionalisation between the different obtained nanoprobes. Contrary to batches 1 and 2, it would be expected a lower mobility of batch 3 nanoprobe in the gel as a result of its lower functionalisation and, consequently, lower size and weight (Veigas, 2009).

Despite these hypotheses, another parameter should be debated. It is needed to emphasize that the 3 batches of synthesized gold nanoprobes were obtained from different batches of gold nanoparticles. Batches 1 and 2 were synthesized from a batch of gold nanoparticles, while batches 3 and 4 were obtained from another as described in **section 3.2.1.**

Gold nanoparticles size might have influenced the functionalisation process. Changes in this characteristic of gold nanoparticles can affect their DNA hybridisation property and the probe loading capacity (Demers et al., 2000). This capacity is higher for smaller diameter nanoparticles when compared with the larger ones, for a given equal surface area (Pellegrino et al., 2007). The probe loading on the gold surface results of the interplay between the covalent gold/thiol interactions and the electrostatic repulsion between DNA strands. Therefore, reducing electrostatic interactions allows more oligonucleotide to attach to the highly curved surface (Hill et al.,2009). This condition is reached in gold nanoparticles of smaller diameter, which have a more curved surface than the larger ones, allowing the oligonucleotide probes attached to these nanoparticles to have more distance from one another, moving radially away from the particle surface (**Figure 3.15**).

These facts may justify the supposed difference of functionalisation between batches 1 and 2 and the last two batches. These speculations were confirmed by TEM data obtained from the two batches of gold nanoparticles used in gold nanoprobes synthesis, which show that gold nanoparticles used for the first and second batches are smaller (13 nm ± 2.8 nm) than the used for batches 3 and 4 (14,3±2.7 nm).

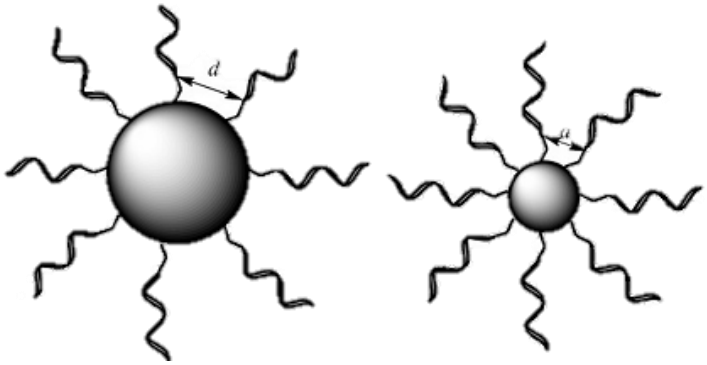

Figure 3.15 Illustration of the effect of solid surface curvature on the probe-loading capacity((Pellegrino et al. 2007) and the images of TEM obtained from gold nanoparticles used in synthesis of batches 1 and 2 (B) and 3 (A) of *ttrRSBCA* gold nanoprobes.

3.3 Applying gold nanoprobes to detection

3.3.1 Synthetic oligonucleotide

Once determined the minimal ionic strength needed to cause nanoprobes aggregation, their capacity to detect ssDNA oligonucleotides (40 pb) was tested. These targets were first used rather than LAMP products, due to their characteristics, namely length, concentration, single stranded structure and high level of purity with less interfering agents, that could influence gold nanoprobe response. The results obtained for the four batches of the synthesized gold nanoprobes are represented below (**Figures 3.16 and 3.17**).

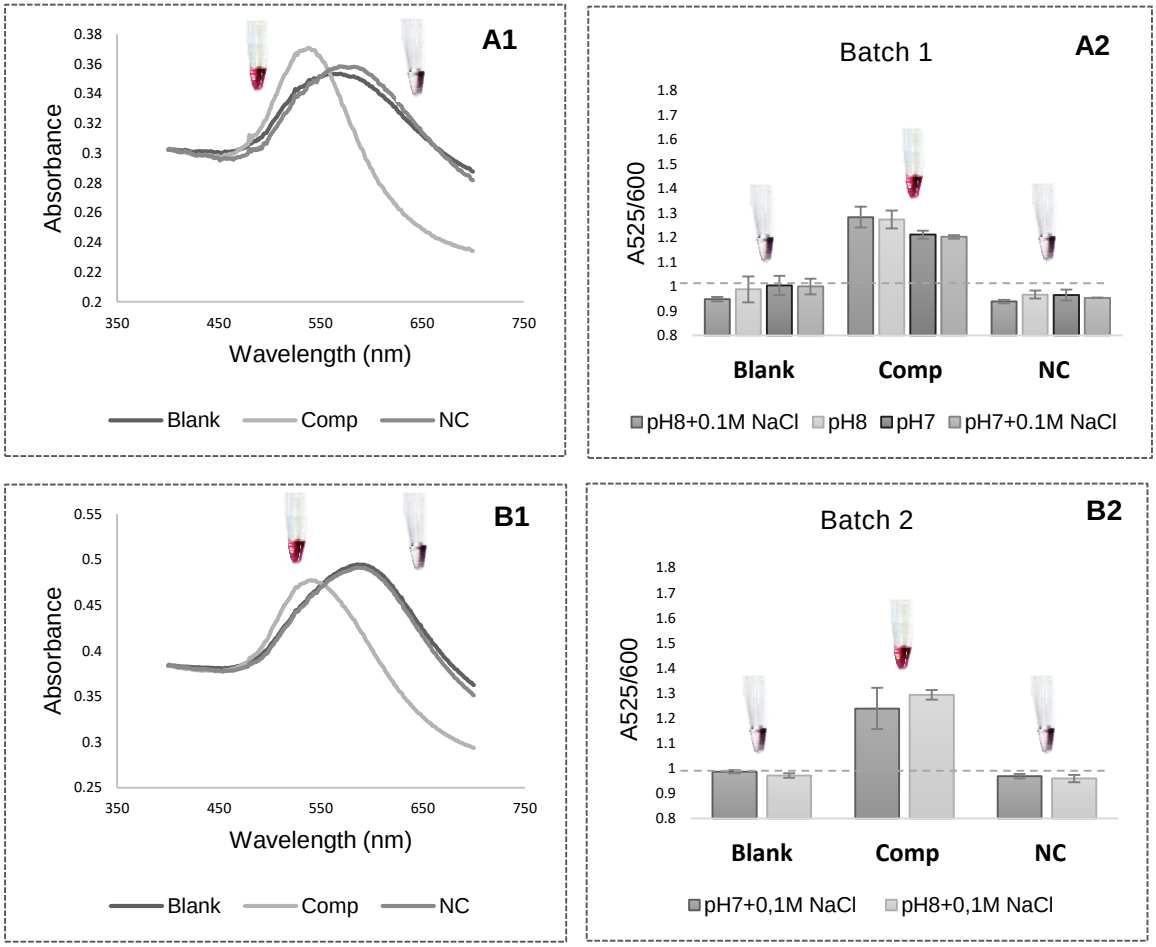

Figure 3.16 Hybridisation assay with ssDNA oligonucleotides for the batches 1 and 2 of *ttrRSBCA* gold nanoprobe. Au-nanoprobes aggregation was measured by ratio of aggregation (ratio of SPR intensity at 525 and 600 nm) for the assay tests - 2.5 nM Au-nanoprobe, 10 mM phosphate buffer pH 8 (**A1** and **B1**) and ssDNA targets at a final concentration of 0.3 pmol. µL-1. All spectrophotometric data were collected 15 minutes after salt addition: **A1 –** 72.5 mM; **B1** – 62.5 mM; **A2 –** 132.5 Mm (pH8+0.1M NaCl); 72.5 mM (pH8); 62.5 mM (pH7) and 102.5 mM (pH7+0.1M NaCl), **B2 –** 112.5 mM (pH7+0.1M NaCl) and 122.5 mM (pH8+0.1M NaCl). Error bars represent the standard deviation of three independent assays.

Upon hybridisation with a complementary target, an increase in AuNPs stability was observed (**Figure 3.16 A1, B1 and Figure 3.17 C1 and D1**). This stabilisation can be explained by the steric hindrance generated by the synthetic oligonucleotides around AuNPs, which is consequence of their non-complementary tail of 20 pb. Therefore, as a result of the formation of

dsDNA structures with higher rigidity than ssDNA(Li & Rothberg, 2004), AuNPs were shielded. Consequently, their probability of aggregation was reduced with a consequent increase in stability. As a result, the solution remained red with a concomitant higher absorbance at 525 nm than at 600 nm (**Figure 3.16. A1, B1 and Figure 3.17 C1 and D1**).

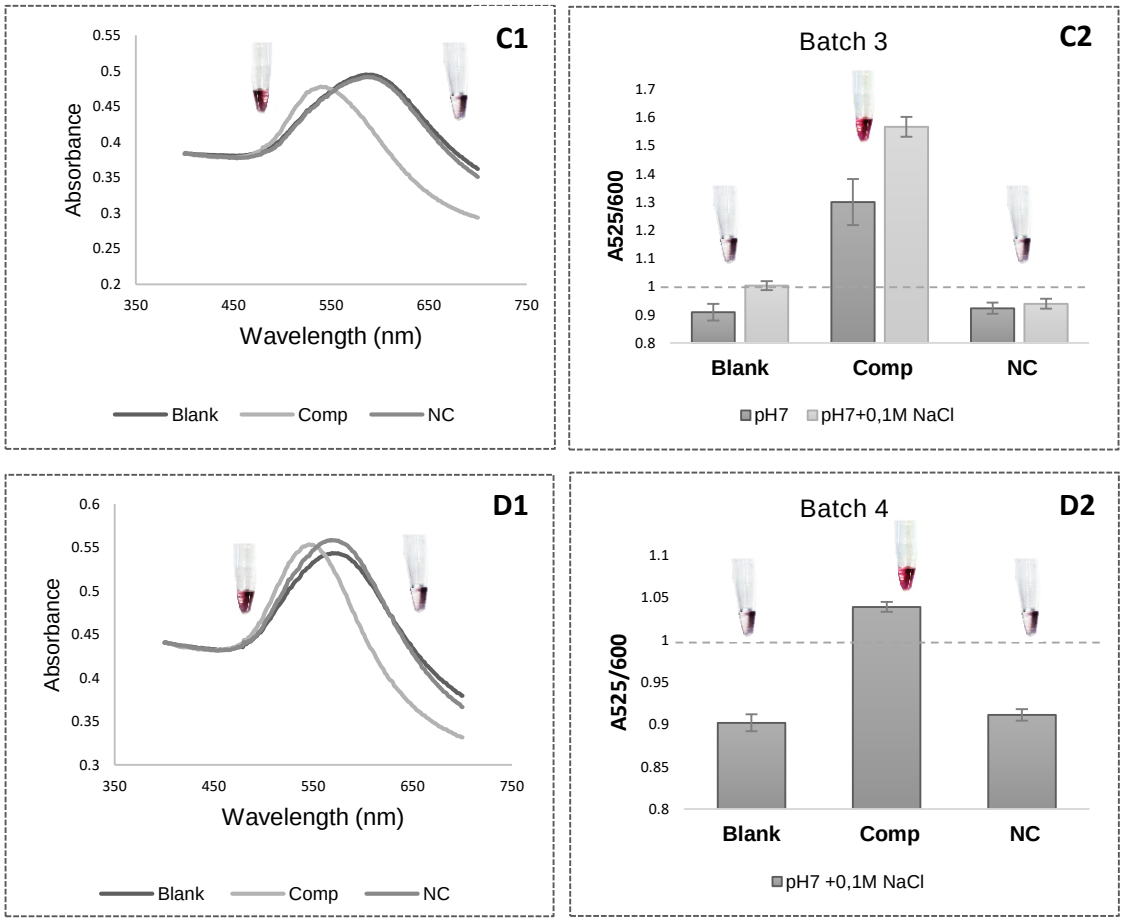

Figure 3.17 Hybridisation assay with ssDNA oligonucleotides for the batches 3 and 4 of *ttrRSBCA* gold nanoprobe. Au-nanoprobes aggregation was measured by ratio of aggregation (ratio of SPR intensity at 525 and 600 nm) for the assay tests - 2.5 nM Au-nanoprobe, 10 mM phosphate buffer pH 7+0.1 M NaCl (**C1** and **D1**), ssDNA targets at a final concentration of 0.3 pmol. µL-1. All spectrophotometric data were collected 15 minutes after salt addition: **C1-** 32.5 mM; **D1 –** 52.5 mM; **C2 –** 22.5 mM (pH7) and 32.5 mM (pH7+0.1M NaCl); **D2 –** 50 mM. Error bars represent the standard deviation of three independent assays.

On the other hand, in the absence of target (blank) or in the presence of non-complementary target, Au-nanoprobes aggregation occurred, which was associated to the expected colorimetric change of the solution from red to blue. The obtained spectrophotometric data confirmed this fact, as the value for absorbance at 600 nm was higher than for 525 nm, which indicates the majority of aggregated species in solution (**Figure 3.16 A2, B2 and Figure 3.17 C2 and D2).**

When comparing the spectrophotometric profile of batches 1 and 3 (**Figure 3.16 A1** and **3.17 C1**) with batches 2 and 4 spectra (**Figure 3.16 B1** and **Figure 3.17 D1**), one can infer that the band at 525 nm from batches 1 and 3 presents broadening. This might be related to an excess of electrolyte added to the solution, which means that the salt concentration decided as the

minimum electrolyte concentration to cause nanoprobes aggregation (**Section 3.2.3**) may be inadequate. As a consequence, populations of gold nanoparticles of different sizes arose in solution, causing the 525 nm peak broadening.

These tests also served as a way of comparison between all used 10 mM phosphate buffers, in order to conclude about their efficiency to discriminate between complementary and non-complementary target. A good discrimination was observed in all used buffers for each batch of nanoprobe. Therefore, taking into account the difference between the ratio obtained for complementary versus non-complementary target, the most suitable phosphate buffer was selected for each probe. For batches 1 and 2, pH8+0.1M NaCl phosphate buffer was considered to be the one who achieved the best discrimination. For the following batch 3 colorimetric tests, pH7+0.1M NaCl phosphate buffer was selected. Based on the results of Batch 3, Batch 4 oligonucleotide detection was only performed in pH7+0.1M NaCl.

The results achieved in this section showed that nanoprobes were correctly discriminating synthetic targets. Thus, the next step was to verify if they maintained this capacity of discrimination when applied to LAMP products obtained from *Salmonella* extracted DNA.

3.3.2 LAMP products

After detecting synthetic oligonucleotides, the system was calibrated for the detection of biological samples using the parameters determined in the previous sections, namely time of reading and salt concentrations. As described previously along this project, the diverse batches of synthesized probes present different characteristics and, consequently, different behaviour. In this section the obtained results will be discussed individually for each batch.

3.3.2.1 Batch 2

Using the electrolyte concentration defined before, the capacity of detection was tested with pH8 +0.1M NaCl phosphate buffer (**Figure 3.18**).

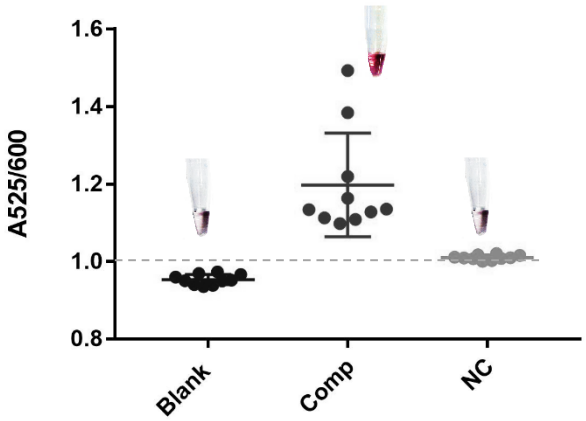

Figure 3.18 Hybridisation assay of LAMP product with batch 2 of *ttrRSBCA* gold nanoprobe. Au-nanoprobes aggregation was measured by ratio of aggregation (ratio of SPR intensity at 525 and 600 nm) for the assay tests - 2.5 nM Au-nanoprobe, 10 mM phosphate buffer (pH 8) +0.1M NaCl, DNA targets at a final concentration of 30 ng/µL. All spectrophotometric data was collected 15 minutes after 65 mM salt addition. Error bars represent the standard deviation of nine independent assays.

As observed in the figure above, *ttrRSBCA* gold nanoprobe batch 2 presented a good detection and discrimination between complementary and non-complementary target. These spectrophotometric data were corroborated by the solution colour, which remained red for the complementary target. The obtained ratio (>1) also indicates the majority of dispersed species in solution. Therefore, the "buffer" role played by ssDNA for increasing ionic strength in section **3.3.1** for increasing ionic strength, which is associated with increased stabilisation of Au-nanoprobes is also verified for LAMP product detection. However, as observed in this figure by the error bar size of complementary target, this effect is not so straight for dsDNA. This fact might be justified by the absence of exposed bases free to interact with the AuNP upon increasing ionic strength (Sandström et al.,2003).

On the other hand, in the absence of target (blank) or in the presence of non-complementary target, Au-nanoprobes aggregation occurred, which was associated to the expected colorimetric change of the solution from red to blue. The obtained spectrophotometric data confirmed this fact, as the value for absorbance at 600 nm was higher than for 525 nm, which indicates the majority of aggregated species in solution.

3.3.2.2 Batch 3

As previously described, the third batch of synthesized probe showed some differences from batches 1 and 2, which might explain its behaviour in LAMP product detection. Using the electrolyte concentration defined before, the capacity of detection was tested with pH7 phosphate buffer (**Figure 3.19**).

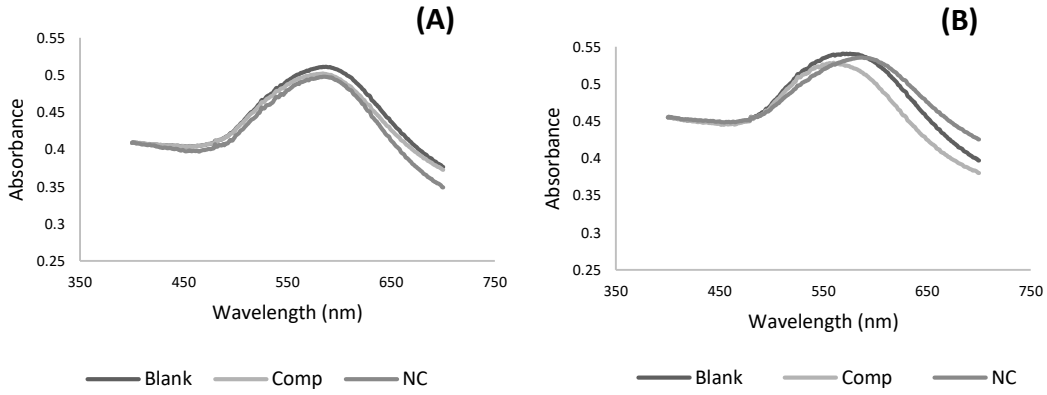

Figure 3.19 Hybridisation assay of LAMP product with batch 3 of *ttrRSBCA* gold nanoprobe. Au-nanoprobes aggregation was measured by ratio of aggregation (ratio of SPR intensity at 525 and 600 nm) for the assay tests - 2.5 nM Au-nanoprobe, 10 mM phosphate buffer (pH 7), DNA targets at a final concentration of 30 ng/µL. All spectrophotometric data was collected 15 minutes after 20 mM(**A**) and 17.5 mM (**B**) salt addition.

As mentioned before, non-cross linking approach is based on the different aggregation profile of Au-nanoprobes in presence/absence of the specific complementary target upon salt induced nanoparticle aggregation (Baptista et al., 2005). Presence of the complementary target

sequence to that of the probe prevents aggregation and the solution remains red (localised surface plasmon resonance (LSPR) band at 525 nm), whereas absence of a specific target sequence leads to extensive aggregation after salt addition and the solution turns blue (red-shift of the LSPR peak) (Baptista et al., 2008).

Based on these statements, one can observe in the figure above (**Figure 3.19 A**) that the discrimination between complementary and non-complementary target was not attained. It means that despite the observation of a colorimetric difference at 5 minutes after salt addition, when reading in a microplate reader after 15 minutes the aggregation has already occurred. Therefore, no discrimination was observed. Another factor that may influence the absence of discrimination was, as indicated in section **3.3.1**, the excess of electrolyte concentration added, which conducted to a faster aggregation.

Taking it into account, other tests were performed with lower concentration of added electrolyte but no changes were observed (**Figure 3.19 B**). It is represented by the red-shift in SPR band from 525 nm to 600 nm of all solutions, corresponding to a colour change of the solution from red to blue, which relates to aggregation. Finally, another parameter that might be responsible for the absence of discrimination is target concentration. In the represented tests (**Figure 3.19**) the LAMP product used was at 30 ng/µL, which may not be enough to cause steric hindrance between gold nanoprobes and avoid their aggregation. Or, as discussed previously in section **3.2.2.**, size of the gold nanoparticle might influence hybridisation. The gold nanoparticles used in this synthesis might have a higher size than the used for batches 1 and 2.

The binding of target strands to the oligonucleotide probes attached to highly curved surfaces (lower size nanoparticles) is more favourable, since it is associated to a relaxation of electrostatic interaction and steric hindrance between neighbouring oligonucleotides(Ravan et al., 2014). Therefore, the target strands can penetrate more easily into the probe layer and be hybridised, which was not verified in this situation.

In order to overcome this issue, more tests with the Au-nanoprobe were performed using pH7+0.1M NaCl phosphate buffer. The assay consisted on the spectrophotometric comparison of a “Blank” (without DNA), 10 mM phosphate buffer (pH 7), 0.1 M NaCl; POSITIVE control containing a complementary control DNA to the Au-nanoprobe and a NEGATIVE control containing non-complementary DNA. The pre-determined $MgCl_2$ amount was added to each reaction and, after 5 min at room temperature for colour development, the mixtures and the blank were assayed by UV/visible spectroscopy in a microplate reader.

Aggregation profiles were analysed in terms of the Abs525nm/Abs600nm ratio (dispersed vs. aggregated species), as represented below (**Figure 3.20**).

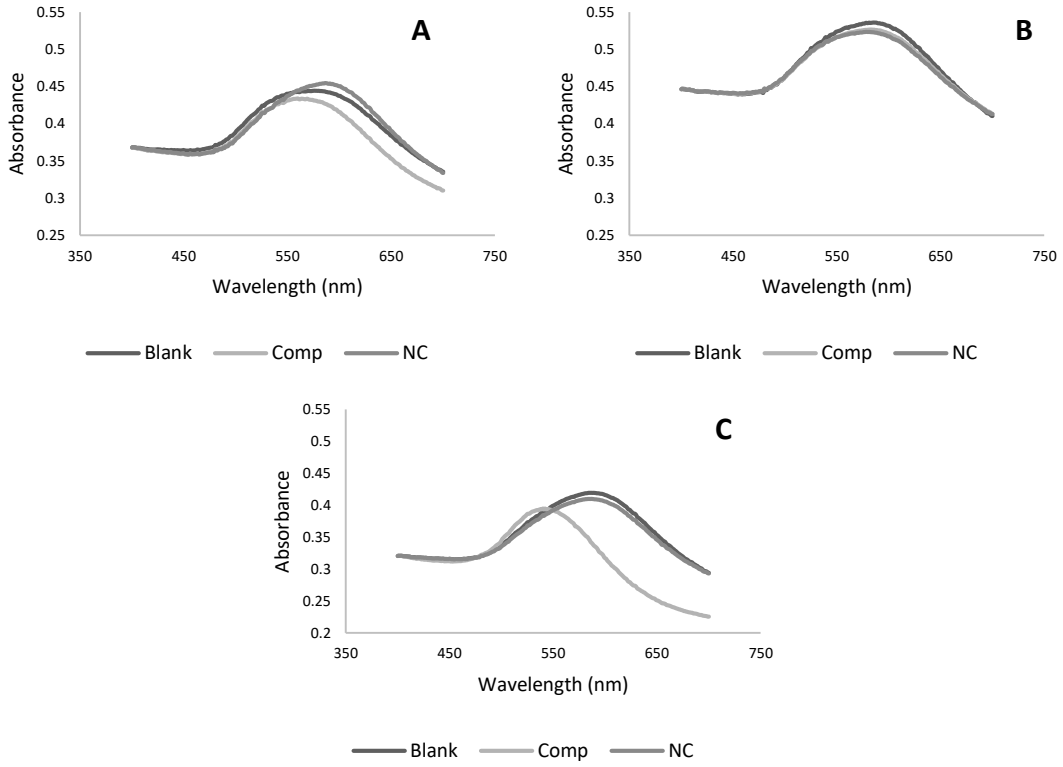

Figure 3.20 Hybridisation assay of LAMP product with batch 3 of *ttrRSBCA* gold nanoprobe. Au-nanoprobes aggregation was measured by ratio of aggregation (ratio of SPR intensity at 525 and 600 nm) for the assay tests - 2.5 nM Au-nanoprobe, 10 mM phosphate buffer (pH 7) +0.1M NaCl, DNA targets at a final concentration of 80 ng/µL (**A**), 30 ng/µL (**B**) and 75 ng/µL (**C**). All spectrophotometric data was collected 15 minutes after 22.5 mM(**A**) and 25 mM (**B**; **C**) salt addition.

After an optimisation process, the condition that allowed the discrimination between complementary and non-complementary target was achieved (**Figure 3.20C**). Then, considering these parameters, the limit of detection (LOD) of the gold nanoprobe was determined as being 75 ng/µL, which is higher than the obtained for the second batch (20 ng/µL) (**Figure A8 Appendix**). This fact supports the idea of the possible lower functionalisation of the last synthesized probe. Since nanoprobe possesses lower oligonucleotide density, the oligonucleotide will be prone to adsorb to the probe surface and take on a mushroom-like conformation, being less accessible to their target (Ravan et al., 2014). Therefore, for nanoprobe batch 3, a higher concentration of target is needed in order to occur recognition.

As previously stated, this study aims to develop a gold nanoprobe for *Salmonella ttrRSBCA* locus detection. Thus, the key of this thesis is to guarantee that the nanoprobe is sufficiently sensitive. Thus, *Salmonella* extracted DNA was submitted to different LAMP reaction times (5,25 and 45 minutes) and purified. Then, the obtained targets were tested at the same conditions (25 mM $MgCl_2$ and reading 5 minutes after electrolyte addition) in the nanoprobe. The probe only had the capacity to detect product which resulted from 45 minutes of reaction. Nanoprobe is not detecting maybe due to the absence of amplification before that reaction time. Even if the nanoprobe could detect without amplification possibly the target concentration used

in the LAMP reaction might not be enough (30ng/µL) to detect if not amplified. Furthermore, DNA purification lowers its yield, which may influence detection by the gold nanoprobe. Moreover, some reagents that are commonly used in molecular biology might also interfere in nanoprobes stability.

3.3.2.2.1 Effect of DMSO

DMSO, which was used to optimise LAMP amplification in this study (**section 3.2**), facilitating DNA hibridisation and increasing stringency, can be present in the biological samples, interfering in the probe behaviour.

Therefore, the stability of the Au-nanoprobe was tested for this reagent. The concentration of DMSO was chosen according to what was used in LAMP reaction (5%) (**Figure 3.21).**

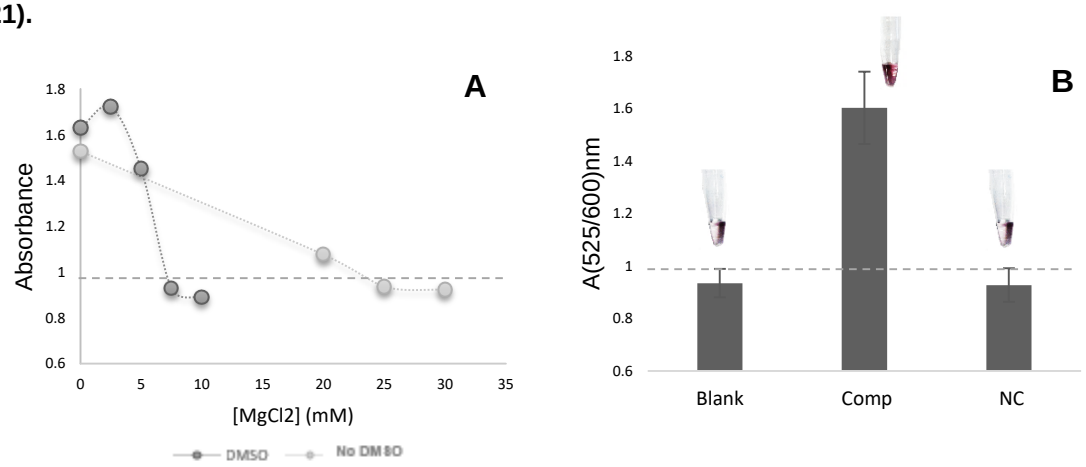

Figure 3.21 *ttrRSBCA* Au-nanoprobe (batch 3) salt induced aggregation profile in presence (blue) and absence (orange) of DMSO (A) and detection of ssDNA oligonucleotides in the presence of DMSO (B) after 7.5 mM salt addition. Determination of *ttrRSBCA* Au-nanoprobe stability profile by $MgCl_2$ concentration increase. All data was collected 5 minutes after salt addition.

As observed in the figure above, in the presence of DMSO, the Au-nanoprobes stability decreased. It might be justified by the DMSO dielectric constant, which is lower than water. Consequently, this change in the dielectric constant of the medium surrounding Au-nanoprobes led to a decrease in the double-layer thickness responsible for the electrostatic repulsion between them. Besides, DMSO is an aprotic reagent, favouring the creation of dipole moments that may facilitate Au-nanoprobes aggregation (Doria, 2010).

The minimum electrolyte needed to cause nanoprobe aggregation in the presence of DMSO was tested in ssDNA oligonucleotides and it was verified that the probe was discriminating correctly (**Figure 3.21 B**). However, when tested in biological samples, different results were obtained (**Figure 3.22**).

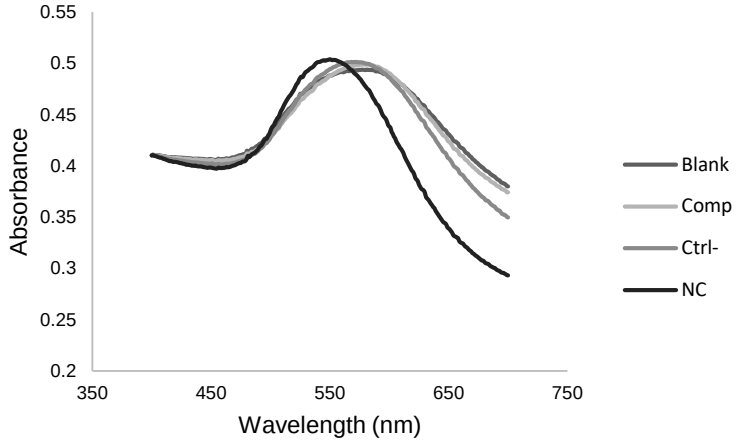

Figure 3.22 Hybridisation assay of LAMP product with batch 3 of *ttrRSBCA* gold nanoprobe. Au-nanoprobes aggregation was measured by ratio of aggregation (ratio of SPR intensity at 525 and 600 nm) for the assay tests - 2.5 nM Au-nanoprobe, 10 mM phosphate buffer (pH 7) +0.1M NaCl, DNA targets at a final concentration of 75 ng/µL. All spectrophotometric data was collected 5 minutes after 7.5 mM salt addition.

A possible explanation for this result may be the nature of the non-complementary target being used. In the figure above, it is observed that the gold nanoprobe is only detecting the non-complementary target. As stated before, the LAMP reaction optimisation for *Salmonella ttrRSBCA* locus amplification was carried out in the presence of DMSO. However, the reaction that originated the non-complementary target does not have this reagent. Therefore, the only way to correctly compare the discrimination of the gold nanoprobe between the two targets is to perform their amplification under the same conditions. Even if it is guaranteed, it is difficult to ensure that after purification no DMSO is remaining in the biological samples and, if remaining, is present at the same amount in both targets.

3.3.2.2.2 Effect of pH in nanoprobe shelf life

Another parameter that can influence the detection is the gold nanoprobe itself. Since nanoprobe batch 3 was synthesized with pH7+0.1M NaCl instead of pH8+0.1M NaCl as the other nanoprobes, it may interfere in its shelf life. In order to check this possibility, the gold nanoprobe was characterised again, namely by UV-vis spectrophotometry and DLS. The obtained results are represented below (**Figure 3.23**).

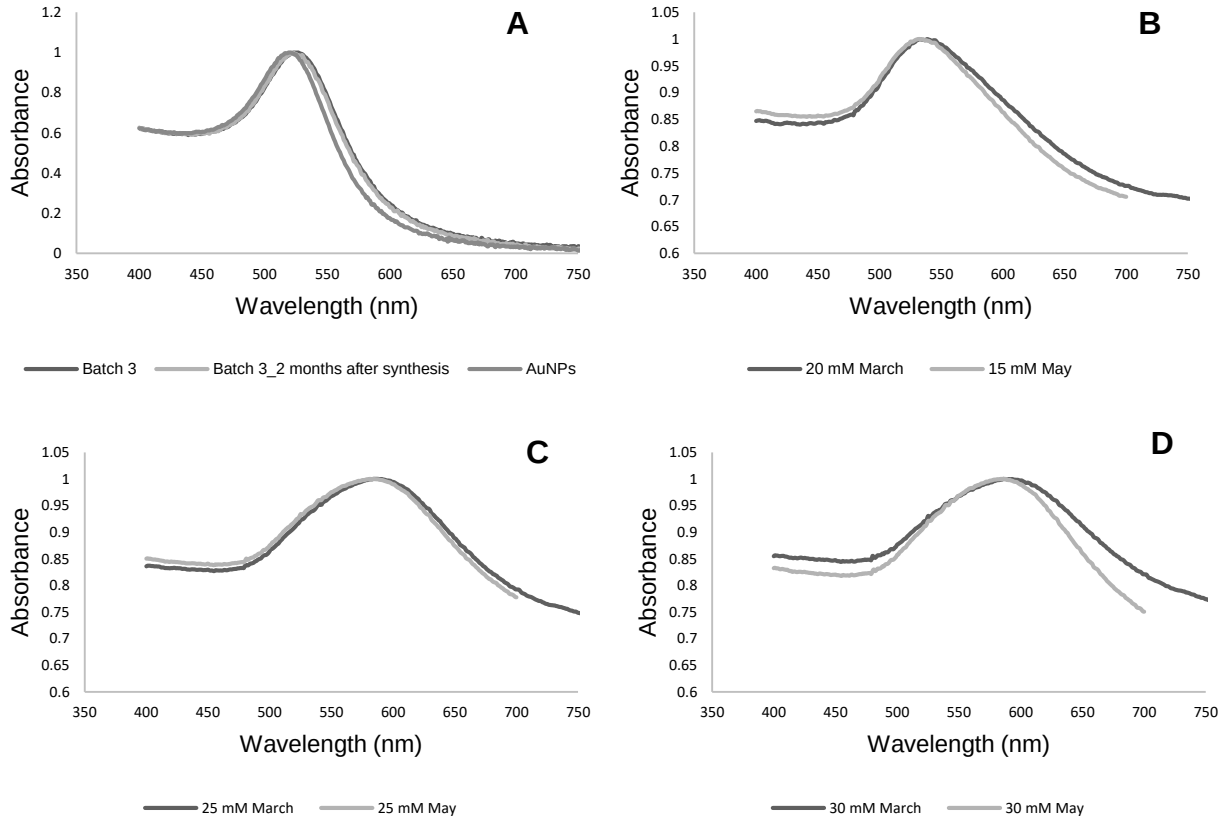

Figure 3.23 *ttrRSBCA* Au-nanoprobe (batch 3) salt induced aggregation profile. A, B, C, D – Analysis of nanoprobe behaviour in the presence of different salt concentrations (15 mM, 20 mM, 25 mM and 30 mM) 2 months after synthesis (May) and comparison with the previous registered data (March). All data was collected 5 minutes after salt addition.

Results show that the spectrophotometric profile exhibited by the gold nanoprobe was maintained since its synthesis as well as its concentration, still presenting a SPR band peak at 525 nm, characteristic of functionalisation (**Figure 3.23 A**). However, upon salt addition some differences were observed two months after synthesis. Interestingly, the nanoprobe exhibits the same behaviour currently as two months ago when less amount of electrolyte is added (15 mM instead of 20 mM $MgCl_2$) (**Figure 3.23 B**). It means that a change in the probe stability has occurred with a consequent change in the minimum electrolyte concentration to cause its aggregation. This may denote a decrease in oligonucleotide density over time, which might be related to the occurrence of non-specific adsorption during salt aging in the synthesis(Hurst et al., 2006).

After analysis of gold nanoprobe stability, its capacity of discrimination was also compared, using ssDNA oligonucleotides (**Figure 3.24**). The obtained graph shows an increase of ratio A525/A600 for the non-complementary and complementary target from March to May. In the case of the complementary target, this observation corroborates the previous stated hypothesis, namely the decrease in oligonucleotide density at the gold nanoparticles surface. This may generate a decrease in the steric hindrance created between oligonucleotides, facilitating

the hybridisation of the nanoprobe to the target (Ravan et al., 2014). In the case of the non-complementary target, the increase in ratio might also be related with the loss of probe functionalisation. Lower density of oligonucleotides at the surface means that the remaining oligonucleotides have tendency to occupy the surface of the particle, hindering its aggregation (Ravan et al., 2014).

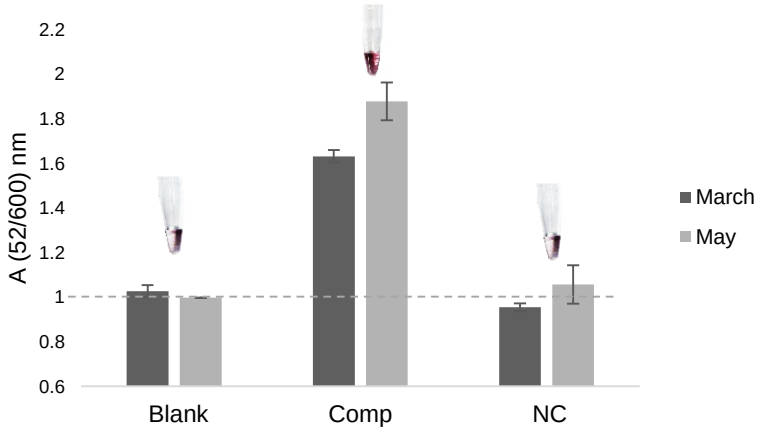

Figure 3.24 Hybridisation assay with ssDNA oligonucleotides for the 3 batches of *ttrRSBCA* gold nanoprobe. Comparison of nanoprobe behaviour 2 months after synthesis (May) with the previous registered data (March). Au-nanoprobes aggregation was measured by ratio of aggregation (ratio of SPR intensity at 525 and 600 nm) for the assay tests - 2.5 nM Au-nanoprobe, 10 mM phosphate buffer (pH 7) +0.1M NaCl, ssDNA targets at a final concentration of 0.3 pmol. µL-1. All spectrophotometric data was collected 5 minutes after 22.5 mM salt addition and error bars represent the standard deviation of three independent assays.

On the other hand, DLS data present an increase in the gold nanoprobes hydrodynamic ratio (**Figure 3.25**), namely from 32.1 nm to 52.8 nm.

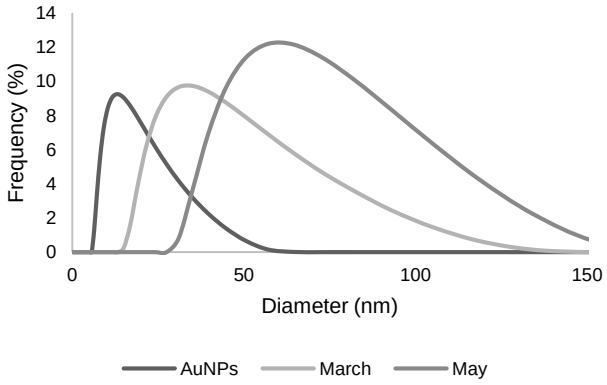

Figure 3.25 DLS of AuNPs and *ttrRSBCA* probe 2 months after synthesis and comparison with previous registered data.

Since the value of ratio obtained 2 months after gold nanoprobe synthesis increased for approximately to double, it could indicate gold nanoparticles aggregation. However, this possibility is not in agreement with the spectrophotometric data obtained. If it has occurred any aggregation, a shift in the SPR peak to 600 nm, characteristic of the inter-particle distance decrease, would have been observed in **Figure 3.23 A**. Therefore, an explanation for this observation might be

the limitations associated to DLS technique. It is easily influenced by the presence of groups of smaller particles or small populations of large particles, which can be translated into a greater overall nanoparticle size (Hinterwirth et al., 2013). This might justify the observed result, indicating that there are several populations of nanoparticles of different sizes in the solution.

3.3.2.3 Batch 4

Spherical nucleic acid conjugates (gold nanoprobes) have become an increasingly powerful tool in Biomedicine. The first step for all downstream applications is to attach thiolated DNA to AuNPs in order to achieve a stable conjugate. In spite of seeming simple, this reaction based on the well-known thiol/gold chemistry turns out not to be very straightforward since both DNA and AuNPs are negatively charged (Zhang et al., 2013). Considering this factor and the effects studied previously in nanoprobe Batch 3 synthesis, the last synthesized probe was studied under similar conditions. The results are presented below (**Figure 3.26**).

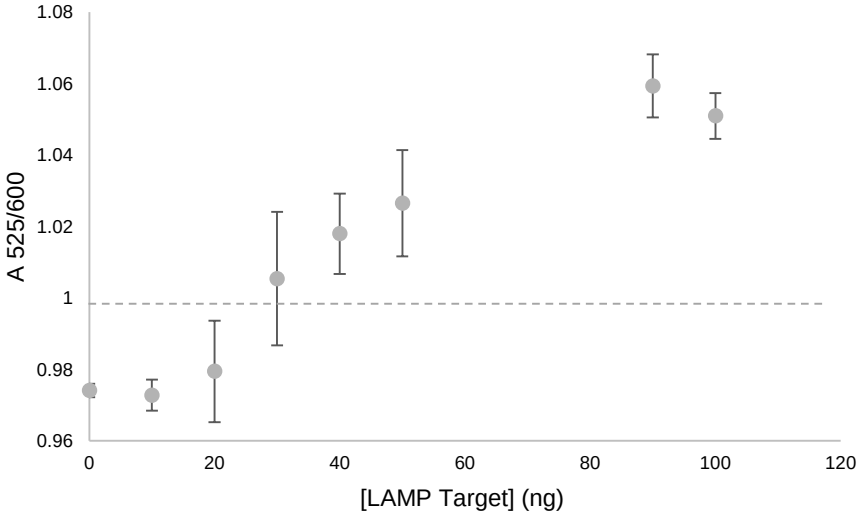

Figure 3.26 Limit of Detection (LOD) profile for *ttrRSBCA* probe Batch 4. Ratio of absorbance for *ttrRSBCA* Au-nanoprobe conducted with 2.5 Nm of Au-nanoprobe on phosphate buffer 10Mm (pH7+0.1M NaCl) and with purified full complementary LAMP products. Aggregation induction was carried out by increasing the ionic strength up to 60 mM with the addition of $MgCl_2$. All spectra were taken 5 min after salt addition. Dots represent the average of three independent measurements and the error bars indicate standard deviation.

Upon hybridisation with LAMP complementary target, an increase in gold nanoprobe stability was observed when compared with synthetic oligonucleotide detection in this batch. Therefore, a higher concentration of electrolyte (60 mM instead of 50 mM) was needed in order to achieve detection of the amplification product. This fact might be justified by the steric hindrance generated by LAMP amplification products, which is higher than the generated by ssDNA, reducing nanoprobe aggregation probability.

Considering the ratio A525/A600 defined in the previous sections, one can observe in the figure above that this gold nanoprobe batch detects complementary product in a concentration

above 50 ng/µL (r>1 which proves the majority of non-aggregated species in solution). This value of LOD is lower than the concentration obtained for batch 3 (75 ng/µL) and higher than the value defined for the second synthesized gold nanoprobe (20 ng/µL) (**Figure A8 Appendix**), which may suggest that the fourth batch of gold nanoprobe presents an intermediate oligonucleotide density comparing with the other synthesized gold nanoprobes.

This figure also shows that gold nanoprobe was detecting correctly its complementary target. The next step was to check its discrimination capacity between complementary and non-complementary targets. Several conditions were tested (**Figure 3.27**).

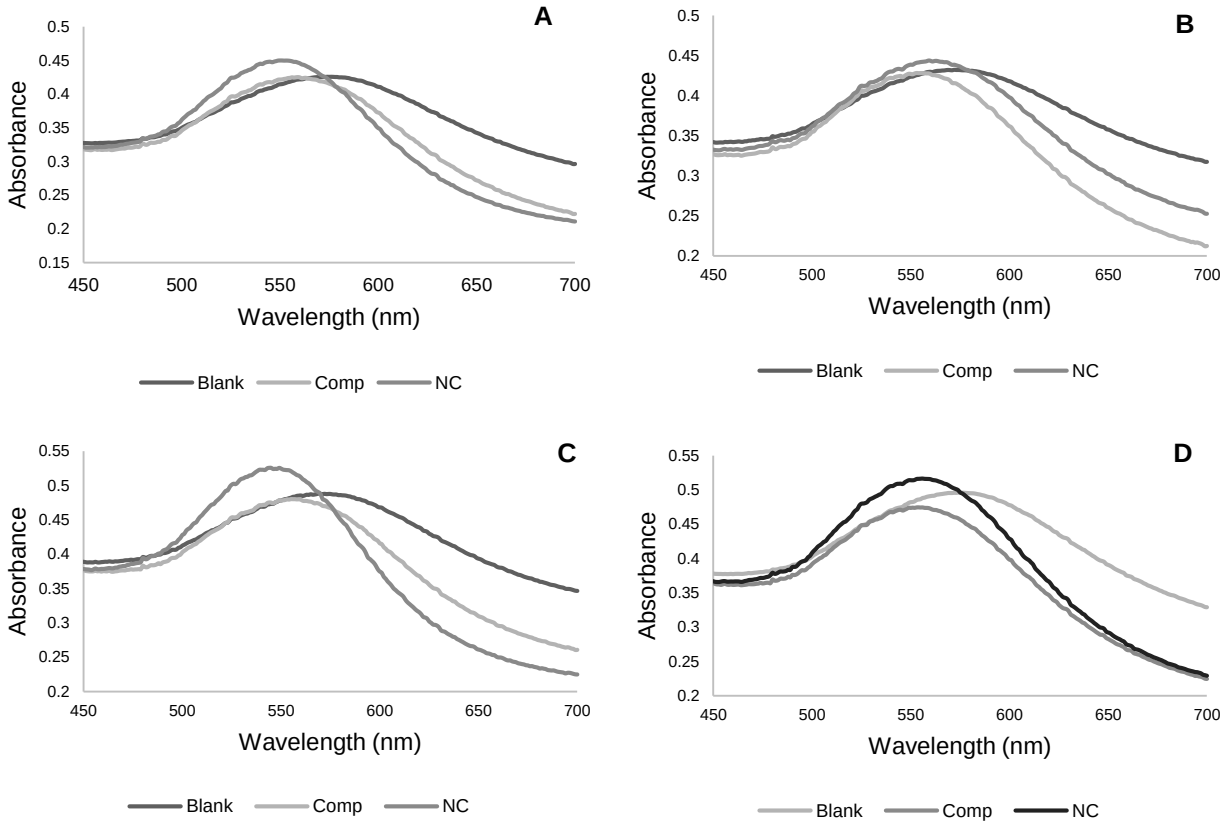

Figure 3.27 Hybridisation assay of LAMP product with batch 4 of *ttrRSBCA* gold nanoprobe. Au-nanoprobes aggregation was measured by ratio of aggregation (ratio of SPR intensity at 525 and 600 nm) for the assay tests - 2.5 nM Au-nanoprobe, 10 mM phosphate buffer (pH 7) +0,1M NaCl. Different DNA target and electrolyte final concentrations were tested, respectively: **A)** 100 ng target DNA and 62.5 mM MgCl2; **B)** 100 ng target DNA and 65 mM $MgCl_2$; **C)** 100 ng DNA target and 67.5 mM $MgCl_2$; **D)** 80 ng target DNA and 65 mM electrolyte. All spectrophotometric data was collected 5 minutes after salt addition

As stated before, this project is based in the non-cross linking method, where a DNA sample is added to the Au-nanoprobes followed by a salt which promotes nanoprobe aggregation. In the presence of complementary DNA, it hybridises with the probe, protecting it from aggregation. On the other hand, if the target is non-complementary, the Au-nanoprobes remain unprotected, aggregating. The colorimetric change of disperse versus aggregated nanoparticles allows a visual analysis which can also be quantified in a spectrophotometer. In **figure 3.27** this

colorimetric change was only observed for the Blank, where the gold nanoprobe aggregation promoted the shift of the SPR peak to 600 nm region. It means LAMP products discrimination between complementary and non-complementary target was not successful, since gold nanoprobe was detecting both targets, appearing red in solution. This situation might be related to probe percentage of GC (70%) which may be responsible to non-specific hybridisation, an issue which was discussed previously (**section 3.1.2**).

In order to overcome this situation, increasing salt concentrations (62.5; 65 and 67.5 mM) were added as a way of promoting gold nanoprobe aggregation and, consequently, preventing recognition of non-complementary target. However, as it can be observed in the figure above, the gold nanoprobe continued to detect it. Target concentration was also decreased from 100 ng to 80 ng (**Figure 3.27 D**) but target discrimination was not achieved.

In order to understand these observations, an alignment between the gold nanoprobe and the non-complementary target sequence and its LAMP primers (which might not be eliminated in DNA purification) was performed. The similarity degree found between these sequences presented a low value, which cannot be used to justify NC target detection **(Figure A9 Appendix).**

Other conditions were tested in the gold nanoprobe and it was found one where discrimination was achieved (**Figure 3.28**).

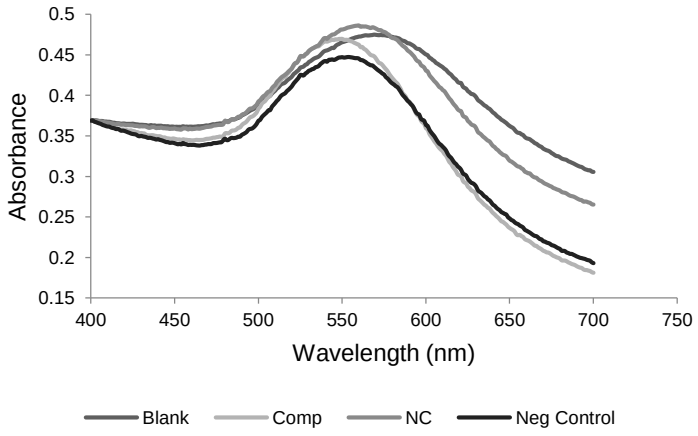

Figure 3.28 Hybridisation assay of LAMP product with batch 4 of *ttrRSBCA* gold nanoprobe. Au-nanoprobes aggregation was measured by ratio of aggregation (ratio of SPR intensity at 525 and 600 nm) for the assay tests - 2.5 nM Au-nanoprobe, 10 mM phosphate buffer (pH 7) +0.1M NaCl and 80 ng complementary, non-complementary target DNA and negative control from 45 minutes' reactions after 67.5 mM salt addition.

In this figure it is observed the deviation of SPR peak from 525 nm to 600 nm in the presence of non-complementary target, which means that gold nanoprobe was not able to detect it, leading to its aggregation. The used conditions are similar to the used in figure **3.27D,** except the LAMP amplification conditions of the non-complementary target. The previous tests (**Figure 3.27**) were performed using non-complementary LAMP products from an amplification reaction of 90 minutes while the complementary target was amplified in 45 minutes. This might explain why the gold nanoprobe was detecting both targets. Although LAMP reaction reaches a threshold

where no more copies of DNA are obtained, probably the number of copies of DNA obtained in 90 minutes is higher than in 45 minutes. Therefore, although the same concentration of complementary and non-complementary target is being applied to the gold nanoprobe, the number of copies of DNA present per ng will be higher, being in excess in the reaction, allowing its detection. This hypothesis undermines the reliability and sensitivity of the test because if non-complementary target is present in a higher amount in the environment the gold nanoprobe detects it equally, which would originate false positives. In **figure 3.28** gold nanoprobe is discriminating between both targets but is still detecting negative control of LAMP reaction, which may indicate that the non-specific amplification observed in the gel electrophoresis might be from *Salmonella* contamination (**see section 3.2**).

The problem of discrimination of the gold nanoprobe for LAMP products might be related with two factors: probe sequence or LAMP products. In order to check these hypotheses, the gold nanoprobe was submitted to tests with PCR products (**Figure 3.29**).

3.3.3 PCR Products

Although LAMP has recently become a promising alternative for pathogen detection, PCR is still a widely used technique (Odumeru & León-Velarde, 2012). Thus, as comparison, a PCR assay targeting *ttrRSBCA* locus was performed using the LAMP primers and the same reagents (**Figure 3.29**).

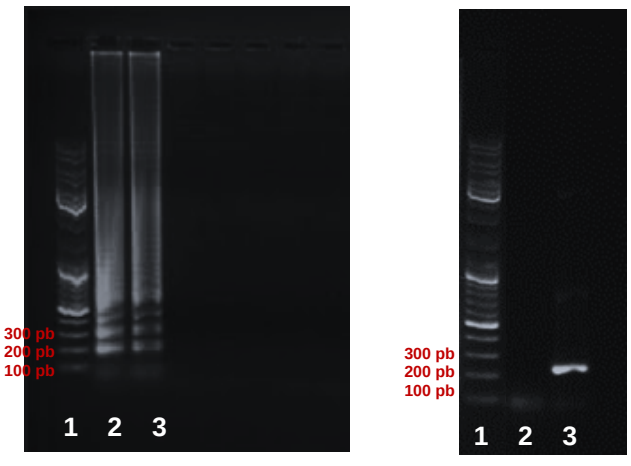

(A) **(B)**

Figure 3.29 Agarose gel 1% electrophoresis in 100 mL TAE 1x + 15µL of gel red (85 V 70 min) of amplification products of *ttrRSBCA* locus from *Salmonella* (A) 1 – Gene ruler DNA ladder; 2 - Negative control of LAMP amplification reaction where non-specific amplification is present; 3- LAMP product at 65ºC for 45 minutes; **(B)** 1 – Gene Ruler DNA ladder**.** PCR amplification product of 232 pb (3) using the same reagents as A**,** where non-specific amplification at negative control is present (2).

Contrary to LAMP, it was observed the absence of non-specific amplification in negative control in PCR. Through this observation we can reach various speculations. First, since the used reagents are the same in both assays, the possibility of contamination of the reagents may be eliminated. On the other hand, this absence of non-specific amplification in PCR negative control

might be related to the sensitivity of PCR. Besides being a highly robust technique, LAMP is very sensitive and specific, having the capability of synthesizing a large amount of DNA (10-20µg/25µl) from an infinitesimal quantity of template (Siyi Chen et al., 2011), which might not be detected by PCR.

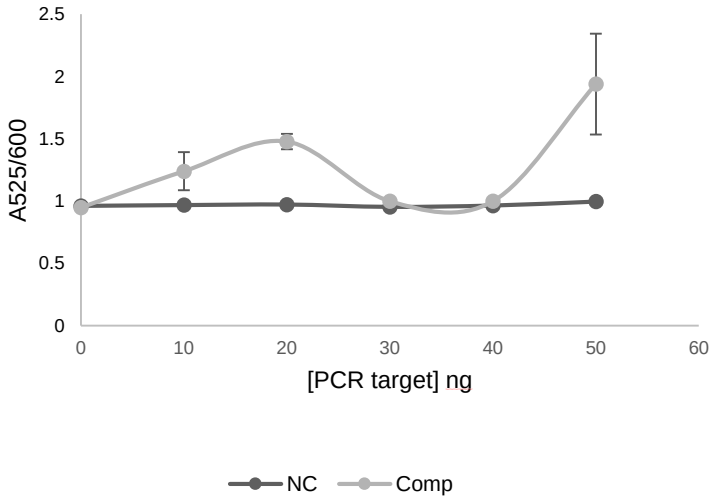

Figure 3.30 Hybridisation assay of PCR product with batch 4 of ttrRSBCA gold nanoprobe. Au-nanoprobes aggregation was measured by ratio of aggregation (ratio of SPR intensity at 525 and 600 nm) for the assay tests - 2.5 nM Au-nanoprobe, 10 mM phosphate buffer (pH 7) +0.1M NaCl. Different DNA target concentrations were tested (from 0 to 50 ng). All spectrophotometric data was collected 5 minutes after 52.5 mM salt addition. Dots represent the average of three independent measurements and the error bars indicate standard deviation.

By analysing this figure one can infer that, contrary to what happened with LAMP products, the gold nanoprobe is correctly discriminating between complementary and non-complementary PCR targets. As the DNA concentration increases (from 0 to 50 ng), A525/600 ratio increases at the same time as expected. The number of aggregated species (A600) has tendency to decrease due to the presence of complementary target which causes steric hindrance, preventing gold nanoprobe aggregation. However, this increase is not linear, since it is observed an abrupt descent of A525/600 ratio for 30 ng and 40 ng of target. It may be explained by the fact that the used targets result from different PCR reactions. Since it is a stochastic process, even though the initial concentrations being tested in the gold nanoprobe are equal, they may contain less amount of DNA than expected. It may be justified by the hyperchromic effect of DNA. The absorption of single strand DNA is higher than double strand DNA (dsDNA). These concentration values were obtained using a UV-Vis Spectrophotometer (Nanodrop ND-1000). The values of absorbance registered may be a result of the hyperchromic effect of DNA. The hydrogen bonds between the paired bases in the double helix limits the resonance behaviour of the aromatic ring of the bases which results in decrease in the UV absorbance of dsDNA (Smith, 2004). On the other hand, ssDNA bases are in free form and do not form hydrogen bonds with complementary bases and ssDNA presents 40% higher absorbance at the same concentration

of dsDNA (Smith, 2004). Even after the purification process some dNTPs might present, contributing to the rising of absorbance value and, consequently, to the rising of concentration.

The non-complementary target curve presents constant values of A525/600 ratio (<1) even with the increase of this target. Thus, the gold nanoprobe is specific for its target. It means that the problem presented by the gold nanoprobe in the discrimination of LAMP products is not derived from its sequence but might be a question of thermodynamics.

In **figure 3.29** it is also observed that the limit of detection for PCR products is lower (10ng) than for LAMP products (50 ng) as observed in **figure 3.26.** This fact might be related with the differences in conformation and length between these products, which may influence their hybridisation with the gold nanoprobe. Since LAMP possesses higher sensitivity and specificity than PCR, it produces large amount product from an infinitesimal quantity of template (Chen et al., 2011). Moreover, the final amplification products are mixtures of many different sizes of stem-loop DNAs with several inverted repeats of the target sequence. Since these products possess much more complementary zones when compared with PCR products it would be expected to make easier the hybridisation with the gold nanoprobe and, consequently, less amount of DNA would be necessary in order to occur detection. However, it was not observed.

On the other hand, these facts may justify the reason why the gold nanoprobe has difficulty discriminating between complementary and non-complementary LAMP products. As discussed before, an alignment between the gold nanoprobe and the non-complementary target sequence and its LAMP primers was performed and the similarity degree found between these sequences presented a low value, which could not be used to justify NC target detection. However, since LAMP products are present in a very high concentration and possess a high number of copies, even if the number of bp complementary to the gold nanoprobe is low, their excess may facilitate the hybridisation with the gold nanoprobe, resulting in false positive results.

As referred before, the aim of this project was the development of a specific, sensitive and rapid test for *Salmonella* detection which allied LAMP amplification technique to gold nanoprobes. The rapidity would lie in LAMP technique, however the nanoprobe was not able to discriminate correctly these products. Therefore, in order to keep the rapidity of the test, the number of PCR cycles and, consequently, reaction time was decreased. The results are represented below.

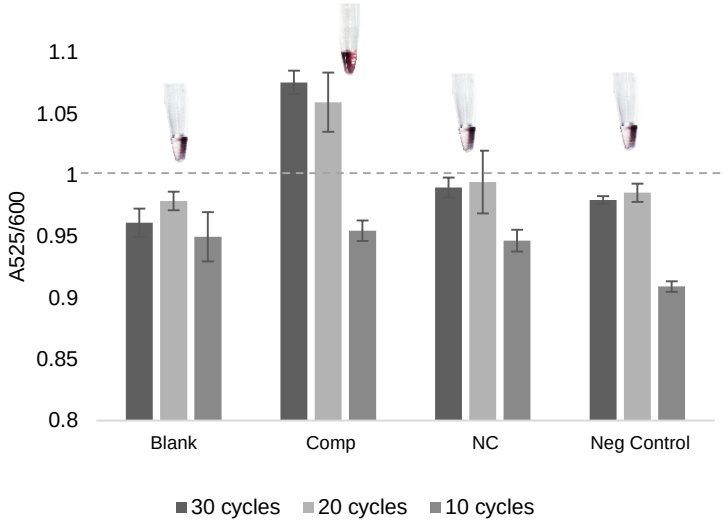

Figure 3.31 Hybridisation assay of PCR product with batch 4 of *ttrRSBCA* gold nanoprobe. Au-nanoprobes aggregation was measured by ratio of aggregation (ratio of SPR intensity at 525 and 600 nm) for the assay tests - 2.5 nM Au-nanoprobe, 10 mM phosphate buffer (pH 7) +0.1M NaCl. PCR products result from reactions of 10, 20 and 30 cycles. All spectrophotometric data was collected 5 minutes after 50 mM salt addition. Dots represent the average of three independent measurements and the error bars indicate standard deviation.

This figure presents the difference in detection performed by the gold nanoprobe between PCR products resultant from the usual 30 cycles reaction and 20 and 10 cycles. One can observe that occurs discrimination between complementary and non-complementary products (NC and Neg Control) from 20 and 30 cycles reactions. On the other hand, products from 10 cycles reaction are not detected. Nanoprobe is not detecting product probably due to the low number of DNA copies obtained from 10 cycles reaction. To enable the detection maybe the template used in PCR reaction needed to have a higher concentration, so less amplification cycles would be necessary. It should also be noticed that, contrary to what happened in LAMP detection (**Figure 3.28**), the gold nanoprobe is not detecting the Negative control of PCR reaction which is in agreement with the obtained agarose gel (**Figure 3.29**).

Very low numbers of *Salmonella* cells are typically found in food. However, such contamination may be fatal because of the possibility of multiplication of the cells, leading to a high risk for consumers (Malorny et al.,2008). Consequently, methods that can enumerate low levels of *Salmonella* are needed. Therefore, using the 20 cycles amplification condition, it was performed a gradient of concentration of template (1,5,10 and 20 ng) in PCR reaction. However, gold nanoprobe was not able to detect these amplification products. Thus, the LOD of the gold nanoprobe for PCR products is 20 cycles of PCR starting from 30 ng template.

4 Conclusion

A wide range of methods for the detection of *Salmonella* in food has been developed in the last decade. However, it still faces many inherent challenges. The complexity of food matrices and the presence of pathogens in low numbers in food products require several methods of concentrating and separating bacteria from food matrices, which make even rapid methods last days instead of hours. Therefore, the aim of this study was to develop a rapid, sensitive and inexpensive colorimetric test based in specific DNA-functionalised AuNPs (Au- Nanoprobes) to detect *Salmonella* amplified by LAMP technique.

Four batches of *ttrRSBCA* gold nanoprobe were synthesized under different conditions. These differences were denoted in their hybridisation capacity and stability. It was verified that a higher stability value (Batches 1 and 2) may be related with higher densities of thiol-modified oligonucleotides bound to AuNPs surface. This divergence in density values between batches might be attributed to synthesis conditions, namely lack of ionic strength and insufficient or absence of ultrasound time which have led to non-specific adsorptions occurred during functionalisation process. These difference in oligonucleotide density might also be explained by the different sizes of gold nanoparticles used in the syntheses of the gold nanoprobe. TEM confirmed that the gold nanoparticles used in batches 1 and 2 are smaller than the used in batches 3 and 4, presenting higher loading capacity and, consequently, leading to gold nanoprobes higher stability.

Batches 1 and 2 where synthesized at pH8 and 25 °C while batches 3 and 4 were resuspended in pH7 buffer and synthesized at 57°C. The increase in synthesis temperature was expected to make easy gold nanoprobe hybridisation since the probability of hairpin formation is lower in this condition, exposing DNA bases to the target. However, it was observed that at this pH and temperature conditions, discrimination between targets did not improve. Besides, pH7 might be related with a lower shelf life of gold nanoprobes as observed with Batch 3 stability change after 2 months.

When compared with Batches 1 and 2, Batches 3 and 4 present less stability and, consequently, are less functionalised due to the higher size of gold nanoparticles used in their syntheses. Therefore, their LOD present different values, which are in agreement with their characteristics. Batch 2 has a higher oligonucleotide loading, thus needs less target concentration in order to occur detection (20 ng/µL). On the other hand, batches 3 and 4, which are less functionalised, have LOD values of 75 ng/µL and 60 ng/µL for LAMP products, respectively. Although LAMP product detection was achieved, its discrimination was unsuccessful for Batch 4, which emphasizes the disadvantage of pH7 buffer for discrimination. PCR products were tested in gold nanoprobe and it was verified that the discrimination obtained for these products was better than for LAMP products. This may be related to thermodynamics, since there are differences in conformation and length between these products, which may influence their hybridisation with the gold nanoprobe. A way to address this issue could be the change of detection temperature from environment temperature to higher temperatures in order to increase

hybridisation specificity. However, this discrimination failure might also be related with the selected sequence for this study.

The sequence of gold nanoprobe used for detection of the target region (*ttrRSBCA* locus) plays a key role in the success of the colorimetric test and maybe has contributed to some problems occurred in its performance. Although the developed nanoprobe works better with PCR products and that the next step would be testing it in food, LAMP stills a more advantageous technique. Thus, an alternative to test this probe in food, would be to redesign its sequence. However, considering that LAMP needs 4 primers which should follow certain criteria it would be difficult to find an alternative to the used primers and sequence for the *ttr* locus. On the other hand, another locus present in *Salmonella* could be used as target but, even if the gold nanoprobe was able to detect the LAMP products that contained this region, the risk of having false negatives would be higher because this region would not be conserved as *ttr* locus and no target sequence would be present in the reaction.

False negative results can also mean that the reaction was inhibited due to malfunction of the thermal cycler, incorrect LAMP mixture, poor polymerase activity, and, not least, the presence of inhibitory substances in the sample matrix, which would turn into a threat for the population (Hoorfar et al., 2003). Therefore, apart from the sequence used as target, the inclusion of an IAC (Internal Amplification Control in the reaction would solve this issue, because a control signal will always be produced when there is no target sequence present. Therefore, it would be a good indicator of LAMP failure in the future.

LAMP was expected to provide robustness, high sensitivity, specificity and simplicity to detection. However, in this study it was observed that this sensitivity can be disadvantageous since this technique synthesizes a large amount of DNA from an infinitesimal quantity of template, which may justify the presence of a non-specific amplification observed in the negative control. Several hypotheses were proposed to explain this amplification, namely the great similarity verified between *Salmonella* and *E. coli*, which may be present in the laboratory as aerosol and affect LAMP amplification; and self-amplification of primers. Different variables were tested in order to optimise the reaction and it was verified that DMSO has great effect in reaction specificity, avoiding primers self-annealing. The presence of this reagent in solution can also further have an effect in the nanoprobes stability and, therefore, should be taken into account when performing non-cross-linking.

The two methods combined in these thesis can bring several advantages to pathogen detection but still need some improvement individually. LAMP is a method, that, in spite of its advantages, namely robustness, specificity and rapidity is very sensitive to cross-over contamination. Besides, a tight control over nanoparticle functionalisation should be considered in this case, as small variations can drastically change their properties and behaviour in detection methods. After optimisation of this test, it could also be applied in the identification and discrimination of *Salmonella* serovars.

The system developed here must be taken as proof-of-concept. For further tests in food samples many questions on sample handling and preparation still need to be addressed, as Au-

NP systems and LAMP technique can be rather unstable in complex media, which may hinder application at point-of-care for pathogen detection.

REFERENCES

Andino, A., & Hanning, I. (2015). Salmonella enterica: Survival, colonization, and virulence differences among serovars. *Scientific World Journal*, *2015.*

Ao, T. T., Feasey, N. A., Gordon, M. A., Keddy, K. H., Angulo, F. J., & Crump, J. A. (2015). Global Burden of Invasive Nontyphoidal *Salmonella* Disease, 2010. *Emerging Infectious Diseases*, *21*(6), 941–949.

Baptista, P., Doria, G., Henriques, D., Pereira, E., & Franco, R. (2005). Colorimetric detection of eukaryotic gene expression with DNA-derivatized gold nanoparticles. *Journal of Biotechnology*, *119*(2), 111–117.

Baptista, P., Pereira, E., Eaton, P., Doria, G., Miranda, A., Gomes, I. & Franco, R. (2008). Gold nanoparticles for the development of clinical diagnosis methods. *Analytical and Bioanalytical Chemistry*, *391*(3), 943–950.

Baptista, P. V, Doria, G., Quaresma, P., Cavadas, M., Neves, C. S., Gomes, I. & Franco, R. (2011). *Chapter 11 - Nanoparticles in Molecular Diagnostics*. *Nanoparticles in Translational Science and Medicine* ,104, 427-488.

Baptista, P. V., Koziol-Montewka, M., Paluch-Oles, J., Doria, G., & Franco, R. (2006). Gold-nanoparticle-probe-based assay for rapid and direct detection of *Mycobacterium tuberculosis* DNA in clinical samples. *Clinical Chemistry*, 52 (7), 1433-1434.

Bhattacharyya, D., Singh, S., & Satnalika, N. (2009). Nanotechnology , Big things from a Tiny World : a Review. *Science and Technology*, *2*(3), 29–38.

Brown, K. A., Park, S., & Hamad-schifferli, K. (2008). Nucleotide - Surface Interactions in DNA-Modified Au - Nanoparticle Conjugates : Sequence Effects on Reactivity and Hybridization, 112 (20),7517–7521.

Baylis, C., Uyttendaele, M., Han Joosten, N.& Davies, & A. (2011). *The Enterobacteriaceae and their Significance to the Food Industry*.

Chakrabarti, R., & Schutt, C. E. (2001). The enhancement of PCR amplification by low molecular-weight sulfones. *Gene*, *274*(1-2), 293–298.

Chandra, P., Singh, J., Singh, A., Srivastava, A., Goyal, R. N., & Shim, Y. B. (2013). Gold Nanoparticles and Nanocomposites in Clinical Diagnostics Using Electrochemical Methods. *Journal of Nanoparticles*, *2013*.

Chau, T. T., Campbell, J. I., Galindo, C. M., Hoang, N. V. M., To, S. D., Nga, T. T. T., & Dolecek, C. (2007). Antimicrobial drug resistance of *Salmonella enterica* serovar Typhi in Asia and molecular mechanism of reduced susceptibility to the fluoroquinolones. *Antimicrobial Agents and Chemotherapy*, *51*(12), 4315–4323.

Chen, S., Wang, F., Beaulieu, J. C., Stein, R. E., & Ge, B. (2011). Rapid Detection of Viable Salmonellae in Produce by Coupling Propidium Monoazide with Loop-Mediated Isothermal Amplification. *Applied and Environmental Microbiology*, *77*(12), 4008–4016.

Coburn, B., Grassl, G. A., & Finlay, B. (2007). *Salmonella*, the host and disease: a brief review. *Immunology and Cell Biology*, *85*, 112–118.

Conde, J., Dias, J. T., Grazú, V., Moros, M., Baptista, P. V, & de la Fuente, J. M. (2014). Revisiting 30 years of biofunctionalisation and surface chemistry of inorganic nanoparticles for nanomedicine. *Frontiers in Chemistry*, *2*(July), 48.

D'Aoust, J.-Y. (1991). Pathogenicity of foodborne *Salmonella. International Journal of Food Microbiology*, *12*(1), 17–40.

Deguo, W., Guicheng, H., Fugui, W., Yonggang, L., & Daxi, R. (2008). Drawback of loop-mediated isothermal amplification. *African Journal of Food Science*, 2, 83–86.

Demers, L. M., Mirkin, C. A., Mucic, R. C., Reynolds, R. A., Letsinger, R. L., Elghanian, R., & Viswanadham, G. (2000). A Fluorescence-Based Method for Determining the Surface Coverage and Hybridization Efficiency of Thiol-Capped Oligonucleotides Bound to Gold Thin Films and Nanoparticles. *Analytical Chemistry*, *72*(22), 5535–5541.

Doktycz, M. J. (1997). Nucleic Acids : Thermal Stability and Denaturation. *Encyclopedia of Life Sciences*, 3123–3140.

Doria, G. M. R. P. (2010). DNA Nanoprobes for Molecular Detection (Nanossondas de DNA para Detecção Molecular), Faculdade de Ciências e Tecnologias da Universidade Nova de Lisboa.

Dreaden, E. C., Alkilany, A. M., Huang, X., Murphy, C. J., & El-Sayed, M. A. (2012). The golden age: gold nanoparticles for biomedicine. *Chem. Soc. Rev.*, *41*(7), 2740–2779.

Eustis, S., & el-Sayed, M. A. (2006). Why gold nanoparticles are more precious than pretty gold: noble metal surface plasmon resonance and its enhancement of the radiative and nonradiative properties of nanocrystals of different shapes. *Chemical Society Reviews*, *35*(3), 209–217.

Feynman, R. P. (1960),There's plenty of room at the bottom. *Engineering and Science*, 23,22-36.

Francois, P., Tangomo, M., Hibbs, J., Bonetti, E. J., Boehme, C. C., Notomi, T.,& Schrenzel, J. (2011). Robustness of a loop-mediated isothermal amplification reaction for diagnostic applications. *FEMS Immunology and Medical Microbiology*, *62*(1), 41–48.

Fukushima, M., Kakinuma, K., & Kawaguchi, R. (2002). Phylogenetic analysis of *Salmonella*, *Shigella*, and *Escherichia coli* strains on the basis of the gyrB gene sequence. *Journal of Clinical Microbiology*, *40*(8), 2779–2785.

G.Doria, R.Franco, & P.Baptista. (2007). Nanodiagnostics: fast colorimetric method for single nucleotide polymorphism/mutation detection. *IET Nanobiotechnology IET*, *1*(4), 53–57.

Ge, B., & Meng, J. (2009). Advanced Technologies for Pathogen and Toxin Detection in Foods: Current Applications and Future Directions. *JALA - Journal of the Association for Laboratory Automation*, *14*(4), 235–241.

Ghosh, D., & Chattopadhyay, N. (2013). Gold nanoparticles: acceptors for efficient energy transfer from the photoexcited fluorophores. *Optics and Photonics Journal*, *3*(March), 18–26.

Haiss, W., Thanh, N. T. K., Aveyard, J., & Fernig, D. G. (2007). Determination of Size and Concentration of Gold Nanoparticles from UV − Vis Spectra, *79*(October), 788–800.

Hara-Kudo, Y., Yoshino, M., Kojima, T., & Ikedo, M. (2005). Loop-mediated isothermal amplification for the rapid detection of Salmonella. *FEMS Microbiology Letters*, *253*(1), 155–161.

Hensel, M., Hinsley, a P., Nikolaus, T., Sawers, G., & Berks, B. C. (1999). The genetic basis of tetrathionate respiration in Salmonella typhimurium. *Molecular Microbiology*, *32*(2), 275–

Hill, H. D., Millstone, J. E., Banholzer, M. J., & Mirkin, C. A. (2009). The role radius of curvature plays in thiolated oligonucleotide loading on gold nanoparticles. *ACS Nano*, *3*(2), 418–24.

Hinterwirth, H., Wiedmer, S. K., Moilanen, M., Lehner, A., Allmaier, G., Waitz, T., & Lämmerhofer, M. (2013). Comparative method evaluation for size and size- distribution analysis of gold nanoparticles. *Journal of Separation Science*, *36*(17), 2952–2961.

Hoorfar, J., Cook, N., Malorny, B., Wagner, M., Medici, D. De, Abdulmawjood, A., & Fach, P. (2003). Making Internal Amplification Control Mandatory for Diagnostic PCR. *Society*, *41*(12).

Hsieh, K., Mage, P. L., Csordas, A. T., Eisenstein, M., & Soh, H. T. (2014). Simultaneous elimination of carryover contamination and detection of DNA with uracil-DNA-glycosylase-supplemented loop-mediated isothermal amplification (UDG-LAMP). *Chemical Communications (Cambridge, England)*, *50*(28), 3747–3749.

Hu, S., Li, M., Zhong, L., Lu, S., Liu, Z., Pu, J.,& Huang, X. (2015). Development of reverse-transcription loop-mediated isothermal amplification assay for rapid detection and differentiation of dengue virus serotypes 1–4. *BMC Microbiology*, *15*(1), 265.

Hur, J., Jawale, C., & Lee, J. H. (2012). Antimicrobial resistance of Salmonella isolated from food animals: A review. *Food Research International*, *45*(2), 819–830.

Hurst, S. J., Lytton-Jean, A. K. R., & Mirkin, C. A. (2006). Maximizing DNA Loading on a Range of Gold Nanoparticle Sizes. *Analytical Chemistry*, *78*(24), 8313–8318.

Jain, P. K., Lee, K. S., El-Sayed, I. H., & El-Sayed, M. A. (2006). Calculated absorption and scattering properties of gold nanoparticles of different size, shape, and composition: Applications in biological imaging and biomedicine. *The Journal of Physical Chemistry B*, 110,7238-7248.

Jasson, V., Jacxsens, L., Luning, P., Rajkovic, A., & Uyttendaele, M. (2010). Alternative microbial methods: An overview and selection criteria. *Food Microbiology*, *27*(6), 710–730.

Ji, X., Song, X., Li, J., Bai, Y., Yang, W., & Peng, X. (2007). Size Control of Gold Nanocrystals in Citrate Reduction: The Third Role of Citrate. *Journal of the American Chemical Society*, *129*(45), 13939–13948.

Kalidasan, K., Neo, J. L., & Uttamchandani, M. (2013). Direct visual detection of *Salmonella* genomic DNA using gold nanoparticles. *Molecular BioSystems*, *9*(4), 618–621.

Kato, H., Suzuki, M., Fujita, K., Horie, M., Endoh, S., Yoshida, Y.,& Kinugasa, S. (2009). Reliable size determination of nanoparticles using dynamic light scattering method for in vitro toxicology assessment. *Toxicology in Vitro : An International Journal Published in Association with BIBRA*, *23*(5), 927–934.

Khlebtsov, N. G., & Dykman, L. A. (2010). Optical properties and biomedical applications of

plasmonic nanoparticles. *Journal of Quantitative Spectroscopy and Radiative Transfer*, *111*(1), 1–35.

Kokkinos, P. A., Ziros, P. G., Bellou, M., & Vantarakis, A. (2014). Loop-Mediated Isothermal Amplification (LAMP) for the Detection of Salmonella in Food. *Food Analytical Methods*, *7*(2), 512–526.

Lee, K.-M., Runyon, M., Herrman, T. J., Phillips, R., & Hsieh, J. (2015). Review of *Salmonella* detection and identification methods: Aspects of rapid emergency response and food safety. *Food Control*, *47*, 264–276.

Lee, P. C., & Meisel, D. (1982). Adsorption and surface-enhanced Raman of dyes on silver and gold sols. *J.Phys.Chem.*, *86*(17), 3391–3395.

Li, H., & Rothberg, L. (2004). Colorimetric detection of DNA sequences based on electrostatic interactions with unmodified gold nanoparticles. *Proceedings of the National Academy of Sciences of the United States of America*, *101*(39), 14036–14039.

Lim, J., Yeap, S. P., Che, H. X., & Low, S. C. (2013). Characterization of magnetic nanoparticle by dynamic light scattering. *Nanoscale Research Letters*, *8*(1), 381.

Liz-Marzán, L. M. (2006). Tailoring surface plasmons through the morphology and assembly of metal nanoparticles. *Langmuir*, *22*(1), 32–41.

Louis, C., & Plucherry, O. (2012). *Gold Nanoparticles for physics, chemistry and biology*. Université Pierre et Marie Curie, France: Imperial College Press.

Lv, B., Dai, Y., Liu, J., Zhuge, Q., & Li, D. (2015). The Effect of Dimethyl Sulfoxide on Supercoiled DNA Relaxation Catalyzed by Type i Topoisomerases. *BioMed Research International*, *2015*.

Maciorowski, K. G., Herrera, P., Jones, F. T., Pillai, S. D., & Ricke, S. C. (2006). Cultural and Immunological Detection Methods for Salmonella spp. in Animal Feeds -- A Review. *Veterinary Research Communications*, *30*(2), 127–137.

Majowicz, S. E., Musto, J., Scallan, E., Angulo, F. J., Kirk, M., O'Brien, S. J., & Hoekstra, R. M. (2010). The Global Burden of Nontyphoidal Salmonella Gastroenteritis. *Clinical Infectious Diseases*, *50*(6), 882–889.

Malorny, B., Lofstrom, C., Wagner, M., Kramer, N., & Hoorfar, J. (2008). Enumeration of Salmonella bacteria in food and feed samples by real-time PCR for quantitative microbial risk assessment. *Applied and Environmental Microbiology*, *74*(5), 1299–1304.

Malorny, B., Paccassoni, E., Fach, P., Martin, A., Helmuth, R., & Bunge, C. (2004). Diagnostic Real-Time PCR for Detection of Salmonella in Food. *Applied and Environmental Microbiology*, *70*(12), 7046–7052.

Manzano, M., Cocolin, L., Astori, G., Pipan, C., Botta, G. ., Cantoni, C., & Comi, G. (1998). Development of a PCR microplate-capture hybridization method for simple, fast and sensitive detection ofSalmonellaserovars in food. *Molecular and Cellular Probes*, *12*(4), 227–234.

Martelli, F., & Davies, R. H. (2012). *Salmonella* serovars isolated from table eggs: An overview. *Food Research International*, *45*(2), 745–754.

McClelland, M., Sanderson, K. E., Spieth, J., Clifton, S. W., Latreille, P., Courtney, L., & Wilson, R. K. (2001). Complete genome sequence of *Salmonella* enterica serovar Typhimurium LT2. *Nature*, *413*(6858), 852–856.

Mead, P. S., Slutsker, L., Dietz, V., McCaig, L. F., Bresee, J. S., Shapiro, C., &Tauxe, R. V. (1999). Food-related illnesses and death in the United States. *Emerging Infectious Diseases*, *5*(5), 607–625.

Meneses, Y. E. (2010). Identification and Characterization of *Salmonella* Serotypes Isolated from Pork and Poultry from Commercial Sources. *Dissertations & Theses in Food Science and Technology*.

Mirkin, C. a, Letsinger, R. L., Mucic, R. C., & Storhoff, J. J. (1996). A DNA-based method for rationally assembling nanoparticles into macroscopic materials. *Nature*, 382 (6592), 607-609.

Morgan, E., Campbell, J. D., Rowe, S. C., Bispham, J., Stevens, M. P., Bowen, A. J., & Wallis, T. S. (2004). Identification of host-specific colonization factors of *Salmonella* enterica serovar Typhimurium. *Molecular Microbiology*, *54*(4), 994–1010.

Notomi, T., Okayama, H., Masubuchi, H., Yonekawa, T., Watanabe, K., Amino, N., & Hase, T. (2000). Loop-mediated isothermal amplification of DNA. *Nucleic Acids Research*, *28*(12).

Odumeru, J. a., & León-Velarde, C. G. (2012). *Salmonella* Detection Methods for Food and Food Ingredients. *Salmonella - A Dangerous Foodborne Pathogen*, 375 – 392.

Parak, W. J., Pellegrino, T., Micheel, C. M., Gerion, D., Williams, S. C., & Alivisatos, A. P. (2003). Conformation of Oligonucleotides Attached to Gold Nanocrystals Probed by Gel Electrophoresis. *Nano Letters*, *3*(1), 33–36.

Park, S. H., Aydin, M., Khatiwara, A., Dolan, M. C., Gilmore, D. F., Bouldin, J. L.,& Ricke, S. C. (2014). Current and emerging technologies for rapid detection and characterization of Salmonella in poultry and poultry products. *Food Microbiology*, *38*, 250–262.

Pellegrino, T., Sperling, R. A., Alivisatos, A. P., & Parak, W. J. (2007). Gel electrophoresis of gold-DNA nanoconjugates. *Journal of Biomedicine & Biotechnology*, *2007*.

Peterson, a W., Heaton, R. J., & Georgiadis, R. M. (2001). The effect of surface probe density on DNA hybridization. *Nucleic Acids Research*, *29*(24), 5163–5168.

Prasad, D., Shankaracharya, & Vidyarthi, A. S. (2011). Gold nanoparticles-based colorimetric assay for rapid detection of Salmonella species in food samples. *World Journal of Microbiology and Biotechnology*, *27*(9), 2227–2230.

Rai, M., & Kon, K. (2015). *NANOTECHNOLOGY IN DIAGNOSIS, TREATMENT AND PROPHYLAXIS OF INFECTIOUS DISEASES*. *Elsevier.*

Ravan, H., Kashanian, S., Sanadgol, N., Badoei-Dalfard, A., & Karami, Z. (2014). Strategies for optimizing DNA hybridization on surfaces. *Analytical Biochemistry*, *444*(1), 41–46.

Rychlik, W., Spencer, W. J., & Rhoads, R. E. (1991). Optimization of the annealing temperature for DNA amplification in vitro. *Nucleic Acids Research*, *19*(3), 698.

Saleh, M. (2009). Entwicklung von Testsystemen auf der Basis der “Loop Mediated Isothermal Amplification (LAMP)” Methode zum Nachweis von Yersinia ruckeri, dem Erreger der

Rotmaulseuche (ERM) und von Renibacterium salmoninarum, dem Erreger der bakteriellen Nierenkrankheit . *Control*.

Sánchez-Vargas, F. M., Abu-El-Haija, M. A., & Gómez-Duarte, O. G. (2011). *Salmonella* infections: An update on epidemiology, management, and prevention. *Travel Medicine and Infectious Disease*, *9*(6), 263–277.

Sandström, P., Boncheva, M., & Åkerman, B. (2003). Nonspecific and Thiol-Specific Binding of DNA to Gold Nanoparticles. *Langmuir*, *19*(18), 7537–7543.

Sato, K., Hosokawa, K., & Maeda, M. (2003). Rapid aggregation of gold nanoparticles induced by non-cross-linking DNA hybridization. *Journal of the American Chemical Society*, *125*(27), 8102–3.

Senarath, K. D., Usgodaarachchi, R. B., Navaratne, V., Nagahawatte, A., Wijayarathna, C. D., Alvitigala, J., & Goonasekara, C. L. (2014). Non Specific Amplification with the LAMP Technique in the Diagnosis of Tuberculosis in Sri Lankan Settings. *Journal of Tuberculosis Research*, *02*(04), 168–172.

Shao, Y., Zhu, S., Jin, C., & Chen, F. (2011). Development of multiplex loop-mediated isothermal amplification-RFLP (mLAMP-RFLP) to detect Salmonella spp. and Shigella spp. in milk. *International Journal of Food Microbiology*, *148*(2), 75–9.

Smith, A. (2004). Background: DNA hyperchromic & hypochromic effect. *Molecular Biochemistry*, 1–6.

Storhoff, J. J., Elghanian, R., Mirkin, C. A., & Letsinger, R. L. (2002). Sequence-Dependent Stability of DNA-Modified Gold Nanoparticles. *Langmuir*, *18*(17), 6666–6670.

Sun, L., Zhang, Z., Wang, S., Zhang, J., Li, H., Ren, L., &Zhang, Q. (2009). Effect of pH on the interaction of gold nanoparticles with DNA and application in the detection of human p53 gene mutation. *Nanoscale Research Letters*, *4*(3), 216–220.

Tirado, C., & Schmidt, K. (2001). WHO surveillance programme for control of foodborne infections and intoxications: preliminary results and trends across greater Europe. World Health Organization. *The Journal of Infection*, *43*(1), 80–84.

Tomita, N., Mori, Y., Kanda, H., & Notomi, T. (2008). Loop-mediated isothermal amplification (LAMP) of gene sequences and simple visual detection of products. *Nature Protocols*, *3*(5), 877–82.

Turkevich, J., Stevenson, P. C., & Hillier, J. (1951). A study of the nucleation and growth processes in the synthesis of colloidal gold. *Discussions of the Faraday Society*, *11*, 55.

Veigas, B. (2009). Au-Nanossondas Aplicação na detecção de *Mycobacterium* tuberculosis e Plasmodium berghei, Faculdade de Ciências e Tecnologias da Universidade Nova de Lisboa.

Veigas, B., Doria, G., & Baptista, P. (2012). Nanodiagnostics for Tuberculosis. *Understanding Tuberculosis - Global Experiences and Innovative Approaches to the Diagnosis*, 257–276.

Veigas, B., Pedrosa, P., Couto, I., Viveiros, M., & Baptista, P. V. (2013). Isothermal DNA amplification coupled to Au-nanoprobes for detection of mutations associated to Rifampicin resistance in *Mycobacterium tuberculosis*. *Journal of Nanobiotechnology*,

11(1), 1–6.

Wang, D. G., Brewster, J. D., Paul, M., & Tomasula, P. M. (2015). Two methods for increased specificity and sensitivity in loop-mediated isothermal amplification. *Molecules*, *20*(4), 6048–6059.

Wang, Y., Zhang, W., Yuan, Y., Ma, X., Zhang, H., Su, X.,& Ma, B. (2009). Study on Loop-Mediated Isothermal Amplification Assay for Detection of *Salmonella* in Meat Products. *2009 3rd International Conference on Bioinformatics and Biomedical Engineering*.

WATSON, J. D., & CRICK, F. H. (1953). The structure of DNA. *Cold Spring Harbor Symposia on Quantitative Biology*, *18*, 123–131.

Watson, P., Paulin, S., Bland, A., Jones, P., & Wallis, T. (1995). Characterization of intestinal invasion by Salmonella typhimurium and Salmonella dublin and effect of a mutation in the invH gene. *Infect. Immun.*, *63*(7), 2743–2754.

Wilcoxon, J. P., & Abrams, B. L. (2006). Synthesis, structure and properties of metal nanoclusters. *Chem. Soc. Rev.*, *35*(11), 1162–1194.

Yang, J. L., Ma, G. P., Yang, R., Yang, S. Q., Fu, L. Z., Cheng, A. C., & Xu, Z. Y. (2010). Simple and rapid detection of *Salmonella serovar* Enteritidis under field conditions by loop-mediated isothermal amplification. *Journal of Applied Microbiology*, *109*(5), 1715–1723.

Yang, Q., Wang, F., Jones, K. L., Meng, J., Prinyawiwatkul, W., & Ge, B. (2015). Evaluation of loop-mediated isothermal amplification for the rapid, reliable, and robust detection of *Salmonella* in produce. *Food Microbiology*, *46*, 485–493.

Yeh, Y.-C., Creran, B., & Rotello, V. M. (2012). Gold nanoparticles: preparation, properties, and applications in bionanotechnology. *Nanoscale*, *4*(6), 1871–1880.

Zadernowska, A., & Chajecka, W. (2012). Detection of *Salmonella spp* . Presence in Food. *Salmonella - A Dangerous Foodborne Pathogen*, 18,394-412.

Zanchet, D., Micheel, C. M., Parak, W. J., Gerion, D., & Alivisatos, A. P. (2001). Electrophoretic Isolation of Discrete Au Nanocrystal/DNA Conjugates. *Nano Letters*, *1*(1), 32–35.

Zhang, J., Lang, H. P., Yoshikawa, G., & Gerber, C. (2012). Optimization of DNA hybridization efficiency by pH-driven nanomechanical bending. *Langmuir : The ACS Journal of Surfaces and Colloids*, *28*(15), 6494–501.

Zhang, X., Gouriye, T., Göeken, K., Servos, M. R., Gill, R., & Liu, J. (2013). Toward fast and quantitative modification of large gold nanoparticles by thiolated DNA: Scaling of nanoscale forces, kinetics, and the need for thiol reduction. *Journal of Physical Chemistry C*, *117*(30), 15677–15684.

Zhao, P., Li, N., & Astruc, D. (2013). State of the art in gold nanoparticle synthesis. *Coordination Chemistry Reviews*, *257*(3-4), 638–665.

Zhuang, L., Gong, J., Li, Q., Zhu, C., Yu, Y., Dou, X., & Wang, C. (2014). Detection of *Salmonella* spp. by a loop-mediated isothermal amplification (LAMP) method targeting *bcfD* gene. *Letters in Applied Microbiology*, *59*(6), 658–664.

Zwirglmaier, K. (2005). Fluorescence in situ hybridisation (FISH) - The next generation. *FEMS Microbiology Letters*, *246*(2), 151–158.

APPENDIX

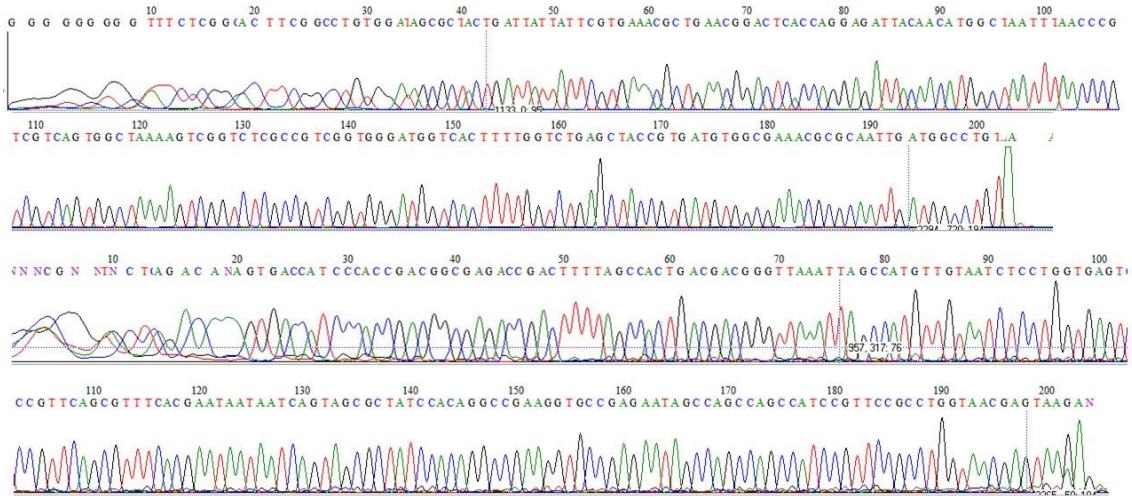

A1. Sequencing of the target region used in this study plus primers.

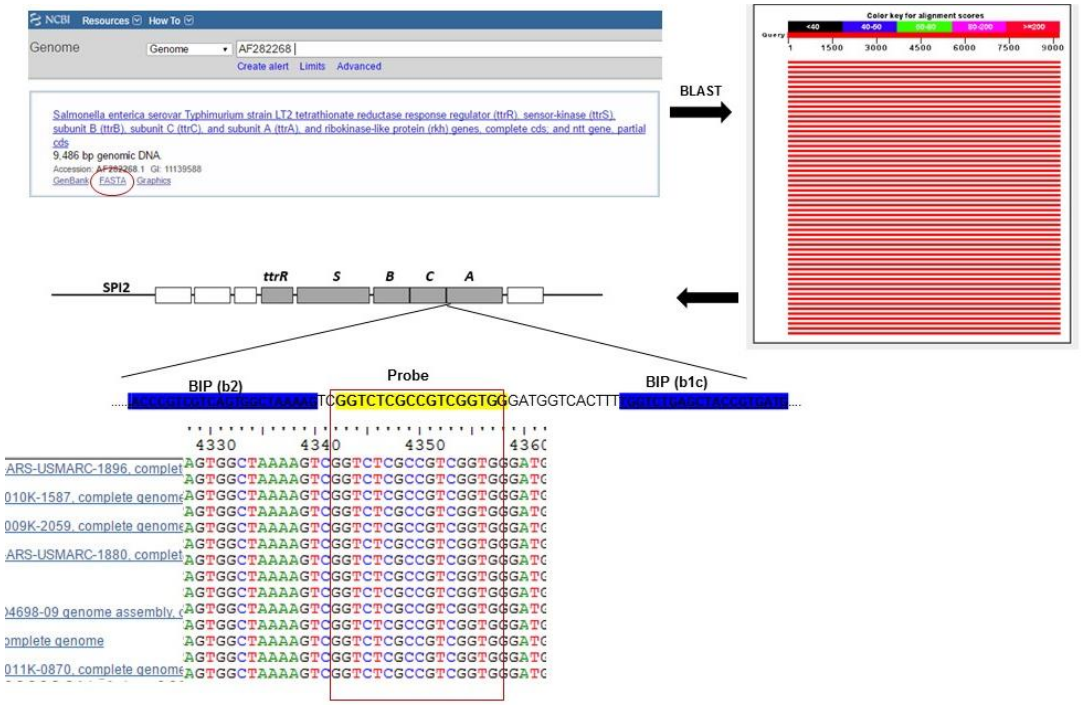

A2. Scheme of the alignment of 103 *Salmonella* strains from GenBank with the DNA sequence of *S.enterica* serotype Typhimurium *ttr* locus (GenBank accession no. AF282268)performed in BioEdit software. The red box indicates the part of the locus shared by all the aligned sequences which was used as target in this study for the gold nanoprobe (yellow).

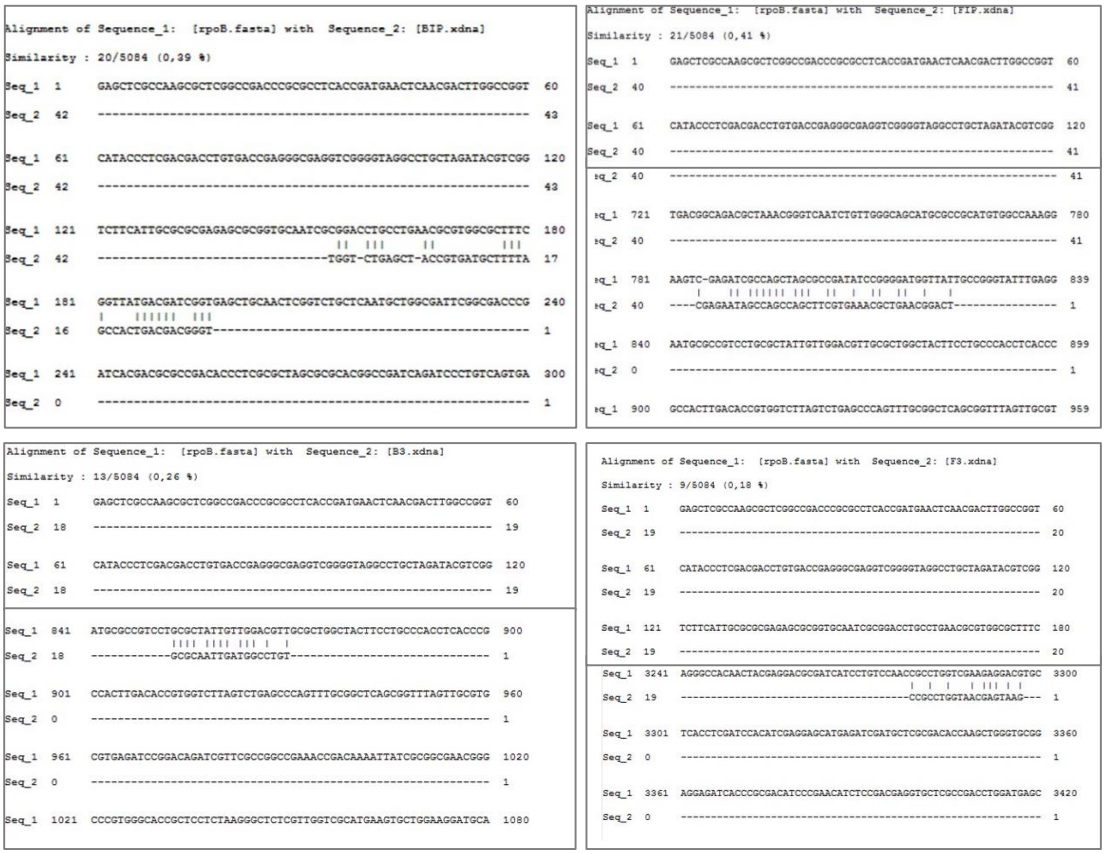

A3. Alignment of r*poB* gene sequence from *E. coli* with *ttrRSBCA* primers (from right to left BIP, FIP, F3, B3) performed in BioEdit software.

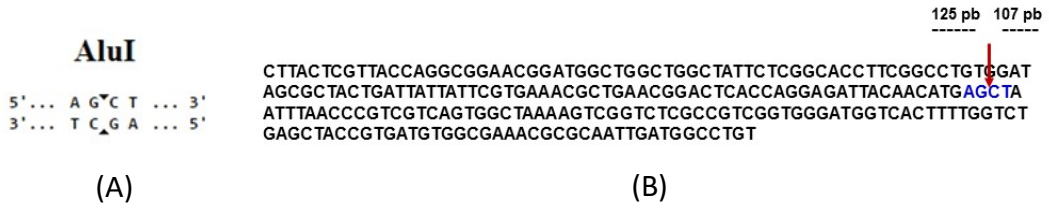

A4. Restriction site of *AluI* enzyme (A) and schematization of the application of *AluI* enzyme in the target region(B). After digestion the 232 bp sequence is divided in two parts of 125 bp and 107 bp.

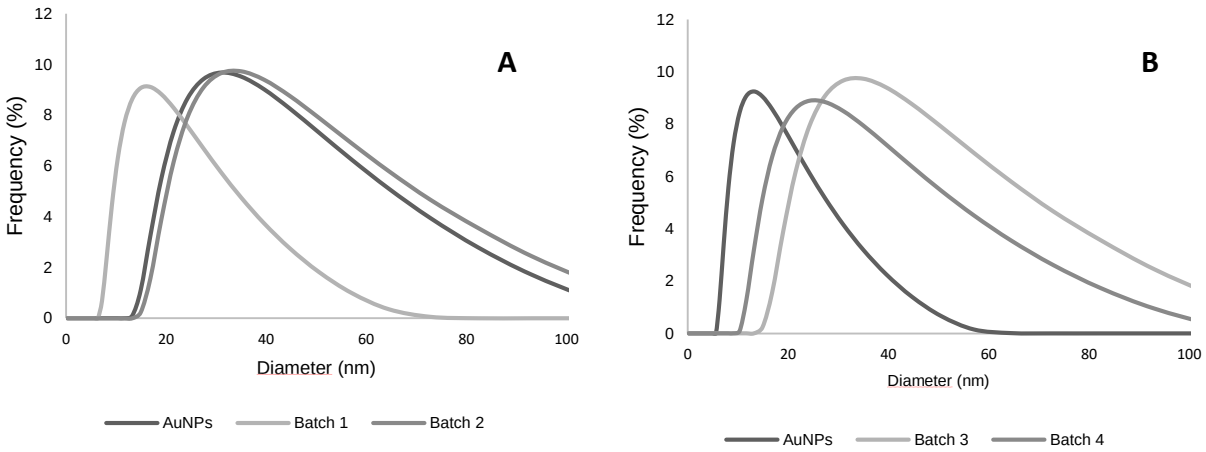

A5. DLS Analysis of AuNPs and Au-nanoprobes. Comparison between Batch 1 gold nanoparticles with gold nanoprobe batches 1 and 2 (**A**) and Batch 2 gold nanoparticles with gold nanoprobe batches 3 and 4 (**B**). An increase in hydrodynamic radius is observed in all synthesized probes when compared to the respective of gold nanoparticles batches.

A6. DLS Data obtained for the studied batches of gold nanoparticles and gold nanoprobes.

	Z-Average (nm)	PI
Nanoparticles Batch 1	15,7	0,237
Nanoprobe Batch 1	29,8	0,26
Nanoprobe Batch 2	31,7	0,47
Nanoparticles Batch 2	14,5	0,07
Nanoprobe Batch 3	32,1	0,439
Nanoprobe Batch 4	23,3	0,303

A7. The four studied probes (Batches 1, 2, 3 and 4) presented different maximum absorbance for the aggregated state. The ratio (A non-aggregated/ A aggregated) with better discrimination (spectrophotometric and colorimetric) was studied for each gold nanoprobe. As example, the study performed with probe batch 2 at pH8 phosphate buffer is represented below.

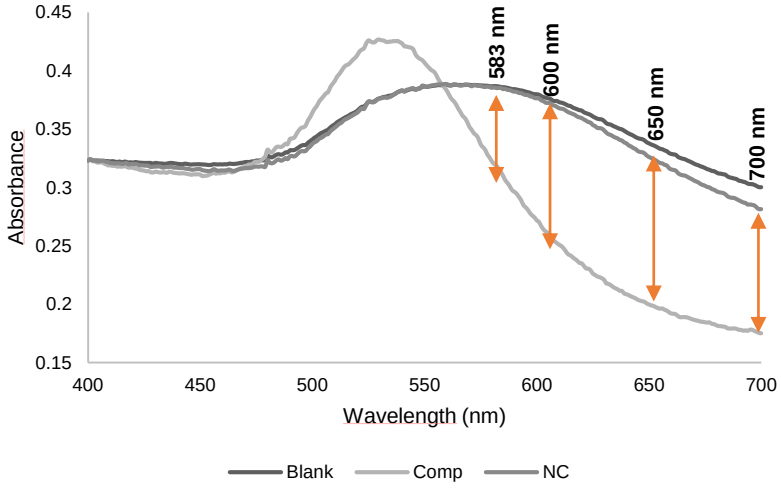

A7 I. Hybridisation profile of gold nanoprobe Batch 2 at pH8 phosphate buffer. The orange arrows represent the diverse values of absorbance registered by aggregated species at different wavelengths. Larger arrows indicate higher difference of absorbance between the non aggregated species (NC) and the aggregated species (C) and possibly a better discrimination between targets.

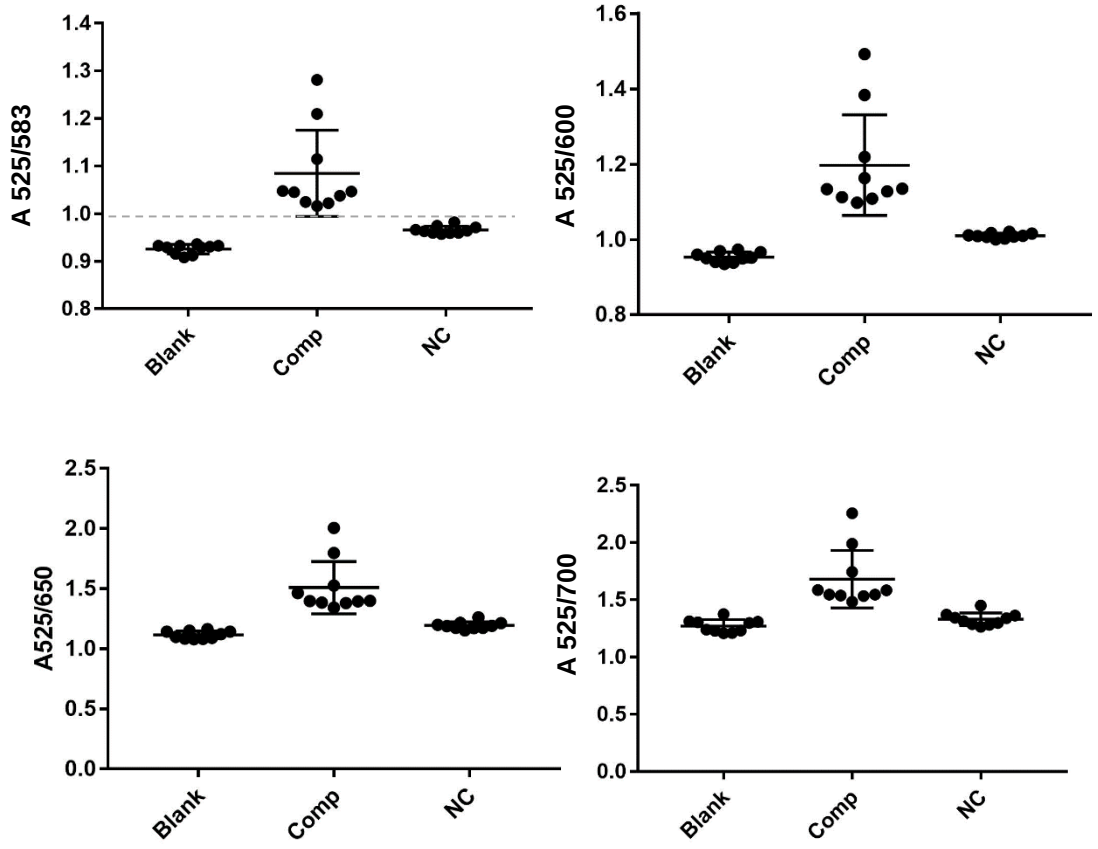

A7 II. Hybridisation profile of gold nanoprobe Batch 2 at pH8 phosphate buffer. Discrimination capacity represented by different ratios between agrgregated species (525nm) and non-aggregated species (538, 600, 650 and 700 nm).

The figure above shows that even though A525/583 and A525/600 ratios present similar discrimination, one can observe that the difference between the A525/600 ratio of complementary target and non-complementary target is higher than for A525/583 ratio. For A525/650 and A525/700 ratios this discrepancy is less visible. Therefore A525/600 was selected as the ratio which allowed the visualization of a better discrimination in agreement with the colorimetric results.

A8. Limit of detection (LOD) profile for *ttrRSBCA* probe Batches 2 (20 ng/µL) and 3 (75 ng/µL).

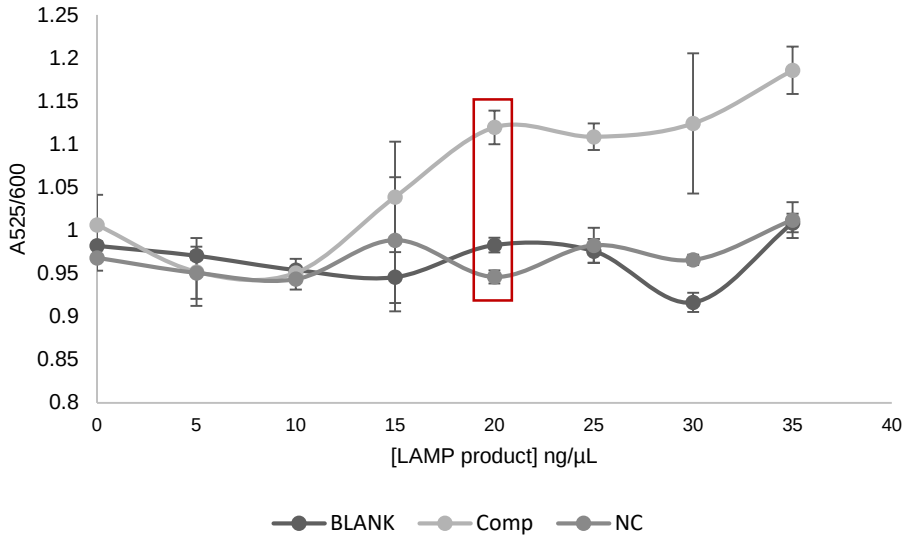

A8 I. Limit of Detection (LOD) profile for *ttrRSBCA* probe Batch 2. Ratio of absorbance for *ttrRSBCA* Au-nanoprobe conducted with 2.5 Nm of Au-nanoprobe on phosphate buffer 10Mm (pH8+0,1M NaCl) and with purified full complementary LAMP products. Aggregation induction was carried out by increasing the ionic strength up to 120 mM with the addition of $MgCl_2$. All spectra were taken 5 min after salt addition. Dots represent the average of three independent measurements and the error bars indicate standard deviation.

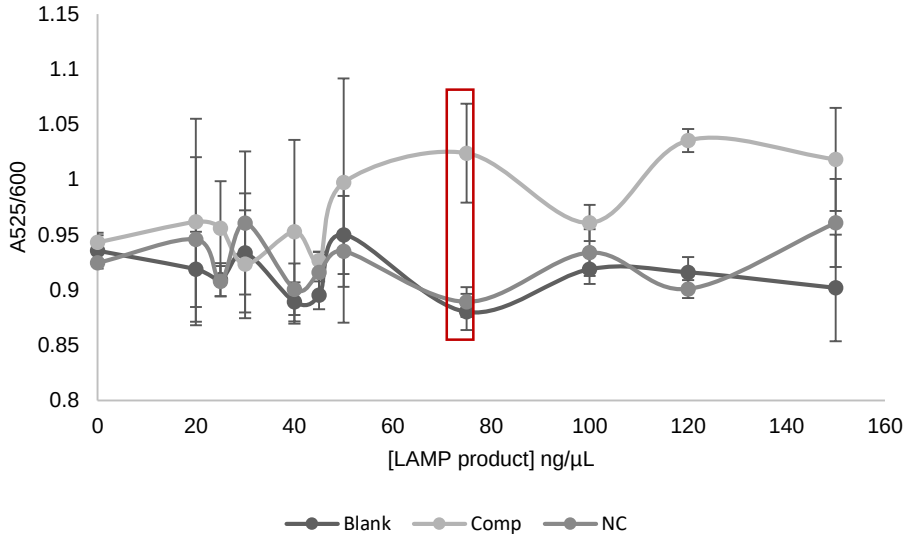

A8 II. Limit of Detection (LOD) profile for *ttrRSBCA* probe Batch 3. Ratio of absorbance for *ttrRSBCA* Au-nanoprobe conducted with 2.5 Nm of Au-nanoprobe on phosphate buffer 10Mm (pH7+0,1M NaCl) and with purified full complementary LAMP products. Aggregation induction was carried out by increasing the ionic strength up to 25 mM with the addition of $MgCl_2$. All spectra were taken 5 min after salt addition. Dots represent the average of three independent measurements and the error bars indicate standard deviation.

```
Alignment of Sequence_1:  [rpoB.fasta] with  Sequence_2: [BIP.xdna]

Similarity : 16/5084 (0,31 %)

Seq_1  1861  ACACCGTCGGCACCGACGAGGCGCTGTTGGACATCTACCGCAAGCTGCGTCCGGGCGAGC  1920
Seq_2  1     ------------------------------------------------------------  0

Seq_1  1921  CCCCGACCAAAGAGTCAGCGCAGACGCTGTTGGAAAACTTGTTCTTCAAGGAGAAGCGCT  1980
Seq_2  1     ------------------------------------------------------------  0

Seq_1  1981  ACGACCTGGCCCGCGTCGGTCGCTATAAGGTCAACAAGAAGCTCGGGCTGCATGTCGGCG  2040
                    ||||       |    || |       | ||||| | |
Seq_2  1     --------ACCCGTCGTCAGTGGCTAAAAGCATCACGGTAGCTCAGACCA----------  42

Seq_1  2041  AGCCCATCACGTCGTCGACGCTGACCGAAGAAGACGTCGTGGCCACCATCGAATATCTGG  2100
Seq_2  43    ------------------------------------------------------------  42

Seq_1  2101  TCCGCTTGCACGAGGGTCAGACCACGATGACCGTTCCGGGCGGCGTCGAGGTGCCGGTGG  2160
```

```
Alignment of Sequence_1:  [rpoB.fasta] with  Sequence_2: [FIP.xdna]

Similarity : 14/5084 (0,28 %)

Seq_2  1     ------------------------------------------------------------  0

Seq_1  241   ATCACGACGCGCCGACACCCTCGCGCTAGCGCGCACGGCCGATCAGATCCCTGTCAGTGA  300
Seq_2  1     ------------------------------------------------------------  0

Seq_1  301   AGCGGTGATGATTTCGTTGGCTCGACTCGTCGCGGACTGCCGAGCCGCGGG-CG-TGCGG  358
                                                                  |  || |  |
Seq_2  1     ----------------------------------------------------A-GTCCGTTCAGC  12

Seq_1  359   CGGTCGGTGAAGCTGACCGACGCTCTCATTGCGGCAACCGCGGAGATCAAGGTGTGACAC  418
                ||    |    |   |    ||||
Seq_2  13    GTTTCACGAAGCTGGCTGGCTATTCTCG------------------------------  40

Seq_1  419   CGAGGACTGATGAAGGTGCCGCTGCACCCTGCCTGATGCCTGACGTCACGATGCCCGTGA  478
Seq_2  41    ------------------------------------------------------------  40
```

```
lignment of Sequence_1:  [rpoB.fasta] with  Sequence_2: [B3.xdna]

imilarity : 12/5084 (0,24 %)

eq_1  4741  TCAACTACCGCACGCTTAAGCCGGAGAAGGACGGCCTGTTCTGCGAGAAGATCTTCGGGC  4800
eq_2  1     ------------------------------------------------------------  0

eq_1  4801  CGACTCGCGACTGGGAATGCTACTGCGGCAAGTACAAGCGGGTGCGCTTCAAGGGCATCA  4860
                                                                 ||| |||||
eq_2  1     ----------------------------------------------------ACAGGCCATCA  11

eq_1  4861  TCTGCGAGCGCTGCGGCGTCGAGGTGACCCGCGCCAAGGTGCGTCGTGAGCGGATGGGCC  4920
              ||||
eq_2  12    ATTGCGC-------------------------------------------------------  18

eq_1  4921  ACATCGAGCTTGCCGCGCCCGTCACCCACATCTGGTACTTCAAGGGTGTGCCCTCGCGGC  4980
eq_2  19    ------------------------------------------------------------  18

eq_1  4981  TGGGGTATCTGCTGGACCTGGCCCCGAAGGACCTGGAGAAGATCATCTACTTCGCTGCCT  5040
```

```
Alignment of Sequence_1:  [rpoB.fasta] with  Sequence_2: [F3.xdna]

Similarity : 12/5084 (0,24 %)

eq_2  1     ------------------------------------------------------------  0

eq_1  1081  TCTTGGCAGATTCCCGCCAGAGCAAAACAGCCGCTAGTCCTAGTCCGAGTCGCCCGCAAA  1140
eq_2  1     ------------------------------------------------------------  0

eq_1  1141  GTTCCTCGAATAACTCCGTACCCGGAGCGCCAAACCGGGTCTCCTTCGCTAAGCTGCGCG  1200
                      | ||||  |||| || |
eq_2  1     ---------CTTACTCGTTACCAGGCGG-------------------------------  19

eq_1  1201  AACCACTTGAGGTTCCGGGACTCCTTGACGTCCAGACCGATTCGTTCGAGTGGCTGATCG  1260
eq_2  20    ------------------------------------------------------------  19

eq_1  1261  GTTCGCCGCGCTGGCGCGAATCCGCCGCCGAGCGGGGTGATGTCAACCCAGTGGGTGGCC  1320
eq_2  20    ------------------------------------------------------------  19
```

A9. Alignment of *rpoB* gene sequence from *M.tuberculosis* with *ttrRSBCA* primers (from right to left BIP, FIP, F3, B3) performed in BioEdit software.